A NEW METHOD TO ASSESS BEST MANAGEMENT PRACTICE EFFICIENCY TO OPTIMIZE STORM WATER MANAGEMENT

A Dissertation

by

MIN-CHENG TU

Submitted to the Office of Graduate and Professional Studies of
Texas A&M University
in partial fulfillment of the requirements for the degree of

DOCTOR OF PHILOSOPHY

Chair of Committee,	Patricia K. Smith
Committee Members,	Anthony M. Filippi
	Raghupathy Karthikeyan
	Fouad H. Jaber
	Ming-Han Li
	Xiuying Wang
Intercollegiate Faculty Chair,	Ronald A. Kaiser

December 2014

Major Subject: Water Management and Hydrological Science

ABSTRACT

For TSS, TN, and TP, this study examined the relationship between BMP pollutant removal efficiency and environmental factors such as ratio of BMP/catchment area, dominant land use, ratio of the dominant land use/catchment area, slope, and BMP type, and derived optimal installation plans based on different criteria.

A SWMM model was built for the Shoal Creek Watershed in Austin, Texas. Inverse modeling (i.e. fitting model to observation data) was used to calibrate the BMP removal efficiency. The relationship can then be derived by using multiple linear regression analysis with BMP removal efficiency as the response variable and the environmental factors as predictive variables.

However, before inverse modeling can be applied, SWMM pollutant buildup and washoff parameters must be derived. A few types of land use were identified as main source of pollutant. The numerical distribution of the parameters suggested that the buildup and the washoff parameters are controlled by forces of different spatial scales.

Also, the SWMM model simulated only direct runoff in order to simplify the calibration. Mean pollutant concentration in base flow is required to convert observed concentration to that in direct runoff. The Shoal Creek Watershed discharges into Lady Bird Lake, and changes of water quality in the lake during base flow dominant dates were used to estimate concentration in base flow from Shoal Creek Watershed. Water quality of the lake was determined by Landsat imagery.

The equations predicting BMP removal efficiency based on environmental factors were analyzed to show the most efficient and least efficient type of BMP and the land use that BMPs will have the highest and lowest removal efficiency for TSS, TN, and TP.

Two planning criteria were utilized for the optimal BMP plans and different time frames were considered. One criterion is goal concentrations in runoff, and the other is a combination of goal concentration and a budget constraint. For each criterion, the associated optimal plan showed an areal ratio between BMP types throughout different time frame. It was also found that the Shoal Creek Watershed needs more BMPs. Suggestions to the Environmental Criteria Manual of Austin were also made based on this study.

DEDICATION

To my mother, my wife, and everyone who is beside me along the way.

ACKNOWLEDGEMENTS

I would like to thank my committee chair, Dr. Smith, for believing in my idea and allowing me to explore it. I would also like to thank my committee members (in alphabetical order), Dr. Filippi, Dr. Jaber, Dr. Karthikeyan, Dr. Li, and Dr. Wang for their guidance and support throughout the course of this research.

I appreciate that Dr. Wilcox enrolled me in 2009 so I had this opportunity to study and develop my research skills in Texas A&M University.

The data, information and support from the city of Austin, Lower Colorado River Authority, National Oceanic and Atmospheric Administration, and the city of Round Rock is crucial to my research and also highly appreciated.

Thanks also go to my friends and colleagues and the program of Water Management and Hydrological Science for making my time at Texas A&M University a great experience (thank you, Dr. Kaiser, Dr. Silvy, and Dr. Sanchez). Finally, thanks to my family for their encouragement, patience and love.

TABLE OF CONTENTS

Page

LIST OF FIGURES

Page

LIST OF TABLES

Page

CHAPTER I

INTRODUCTION

1.1. The Need for Predicting Pollutant Removal Efficiency of BMPs

The impact of urban stormwater on water resources, human health, and natural habitats is a major issue in managing urban watersheds (Al Bakri et al., 2008). Urbanization increases impermeable surfaces which allow pollutants such as oil, fertilizer, pesticides, soil, and animal wastes to directly wash into local waterbodies via municipal separate stormwater sewer systems (MS4s). Untreated, these discharges threaten designated uses of waterbodies.

The Clean Water Act (33 U.S.C. §1251 et seq. (1972)) mandates that a municipality's Stormwater Management Program (SWMP) obtain a permit from the National Pollutant Discharge Elimination System (NPDES) (Debo and Reece, 2003). Unlike point sources, NPDES permits for non-point stormwater do not specify the limits of pollutants; rather, they require a reduction in the discharge of pollutants to the "maximum extent practicable" (U.S. EPA, 2000; Roesner and Traina, 1994) through the use of Best Management Practices (BMPs). Compliance is usually evaluated by the number of applied BMPs (U.S. EPA, 2014a), not the effluent water quality.

A BMP can be defined as non-structural (e.g. good housekeeping and public education) or structural (e.g. infiltration and detention facilities) measures that do not involve active wastewater treatment (Urbonas and Stahre, 1993). For convenience, "BMP" will refer to "structural BMP" from this point forward unless noted otherwise.

Using the city of Austin, Texas, as an example, the Land Development Code (LDC) of the city of Austin (City of Austin, 2014c) stipulates that most land developments must have a water quality control plan. BMP approval and application are based on the individual site development plan. But design criteria of BMPs are based only on area of impervious surface, which is a proper criterion for flood control but probably not for water quality control. Sediment is the main concern in current storm water management practice in Austin. In addition, there is no coordination *per se* in watershed-wide BMP installation. It is important to coordinate BMP installation since BMPs are space and capital intensive (Islam et al., 2011). Optimizing BMP installation has been proven to be able to save significant capital investment even in a small urban watershed (Jia et al., 2012). Jia et al. showed that the potential saving for a small urban plot of 36 hectares can be as much as $35,000 (U.S. dollars) by comparing the most and least expensive scenarios for the same reduction of annual flow volume. The actual saving could be more because Jia et al. considered only the construction cost in the optimization.

Even though a few studies (such as Jia et al., 2012) have investigated the benefit of optimizing BMP installations considering the reduction in runoff and peak flow rate, few have attempted optimization based on the reduction of pollutant concentration in runoff. The reason for this phenomenon probably is the fact that removal efficiency (the ability to reduce pollutant concentration in runoff) of BMPs is hard to quantify (Urbonas and Stahre, 1993). This is shown through data from the International Stormwater BMP Database. The International Stormwater BMP Database was established in 1996 and is

comprised of data from more than 400 studies (Moeller and Connor, 2014). The data from the International Stormwater BMP Database showed that the removal efficiency of BMPs is highly variable. An example of retention pond removal efficiency at removing total suspended solids is shown in Figure 1.1, comparing the influence and effluence concentrations. Note that the axes in Figure 1.1 are on a log scale.

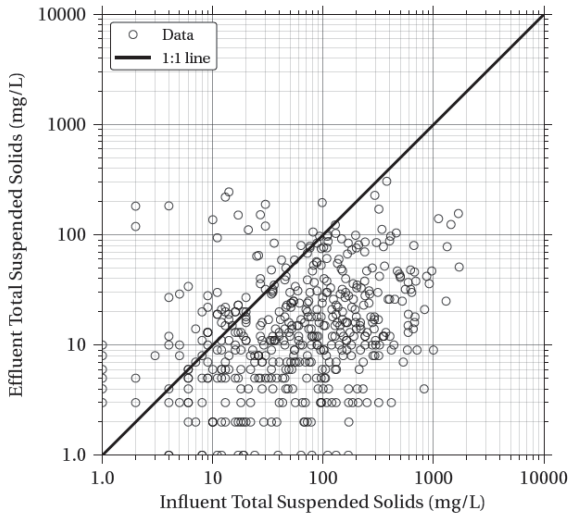

Figure 1.1. Influent and Effluent Plots of Total Suspended Solids at Retention Pond BMPs (Moeller and Connor, 2014)

TSS (total suspended solids), TN (total nitrogen), and TP (total phosphorous) are three water quality constituents removed by BMPs. TSS not only has an impact on

aquatic life (reducing photosynthesis activity) and aesthetics, but also the adsorbtion by sediment with various other pollutants such as phosphorus, pesticide, and metals (Leisenring et al., 2011). TN causes eutrophication and some forms of nitrogen (such as ammonia) can be toxic to aquatic life in low concentrations (Leisenring et al., 2010). TP also causes eutrophication, and since phosphorus is usually the limiting nutrient in freshwater systems, the availability of phosphorus from stormwater runoff has the potential to cause serious water quality problems (Leisenring et al., 2010).

The literature showed that BMP removal efficiency for these water quality constituents (TSS, TN, and TP) is affected by numerous factors in water, such as (Leisenring et al., 2010; 2011):

1. Factors affecting sedimentation: temperature, particle size distribution, density, electric charge associated with clay particles;

2. Factors affecting removal of nitrogen: temperature, pH, bacterial community, DO (dissolved oxygen); and

3. Factors affecting removal of phosphorous: particulate association (sizing of sediments), pH and oxidation reduction potential, cation exchange coefficient/P-index, and temperature.

In addition, studies implied that land use can be an important factor for BMP removal efficiency (ASCE, 2001). Numerous attributes in the environment such as slope (Yu et al., 2001; Liu et al., 2008) and the ratio of BMP area to the catchment area (Yu et al., 2001) have also been considered important. Indeed, Strecker et al. (2001) suggested a long list of factors to be reported in the BMP database (Moeller and Connor,

2014) so BMP removal efficiency can be better evaluated, including factors about the tributary watershed (e.g. soil type, vegetation type), about general hydrology (e.g. peak flow rate, intervals between storms), about water (e.g. alkalinity, temperature), about general facility (e.g. type and frequency of maintenance), etc. All these factors and their interactions made prediction of BMP pollutant removal efficiency a daunting task.

There has been no study attempting to relate BMP pollutant removal efficiency to these factors. A few studies such as Barrett et al. (2005) did find a linear relationship between influence and effluence pollutant concentrations for some types of BMPs, but their finding was based on a small set of data and didn't consider any of the factors above. Similarly, existing BMP planning software such as STEPL (U.S. EPA, 2013), SUSTAIN (U.S. EPA, 2014e), and SELECT (WERF, 2014) do not consider these factors either.

We need to have a better understanding about how BMP removal efficiency is affected by these factors so BMP installation can be fine-tuned in order to save capital cost and building space in the future. This research hypothesized that certain environment factors affect pollutant reduction removal efficiency of BMPs, and had the following objectives:

1. Derive the relationship between BMP pollutant removal efficiency and environment factors;

2. Provide a computer program to optimize BMP planning by using the relationship; and

3. Provide recommendations to improve municipal regulations regarding BMP installation based on the relationship.

1.2. A Short Introduction to the Approach

As Strecker et al. (2001) and other studies suggested, a long list of factors can influence BMP removal efficiency. This study narrowed down the list by using BMPs from the same urban watershed so region-specific factors such as intervals between storms, soil group, and water temperature can be ignored.

BMPs in the Shoal Creek Watershed in Austin, TX were used in this study. There are two main reasons that the Shoal Creek Watershed was chosen in this study as the watershed of interest:

1. The Shoal Creek Watershed discharges into Lady Bird Lake (a.k.a. Town Lake), and multiple water quality monitoring sites have been maintained by the USGS to provide detailed data in water quality of the lake (USGS, 2014b); and

2. The city of Austin maintained a detailed GIS database on the Internet (City of Austin, 2014b), including aerial photography and land use GIS shape files, which made data acquisition easier.

The core methodology utilized by this study is "inverse modeling", which is synonymous to calibration of certain model parameters. Calibration means adjusting parameters in a model so that the behaviors of the model and of the real system are as close as possible (Goegebeur and Pauwels, 2007). When a global minimum of

difference of the observed and simulated response variables is achieved, the associated set of parameters can be considered the real properties of the system (Sun et al., 2013). Following this methodology, this study used SCEUA (Shuffled Complex Evolution – University of Arizona), which is a global optimization algorithm, to derive pollutant removal efficiency of BMPs by matching simulated pollutant concentration to observed pollutant concentration. By linking the derived BMP removal efficiency and associated BMP attributes (i.e. "factors" mentioned before), statistical analysis can be applied to derive their statistical relationship. This part is discussed in Chapter 4.

However, this approach requires two additional pieces of essential information. The first piece of information is the pollutant buildup and washoff parameters, which have not been well established yet for the model of choice (i.e. SWMM: Storm Water Management Model) (U.S. EPA, 2014b). Pollutant buildup and washoff parameters are required in simulating the rate of pollutant building up on the ground when there is no runoff, and how fast pollutant is washed off when runoff is present. These parameters govern the pollutant "input" to BMPs, so they need to be chosen correctly in order to get correct BMP removal efficiency. By using flow rate and water quality data in the 1980s, these parameters were calibrated from a neighboring watershed in the same city. BMP construction is not significant prior to 1990, so the interference in hydrology and water quality from BMPs can be ignored by using data from 1980s. This part is discussed in Chapter 3.

The second piece of information is the mean concentrations in base flow. In order to simplify simulation, the groundwater module was turned off in SWMM, which

means only direct runoff was simulated. Such simplification is valid because SWMM does not consider lateral flow in the soil unsaturated zone (U.S. EPA, 2014b). To accommodate this approach, all observed flow rate and water quality data must be converted to that of direct runoff before being used in calibration. The technique of base flow separation (Lim et al., 2005) was used to separate flow rate into components of direct runoff and base flow. However, the water quality of base flow must be known prior to converting observed water quality to water quality of direct runoff. In this study, water quality of base flow was estimated from two sources: 1) the change of water quality in Lady Bird Lake (which the Shoal Creek Watershed discharges into) on base flow dominant days, and 2) groundwater samples. The change of water quality in Lady Bird Lake was measured from Landsat imagery (EROS, 2014a). Reflectance of spectral bands in satellite imagery is known to be used to build predictive equations to estimate water quality in reservoirs, but the equations used in estimation are site-specific (Liu et al., 2003). Chapter 2 describes the procedure to establish the water quality predictive equations for Lady Bird Lake.

CHAPTER II

WATER QUALITY DETECTION USING LANDSAT TM AND ETM+ IMAGES

2.1. Overview

The ability to monitor water bodies with high spatial and temporal resolution is crucial to maintaining water quality because correction after pollution occurs is typically more costly than early prevention/intervention. Current sampling of Lady Bird Lake in Austin, TX by USGS has low spatial and temporal resolution. Since satellite images have better spatial and temporal resolution than field measurements, this study utilized satellite images from Landsat TM/ETM+ to establish a multiple regression derived relationship between satellite band reflectance and concentrations of total suspended solids (TSS), total nitrogen (TN) and total phosphorus (TP) . Satellite images were atmospherically corrected by FLAASH based on ground temperature. Two methods were used to select predictor variables in multiple regression derived equations considering the variation inflation factor (VIF): forward selection of variables using a p-value threshold, and quasi second order Akaike Information Criteria (AICc). The derived equation for TSS yielded the lowest coefficient of determination ($R^2 = 0.53$), implying a possible weak linkage between turbidity and sediment in this waterbody. Infrared bands (bands 4 to 6) of Landsat TM/ETM+ were found to be important in detection of TN and TP. By comparing the results from the two multiple regression selection methods, the conventional forward selection method coupled with VIF was

found to yield more robust equations. The derived relationships will be useful in extending the temporal and spatial availability of water quality data in Lady Bird Lake.

2.2. Introduction

Continuous water quality monitoring of our nation's water bodies is essential for the health and welfare of the people and ecosystems reliant on them. Urbanization, agriculture and other anthropogenic factors can alter water quality (Kannel et al., 2007); and waiting until a change is clearly visible, can be much more costly than early prevention. Despite the importance of continuous water quality monitoring the cost of adequate temporal and spatial physical measurements can be cost prohibitive (Harmel et al., 2006).

In recent decades, the increasing availability and affordability of satellite imagery has provided an alternative to monitor water quality with a higher frequency and at a lower cost. Each water quality constituent exhibits a specific spectral response that can be observed by satellites (Liu et al., 2003). For instance, suspended sediment usually exhibits strong backscattering of incident light (Liu et al., 2003), but the actual color depends on the terrestrial origin (Bukata, 2005). Colored dissolved organic matter is composed of algae, yellow substance, and organic plumes (Liu et al., 2003), and shows a broad-band solar-induced fluorescence of 490-530 nm (Bukata, 2005). Phytoplankton, on the other hand, show reflectance at a well-defined Gaussian distribution around 685 nm from chlorophyll-a (Bukata, 2005; Liu et al., 2003).

Studies have indicated that multispectral satellite imagery can be used to estimate water quality using a variety of methods, with the majority using either multiple regression analysis or artificial neural networks (ANN) (Kloiber et al., 2002; Liu et al., 2003; Kishino et al., 2005). Conventionally, visible bands are used to measure water quality by virtue of their capability to penetrate the water column (Liu et al., 2003). However, data from infrared bands, including thermal infrared, have also been directly used in multiple regression analysis (Barbini et al., 1997) or incorporated into hydrodynamic models (Schott et al., 2001; Pahlevan et al., 2012) to measure water quality constituents. The applicability of the derived result is usually limited to the same water body (Liu et al., 2003) because the spectral response of suspended sediment depends on the terrestrial origin (Bukata, 2005), and the distribution of sediment particle size affects turbidity even when the sediment concentration is the same (Liu et al., 2003). For a particular wavelength the spectral radiance observed vertically, known as the upwelling radiance, L_u, is given by Equation 2.1 (Doxaran et al., 2002):

$$L_u(\lambda) = L_w(\lambda) + \Omega L_s(\lambda) \tag{2.1}$$

Where L_w is the water-leaving radiance, or the radiance reflected/backscattered by the water column, in-water constituents and the bottom if the depth is shallow; L_s is the skylight radiance; Ω is the ratio of radiance directly reflected by the water surface to L_s; and λ is the wavelength (nm). Note that the radiance observed by a satellite is composed of the upwelling radiance, L_u, plus atmospheric interference, therefore, it requires atmospheric correction (discussed later). L_w, L_s and Ω are influenced by a variety of factors. If the water column is deep enough, allowing the bottom reflection to

be ignored, L_w can be assumed to be a measure of in-water constituents alone. The sky conditions (clear, cloudy, overcast) affect both Ω and L_s, while Ω can be further affected by wind speed in the form of surface ripples (Doxaran et al., 2002).

The objective of this study was to utilize multiple regression analysis to determine the coefficients of an equation that can be used to estimate water quality of Lady Bird Lake (formerly Town Lake) in Austin, TX from band reflectance of Landsat TM and ETM+. The detail of bands from Landsat TM and ETM+ are listed in Table 2.1 (USGS, 2013c). There have been no similar studies performed on Lady Bird Lake. This research is needed because such equations are usually only valid for the same water body, so equations derived from other places cannot be used in Lady Bird Lake.

Table 2.1. Band attributes of Landsat TM and ETM+

		Band 1	Band 2	Band 3	Band 4	Band 5	Band 6	Band 7	Band 8
TM	**wavelength (μm)**	0.45-0.52	0.52-0.60	0.63-0.69	0.76-0.90	1.55-1.75	10.40-12.50	2.08-2.35	n/a
	resolution (m)	30	30	30	30	30	60*	30	n/a
ETM+	**wavelength (μm)**	0.45-0.52	0.52-0.60	0.63-0.69	0.77-0.90	1.55-1.75	10.40-12.50	2.09-2.35	0.52-0.90
	resolution (m)	30	30	30	30	30	60*	30	15

* Products in 60-meter resolution before 2/25/2010 and resampled to 30-meter after that.

This is the first attempt to derive the relationship between water quality and satellite-derived reflectance for Lady Bird Lake. The Landsat mission provides an opportunity to derive at most two water quality measurements each month, which are ideally 24 measurements per year at any location in the lake, thus can be a useful auxiliary data source to stretch the temporal and spatial availability of water quality data in Lady Bird Lake. As a major water body in metropolitan Austin, it is essential that local authorities can detect anomalies in its water quality in a timely manner.

2.3. Research Area

The location of Lady Bird Lake, situated in the heart of Austin, provides an excellent opportunity to monitor water quality in an urban watershed (Figure 2.1). The population of Austin has increased dramatically from 250,000 in 1970 to 850,000 in 2013 (City of Austin, 2014a). With significant population growth comes an increase in impervious area, higher runoff and lower water quality in local water bodies. Therefore, it would be beneficial to have a means to monitor the change in water quality of Lady Bird Lake in order to evaluate the impact of urbanization on local water resources.

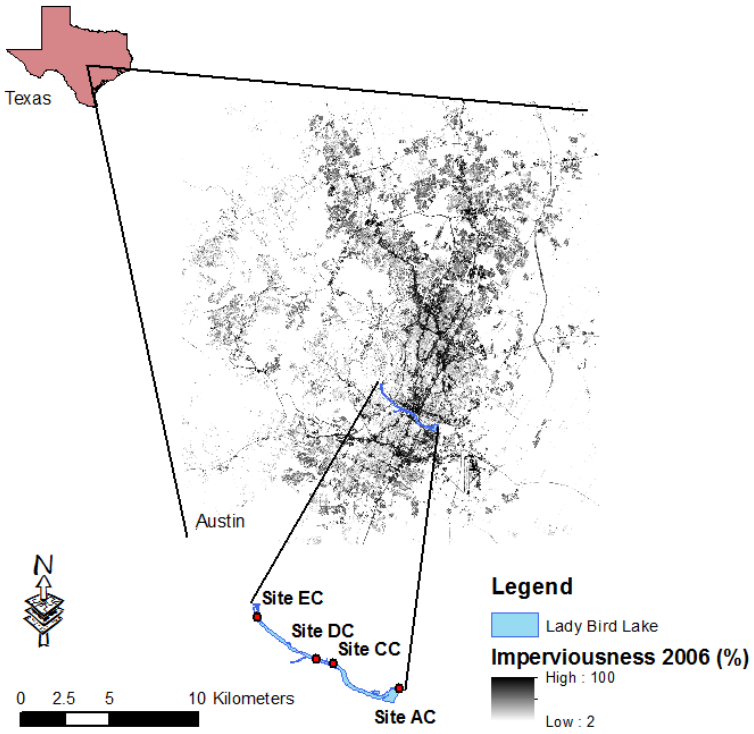

Figure 2.1. Locations of water quality sampling stations on Lady Bird Lake

The USGS monitors water quality in Lady Bird Lake regularly, but the frequency is only about twice per year at a single point in the outlet in the past decade (USGS, 2013b). Additionally, field measurements from year to year do not occur in the same months. As a result, it is difficult to distinguish whether a field-measured change in water quality is truly a long-term change or the result of a seasonal difference or recent event (e.g. a large precipitation event) (McCullough, 2012). Additionally, it is impossible to evaluate the spatial variation in water quality from single point measurements.

Two lakes were formed within the Austin city limits by damming the Colorado River: Lake Austin, formed by Tom Miller Dam, and further downstream Lady Bird Lake, formed by Longhorn Dam (LCRA, 2012). Longhorn Dam is a "pass-through" dam which maintains Lady Bird Lake at a constant level. The surface area of Lady Bird Lake is approximately 429 acres (173.6 hectares) with a capacity of 7,338 acre-ft (905.1 ha-m). The mean depth of Lady Bird Lake is about 18 feet (6 meters) with a maximum depth over 35 feet (11.7 meters) (TWDB, 2009).

USGS has a number of water quality stations on Lady Bird Lake, but only four of them (EC, DC, CC and AC) (Figure 2.1) monitor the water quality constituents of interest in this research: total suspended solids (TSS), total nitrogen (TN) and total phosphorus (TP) within the time frame of available satellite images (USGS, 2013a). Table 2.2 provides basic information for these four stations, and Figure 2.1 shows their locations. Summary statistics for TSS, TN and TP derived from water quality samples used in this research are given in Table 2.3. The transparency measurements (by Secchi disc) accompanying water quality samples used in this research are provided for the four locations in Table 2.4. The transparency is much lower than average depth (6 meters) of the lake, so bottom reflectance can be ignored in this study.

Table 2.2. Coordinates of water quality sample sites in Lady Bird Lake

Site Code	USGS Water quality sample site	Coordinates
EC	USGS 301712097470701	N 30°17'14.4", W 97°47'08.0"
DC	USGS 301558097452201	N 30°15'58.3", W 97°45'22.4"
CC	USGS 301546097445101	N 30°15'47.0", W 97°44'51.1"
AC	USGS 301500097424801	N 30°15'01.5", W 97°42'49.8"

Table 2.3. Summary statistics for Total Suspended Solids (TSS), Total Nitrogen (TN) and Total Phosphorus (TP) from water quality stations in Lady Bird Lake (The number of water quality samples used in this study is denoted by "#")

	TSS (mg/L)			TN (mg/L)			TP (mg/L)		
USGS Water Constituent Parameter Code	**00530**			**00600**			**00665**		
	#	**Mean**	**Std. Dev.**	**#**	**Mean**	**Std. Dev.**	**#**	**Mean**	**Std. Dev.**
Site EC	7	4.57	4.24	11	0.58	0.22	4	0.015	0.0058
Site DC	8	5.75	5.39	8	0.71	0.36	8	0.023	0.017
Site CC	4	9.50	5.26	6	0.53	0.14	3	0.023	0.012
Site AC	8	7.38	10.51	11	0.67	0.25	8	0.028	0.034
All	27	6.48	6.91	36	0.63	0.25	23	0.023	0.022

Table 2.4. Secchi disc transparency for water quality stations in Lady Bird Lake

Site Code	# of measurements	Mean (m)	Std. Dev. (m)
EC	11	2.22	0.86
DC	10	1.68	0.77
CC	8	1.23	0.62
AC	13	1.49	0.64

2.4. Methodology

2.4.1. Data Analysis

Thirteen Landsat TM/ETM+ images (EROS, 2014a) collected within seven days of USGS water quality measurements (USGS, 2004; Kloiber et al., 2002) were selected for this research. After analyzing the relationship between direct runoff and precipitation at the USGS river gage of Shoal Creek at West 12th Street (site number: 08156800), precipitation events less than 1.25 cm (0.5 in) were considered not likely to cause significant runoff (i.e. creating daily direct runoff higher than the average daily value) and alter the water quality constituent concentrations in the lake (USGS, 2013b). There were no precipitation events with depths over 1.25 cm observed between the dates of the selected images and their associated water sample dates (Table 2.5). Only cloud-free images in the vicinity of the city of Austin were selected (Kloiber et al., 2002). The image from December 20, 2001 was excluded from subsequent processing because it yielded negative reflectance values after FLAASH atmospheric correction (discussed

below). All USGS water quality measurements used in this study were made at the depth of 1 foot.

Table 2.5. Dates of satellite images and water quality samples

Sensor Name	Image Date	Water Quality Sampling Date
Landsat4 TM	January 9, 1983	January 6, 1983
Landsat5 TM	August 18, 1985	August 20, 1985
Landsat5 TM	January 15, 1988	January 19, 1988
Landsat5 TM	April 20, 1988	April 19, 1988
Landsat5 TM	July 25, 1988	July 27, 1988
Landsat5 TM	March 6, 1989	February 27, 1989
Landsat5 TM	April 7, 1989	April 12, 1989
Landsat5 TM	August 5, 1992	August 10, 1992
Landsat5 TM	July 24, 1999	July 22, 1999
Landsat5 TM	December 20, 2001	December 16, 2001
Landsat7 ETM+	April 22, 2009	April 18, 2009
Landsat5 TM	June 4, 2010	June 3, 2010
Landsat7 ETM+	May 14, 2011	May 13, 2011

Atmospheric correction using FLAASH was used to obtain reflectance values (ρ) without the effect of path radiance from the atmosphere (Exelis Inc., 2009). Images were first converted from digital number to spectral radiance (L) and then processed by FLAASH atmospheric correction using ENVI to find the surface reflectance as:

$$L = \left(\frac{A\rho}{1-\rho_e S}\right) + \left(\frac{B\rho_e}{1-\rho_e S}\right) + L_a \quad (2.2)$$

Where L is the spectral radiance observed by the sensor, ρ is the "correct" surface reflectance for the pixel of interest, ρ_e is the average surface reflectance from the pixel of interest and the surrounding region, S is the albedo of the atmosphere, L_a is the radiance back-scattered by the atmosphere, and A and B are coefficients depending on atmospheric and geometric conditions but not on the surface (Exelis Inc., 2009).

Because water bodies like Lady Bird Lake are typically very dark, the reflectance from water is low while the surrounding urban area would have a much higher reflectance. The FLAASH manual cautions users that significant errors can occur when strong contrasts occur among the materials in the scene (Exelis Inc., 2009). To avoid this problem, a mask was created to exclude all surrounding regions (Figure 2.2) (Hadjimitsis et al., 2004).

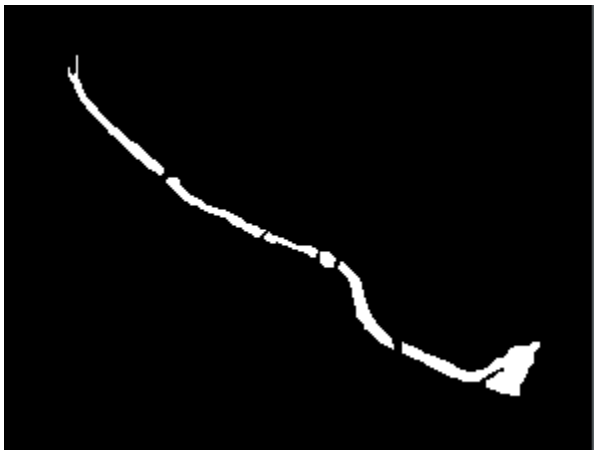

Figure 2.2. Mask for Town Lake in FLAASH processing

FLAASH requires two additional parameters, visibility and choice of atmospheric model. Visibility obtained from historical airport records (NWS, 2014b) was found to cause FLAASH to over-compensate and yield negative reflectance. Therefore, the 2-band (K-T) aerosol retrieval method with "urban" setting in FLAASH was used to estimate visibility. When choosing an atmospheric model, the FLAASH manual suggests selecting an atmospheric model based on (from most preferred to least preferred): known standard column water vapor amount, expected surface air temperature, or tabulated seasonal-latitude combinations (Exelis Inc., 2009). Although there are several products of atmospheric water content available (NASA, 2013a; NOAA, 2013), they do not cover all dates of interest in this research. On the other hand, the surface temperature has been continuously recorded and archived by Camp Mabry Austin City Airport and Austin Bergstrom International Airport every hour over the past

thirty years (NWS, 2014b). Therefore, atmospheric models were selected based on the surface air temperature at the time when the satellite image was taken (Table 2.6).

Table 2.6. Selection of atmospheric model based on surface air temperature

Image Date	Surface Temperature (°C)	Atmospheric Model	Suggested Temperature for Model (°C)
January 9, 1983	11	Sub-Arctic Summer	14
August 18, 1985	33	Tropical	27
January 15, 1988	11	Sub-Arctic Summer	14
April 20, 1988	23	Mid-Latitude Summer	21
July 25, 1988	32	Tropical	27
March 6, 1989	2	Mid-Latitude Winter	-1
April 7, 1989	25	Tropical	27
August 5, 1992	31	Tropical	27
July 24, 1999	31	Tropical	27
December 20, 2001	10	Sub-Arctic Summer	14
April 22, 2009	30	Tropical	27
June 4, 2010	29	Tropical	27
May 14, 2011	23	Mid-Latitude Summer	21

Reflectance values at the water quality stations were extracted from atmospherically corrected satellite images for analysis. However, pixels selected by the coordinates of the water quality sampling stations are not likely to be the ideal pixel to extract reflectance values for several possible reasons including: the error between coordinates and actual sampling locations, random surface debris, reflected light from nearby objects on the shore due to atmospheric scattering, and/or water near the sampling stations may be shallow making bottom reflection a concern. In order to get the reflectance values that have the least error, the search range was expanded to 60 m around the pixel located by the station coordinates. The pixel within the search zone with the lowest value in band 4 was considered to contain the most information from water (Frazier and Page, 2000; USGS, 2013c). If two pixels have the same band 4 values, the one closest to the coordinates of water quality sampling location (i.e. the center of the search zone) was selected.

2.4.2. Multiple Regression Analysis

This study adopted the multiple regression analysis because it generates portable results (i.e. equations) that anyone can use without specialized software. Also, the low sample size in this study does not warrant the use of artificial neural network (ANN).

A total of three equations was derived, one for each of the water constituents of interest (TSS, TN, and TP) in order to establish a quantitative relationship between reflectance from each band at a cell (independent variables) and the water constituent concentration at the cell (dependent variables). The FLAASH atmospheric correction tended to over compensate band 7 and render negative values. Therefore, band 7 was

not included in the regression. The panchromatic band 8 was not used since its wavelength overlaps with other bands. Among the other bands (1 to 6), if any band was found to have a negative value after atmospheric correction, the data containing the negative value was discarded in subsequent calculations. Additionally, band ratios were included as independent variables in the regression analysis because they are less likely to be influenced by lighting conditions (Jensen, 2007). The initial independent variables considered for the subsequent variable selection process are provided in Table 2.7 (all band values and band ratios are based on reflectance).

Table 2.7. Initial band reflectance values and band reflectance ratios considered in the variable selection process ("B" is the shorthand of "band")

Water constituent	# of valid observations	Initial predictor variables before p-threshold test
TSS	27	B1, B2, B3, B4, B5, B6, B2/B1, B3/B1, B4/B1, B5/B1, B3/B2, B4/B2, B5/B2, B4/B3, B5/B3, B5/B4, B6/B1, B6/B2, B6/B3, B6/B4, B6/B5
TN	36	
TP	23	

In order to choose the most robust predictors for water quality, selection of predictor variables was based on two selection methods: forward selection with p-value threshold, and quasi second-order Akaike Information Criterion (QAICc).

In forward selection, variables are added to the regression one at a time, starting with no predictor variables. The p-value threshold includes a predictor in the regression equation if its p-value is below a "probability to enter", and includes a predictor that will most improve the fit first (i.e. "forward"). A default value of 0.25 in JMP (SAS, 2014) was used for "probability to enter". In addition to the classical forward selection method, the variation inflation factor (VIF) was further considered to avoid multicollinearity of the model. Multicollinearity occurs when a predictor variable is a linear combination of other predictor variables in the model. The direct consequence of multicollinearity is that the error variance is inflated, which may result in low prediction power if the over fitted model is used in a new set of data. VIF is calculated as:

$$VIF_j = {1}\Big/{(1 - R_j^2)} \tag{2.3}$$

Where R_j^2 is the multiple coefficient of determination between the predictor variable of interest and the rest of the predictor variables. The rule of thumb to avoid serious multicollinearity is all chosen predictor variables should have VIF less than 10 (Chatterjee and Simonoff, 2013; Hocking, 2013). To incorporate VIF in forward selection, the following procedure was proposed. First, perform the forward selection. Second, check whether all selected variables have p- values below 0.05, and start deleting variable(s) beginning with those with the highest p- value until all variables have p- values below 0.05. Third, check the VIF of the remaining predictor variable(s), and delete the variable with the highest VIF if any of them is above 10. Fourth, follow the second step, and if all variables have both p values below 0.05 and VIF below 10,

stops the procedure. The proposed procedure can be illustrated in Figure 2.3. Coefficients of variables, p-values, and VIF are dynamically recalculated when any variable is deleted from the model.

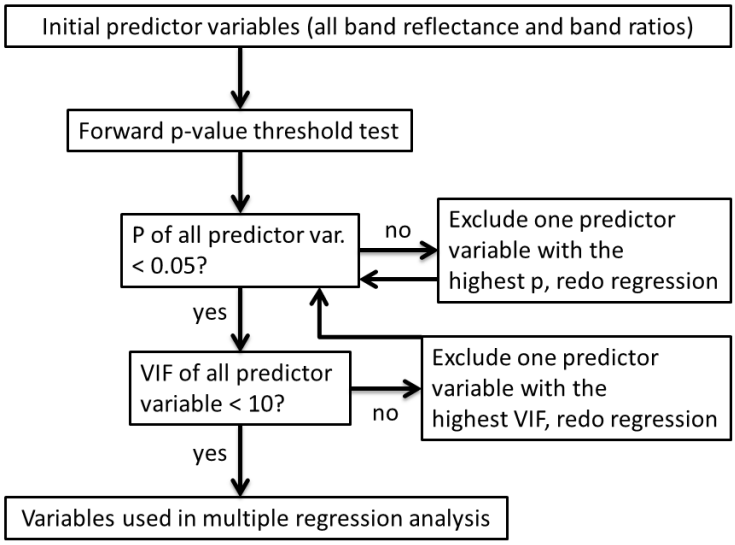

Figure 2.3. Flow chart of the process for selecting predictor variables in multiple regression analysis

AIC is a statistical criterion for model selection that strives to address the "principle of parsimony", striving to reach a balance between strength of fit and model simplicity (Chatterjee and Simonoff, 2013). AIC is an estimation of the information lost in approximating a true model by the regression model. The second-order AIC (i.e. AICc) is used in the case when the number of samples is small (like the current study),

which is usually defined as the number of observations divided by the number of parameters being less than 40 (Burnham and Anderson, 2002). The equation of AICc is calculated as (Anderson and Burnham, 1999; Royston and Sauerbrei, 2008; Yan, 2009):

$$AIC_c = -2\log\left(L\left(\hat{\theta}\right)\right) + pk + \frac{2k(k+1)}{n-k-1} \tag{2.4}$$

Where n is the number of observations, $L(\hat{\theta})$ is the maximum likelihood estimate (proportional to the residual mean square when the distribution is normal) (Konishi and Kitagawa, 2007) and k is the number of predictors in the equation. The term "pk" is the penalty term for each added predictor variable and the penalty constant p is 2 in classical AIC (Barton, 2014). The goal is to minimize AICc, therefore the penalty term is to guard against overfitting.

In Equation 2.4, p=2 has been used frequently in literature. However, some statisticians questioned the use of p=2 as not adequate (Bozdogan, 2000). Such questioning is admissible in this study because some regression equations selected with p=2 are not accepted for high VIF. This is discussed below.

Even though AIC (or AICc for small sample size) considers both goodness-of-fit and over-fitting, it is apparent from Equation 2.4 that it does not consider dispersion of the model. Over-dispersion is a phenomenon which happens when the variance is relatively large compared to the mean (Agresti, 2014). Small error variance is preferred in order to obtain good predictive power, thus over-dispersion of the model should be avoided. Quasi-AICc (QAICc) is the modified criterion considering model dispersion:

$$QAICc = -\left[\frac{2\log\left(L\left(\hat{\theta}\right)\right)}{c}\right] + pk + \frac{2k(k+1)}{n-k-1} \tag{2.5}$$

Where c is analogous to VIF (Anderson and Burnham, 1999). C is calculated as:

$$c = \frac{\chi^2}{d.f.} \tag{2.6}$$

Where χ^2 is the chi-square statistic of the global model, and d.f. are the degrees of freedom of the model. Similar to the variation inflation factor, the value of 1 for c means no dispersion. The package "MuMIn" was used to calculate quasi-AICc for all possible combinations of variables. All available observations were used to derive the regression, rather than dividing observations into two groups (i.e. calibration and validation). There were two reasons for this approach. First, the more observations, the more reliable the derived regression relationship is. Second, the minimum number of calibration data points used in many literature studies is around 20 (Alparslan et al., 2010; Sarangi et al., 2011; Dewidar and Khedr, 2001), so significantly dropping the number of data points below 20 in calibration is not desirable.

2.5. Results

The best fitting regression equations chosen by forward selection and QAICc for each water quality constituent (TSS, TN and TP) are provided in Tables 2.8 through 2.13. Note that the results from QAICc comprise results with different penalty constants, and results from p=4 and p=5 were identical (Table 2.11). The results in Tables 2.8 through 2.13 include the predictor variables (in reflectance), associated regression coefficients and standard error, 95% confidence intervals for the regression coefficients, p-values and VIF values for each of the response variables (TSS, TN, and TP). Note that names of predictors are abbreviated, for example, "B6" means the

reflectance of band 6, and "B3/B1" means the band ratio of reflectance of band 3 divided by that of band 1.

Table 2.8. Best fitting multiple regression models for TSS, TN and TP using forward selection based on p-value and VIF

				Coefficient of predictor		Confidence Interval for mean of coefficient			
	R^2	Number of obs.	Predictor	Value	Std. Error	Lower 95%	Upper 95%	p	VIF
TSS	0.53	27	intercept	-2.98	2.0055	-7.11	1.15	0.1498	n/a
			B3/B1	7.52	1.41	4.61	10.43	<0.0001	1
TN	0.59	36	intercept	-0.19	0.22	-0.63	0.26	0.39	n/a
			B6	2.02	0.36	1.28	2.75	<0.0001	1.06
			B5/B3	-0.5	0.14	-0.77	-0.22	0.0009	1.04
			B5/B4	0.057	0.025	0.0048	0.11	<0.033	1.1
TP	0.76	23	intercept	-0.04	0.014	-0.070	-0.0095	0.013	n/a
			B4/B2	0.047	0.011	0.024	0.070	0.0004	2.20
			B5/B4	0.018	0.0024	0.013	0.023	<0.0001	1.89
			B6/B5	0.00052	0.00023	0.000042	0.0010	0.035	1.75

Table 2.9. Best fitting multiple regression models for TSS, TN and TP using QAICc with a penalty constant p = 2

				Coefficient of predictor		Confidence Interval for mean of coefficient			
	R^2	Number of obs.	Predictor	Value	Std. Error	Lower 95%	Upper 95%	p	VIF
TSS	0.53	27	intercept	-2.98	2.0055	-7.11	1.15	0.1498	n/a
			B3/B1	7.52	1.41	4.61	10.43	<0.0001	1
TN	0.82	36	intercept	-1.19	0.23	-1.67	-0.71	<0.0001	n/a
			B1	9.32	3.69	1.75	16.89	0.018	6.15
			B4	23.38	4.94	13.25	33.51	<0.0001	17.12
			B4/B2	-1.97	0.41	-2.81	-1.13	<0.0001	62.55
			B4/B3	0.69	0.33	0.014	1.36	0.046	42.65
			B6/B2	0.20	0.026	0.15	0.25	<0.0001	10.9
			B6/B3	-0.06	0.013	-0.087	-0.033	<0.0001	12.27
			B6/B4	0.0025	0.00098	0.00048	0.0045	0.017	2.2
			B6/B5	0.0058	0.0018	0.0021	0.0096	0.0058	1.5
TP	0.95	23	intercept	-0.017	0.015	-0.049	0.015	0.27	n/a
			B2	-0.67	0.21	-1.11	-0.23	0.0052	3.53
			B4	2.40	0.33	1.70	3.10	<0.0001	17.16
			B4/B1	-0.053	0.011	-0.076	-0.030	0.0002	27.33
			B5/B1	0.083	0.015	0.051	0.11	<0.0001	14.62
			B5/B4	0.015	0.0014	0.012	0.018	<0.0001	2.4
			B6	-0.12	0.019	-0.16	-0.077	<0.0001	1.54
			B6/B5	0.0015	0.00020	0.0011	0.0019	<0.0001	4.56

Table 2.10. Best fitting multiple regression models for TSS, TN and TP using QAICc with a penalty constant p = 3

				Coefficient of predictor		Confidence Interval for mean of coefficient			
	R^2	Number of obs.	Predictor	Value	Std. Error	Lower 95%	Upper 95%	p	VIF
TSS	0.53	27	intercept	-2.98	2.0055	-7.11	1.15	0.1498	n/a
			B3/B1	7.52	1.41	4.61	10.43	<0.0001	1
TN	0.75	36	intercept	-0.22	0.16	-0.56	0.11	0.18	n/a
			B4	36.00	3.97	27.89	44.11	<0.0001	8.67
			B4/B2	-1.83	0.21	-2.27	-1.40	<0.0001	13.41
			B5	-11.28	3.37	-18.16	-4.40	0.0022	1.45
			B6/B2	0.15	0.022	0.11	0.20	<0.0001	6.22
			B6/B3	-0.034	0.0078	-0.050	-0.018	0.0001	3.41
TP	0.95	23	intercept	-0.017	0.015	-0.049	0.015	0.27	n/a
			B2	-0.67	0.21	-1.11	-0.23	0.0052	3.53
			B4	2.40	0.33	1.70	3.10	<0.0001	17.16
			B4/B1	-0.053	0.011	-0.076	-0.030	0.0002	27.33
			B5/B1	0.083	0.015	0.051	0.11	<0.0001	14.62
			B5/B4	0.015	0.0014	0.012	0.018	<0.0001	2.4
			B6	-0.12	0.019	-0.16	-0.077	<0.0001	1.54
			B6/B5	0.0015	0.00020	0.0011	0.0019	<0.0001	4.56

Table 2.11. Best fitting multiple regression models for TSS, TN and TP using QAICc with a penalty constant p = 4 and p=5

				Coefficient of predictor		Confidence Interval for mean of coefficient			
	R^2	Number of obs.	Predictor	Value	Std. Error	Lower 95%	Upper 95%	p	VIF
TSS	0.53	27	intercept	-2.98	2.0055	-7.11	1.15	0.1498	n/a
			B3/B1	7.52	1.41	4.61	10.43	<0.0001	1
TN	0.75	36	intercept	-0.22	0.16	-0.56	0.11	0.18	n/a
			B4	36.00	3.97	27.89	44.11	<0.0001	8.67
			B4/B2	-1.83	0.21	-2.27	-1.40	<0.0001	13.41
			B5	-11.28	3.37	-18.16	-4.40	0.0022	1.45
			B6/B2	0.15	0.022	0.11	0.20	<0.0001	6.22
			B6/B3	-0.034	0.0078	-0.050	-0.018	0.0001	3.41
TP	0.69	23	intercept	-0.010	0.0072	-0.025	0.0045	0.16	n/a
			B4/B2	0.031	0.0093	0.011	0.050	0.0036	1.32
			B5/B4	0.015	0.0022	0.010	0.019	<0.0001	1.32

Table 2.12. Best fitting multiple regression models for TSS, TN and TP using QAICc with a penalty constant p = 6

				Coefficient of predictor		Confidence Interval for mean of coefficient			
	R^2	Number of obs.	Predictor	Value	Std. Error	Lower 95%	Upper 95%	p	VIF
TSS	0.53	27	intercept	-2.98	2.0055	-7.11	1.15	0.1498	n/a
			B3/B1	7.52	1.41	4.61	10.43	<0.0001	1
TN	0.52	36	intercept	-0.066	0.22	-0.52	0.39	0.77	n/a
			B5/B3	-0.44	0.14	-0.73	-0.15	0.0039	1.004
			B6	1.83	0.37	1.072	2.58	<0.0001	1.004
TP	0.69	23	intercept	-0.010	0.0072	-0.025	0.0045	0.16	n/a
			B4/B2	0.031	0.0093	0.011	0.050	0.0036	1.32
			B5/B4	0.015	0.0022	0.010	0.019	<0.0001	1.32

Table 2.13. Best fitting multiple regression models for TSS, TN and TP using QAICc with a penalty constant p = 7

				Coefficient of predictor		Confidence Interval for mean of coefficient			
	R^2	Number of obs.	Predictor	Value	Std. Error	Lower 95%	Upper 95%	p	VIF
TSS	0.53	27	intercept	-2.98	2.0055	-7.11	1.15	0.1498	n/a
			B3/B1	7.52	1.41	4.61	10.43	<0.0001	1
TN	0.52	36	intercept	-0.066	0.22	-0.52	0.39	0.77	n/a
			B5/B3	-0.44	0.14	-0.73	-0.15	0.0039	1.004
			B6	1.83	0.37	1.072	2.58	<0.0001	1.004
TP	0.52	23	intercept	0.010	0.0043	0.0013	0.019	0.027	n/a
			B5/B4	0.011	0.0023	0.0063	0.016	0.0001	1

A comparison of models derived from different p is given in Table 2.14 based on the highest VIF in the model and model accuracy (R-squared). Based on Table 2.14, the best model for TSS from QAICc was kept the same for all penalty constants. The models for TN and TP both became acceptable when p equaled to 6 because the cut-off criterion of VIF is 10. One additional trial was performed to see what the results turn to be after p=6. Any result with a VIF > 10 is not accepted.

Table 2.14. Comparison of statistical equations selected by QAICc with different penalty constants

Penalty constant p	TSS		TN		TP	
	R^2	Highest VIF	R^2	Highest VIF	R^2	Highest VIF
2	0.53	1	0.82	62.55	0.95	27.33
3	0.53	1	0.75	13.41	0.95	27.33
4	0.53	1	0.75	13.41	0.69	1.32
5	0.53	1	0.75	13.41	0.69	1.32
6	0.53	1	0.52	1.004	0.69	1.32
7	0.53	1	0.52	1.004	0.52	1

The best models chosen by QAICc (Table 2.12) and by forward selection (Table 2.8) are then compared as shown in Table 2.15. VIF in Table 2.15 are all lower than 10, which is the commonly accepted criterion. After the criterion of VIF is accepted, the model accuracy (R-squared) is compared. From Table 2.15, it showed that the accuracy

is higher for models derived from forward selection (Table 2.8). The TSS models derived from QAICc and forward selection are identical.

Table 2.15. Comparison of best models from QAICc and forward selection

	TSS		TN		TP	
	R^2	Highest VIF	R^2	Highest VIF	R^2	Highest VIF
Table 2.12 (QAICc)	0.53	1	0.52	1.004	0.69	1.32
Table 2.8 (forward selection)	0.53	1	0.59	1.1	0.76	2.20

The resulting equations are:

$$TSS = -2.98 + 7.52(B3/B1) \quad (2.7)$$

$$TN = -0.19 + 2.02(B6) - 0.5(B5/B3) + 0.057(B5/B4) \quad (2.8)$$

$$TP = -0.04 + 0.047(B4/B2) + 0.018(B5/B4) + .00052(B6/B5) \quad (2.9)$$

The band ratio of B3/B1 has been previously used by Kloiber et al.(2002) for predicting the Secchi disk transparency, which is related to TSS. For TN and TP, it was found that bands from the infrared frequency (bands 4 to 6) play a role because they make up all or part of the ration of all of the predictor variables. One USGS study (2004) concluded that infrared bands can be contributive in predicting chlorophyll-a concentration, which is related to the trophic condition of water, and in turn is related to nutrient level (i.e. TN and TP) in water. However, the USGS study used band 7 instead.

The observed vs. multiple regression predicted water quality coefficient concentrations for TSS, TN and TP are plotted in Figures 2.4, 2.5, and 2.6, respectively. The predictive equations for TSS has the lowest accuracy among all three water quality constituents, implying that for this particular waterbody, the correlation between suspended sediment and turbidity might not be high. For TP (Figure 2.6), the observed values from USGS seem to be clustered because the method used to measure TP has a minimum detection limit of 0.01 mg/L (Patton and Truitt, 1992).

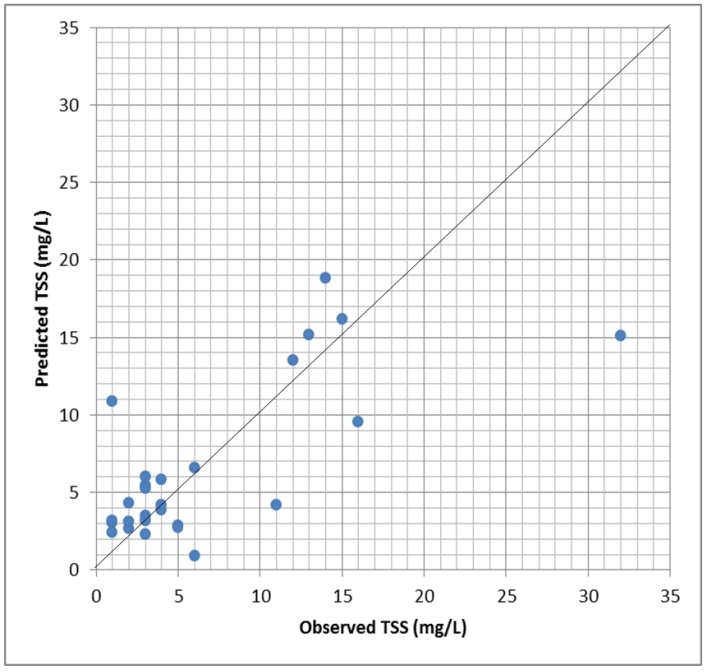

Figure 2.4. Observed vs. predicted values for TSS

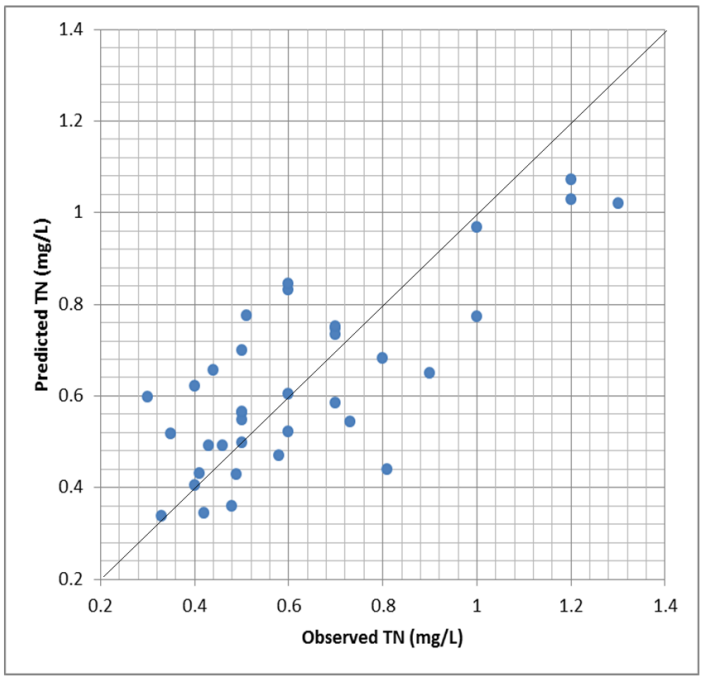

Figure 2.5. Observed vs. predicted values for TN

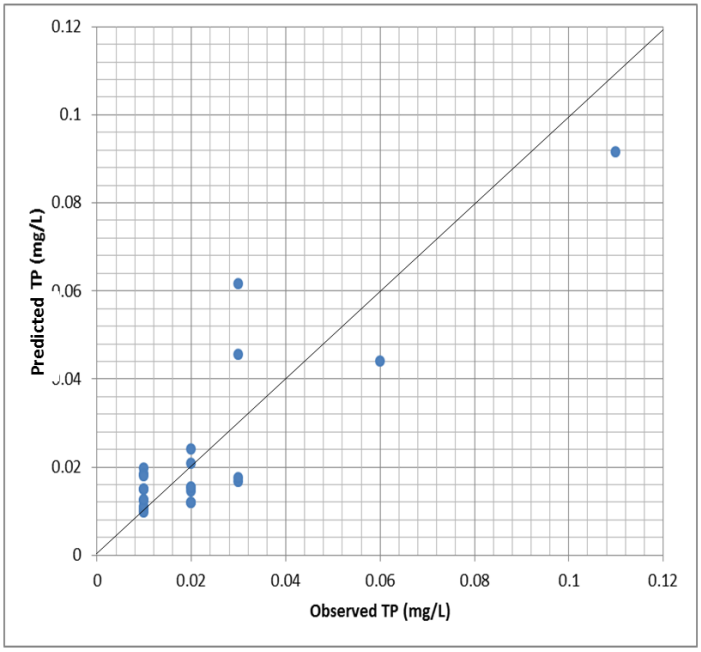

Figure 2.6. Observed vs. predicted values for TP

2.6. Discussion and Conclusion

Multiple regression derived equations using band reflectance as predictor variables to predict concentrations of each of the water quality constituents: TSS, TN, and TP were derived using forward selection based on p-value and QAICc. The coefficients of determination of the best fitting resulting equations varied from 0.53 to 0.76. TSS had the lowest coefficient of determination amount the three equations. Since the chosen predictive variable for TSS (i.e. B3/B1) was also chosen by a study in literature for Secchi disc transparency (Kloiber et al., 2002), such coincidence showed that the predictive equation for TSS of this study actually measures transparency. The

low accuracy for TSS predictive equation may indicate a weak correlation between suspended sediment and turbidity in this particular waterbody. Infrared bands (bands 4 to 6 of Landsat TM/ETM+) were found to play a crucial role in detecting nutrients (N and P) in water.

To show the importance of water quality monitoring by satellites, water quality in Lady Bird Lake from two dates (Table 2.16) was estimated using Equations 2.7, 2.8 and 2.9. Both dates are in summer 2013. Both dates were preceded by a major precipitation event four days earlier, but the magnitude and distribution of these precipitation events were different. Figures 2.7, 2.8, and 2.9 show that even though both dates are in the summer of the same year, moderate differences in precipitation patterns can have profound impacts on water quality distribution in the Lake.

The precipitation event prior to May 3 showed a slightly deteriorating trend of water quality from upstream to downstream locations. The water quality in the northwestern corner part of the lake is generally better than that in the southeastern corner. This trend is more visible for TSS (Figure 2.7) and TN (Figure 2.8). Also note that the May 3 event has a "hotspot" in TN (marked in Figure 2.8), which is the confluence of Eanes Creek and Lady Bird Lake. Eanes Creek is a bacteria impaired waterbody according to section 303(d) of the Clean Water Act (U.S. EPA, 2014f). The precipitation event prior to September 24 has a much less predictable distribution pattern compared to the event of May 3. Such spatial resolution in observations can only be achieved via satellite-derived water quality predictions.

Table 2.16. Data describing events related to water quality predictions made using data from satellites and multiple regression analysis

Date	Prior event precipitation(mm)	Precipitation distribution	Ground temp. of image (^{o}C)	FLAASH model used
May 3, 2013	48.0	Isolated	16	U.S. Standard
Sep. 24, 2013	74.2	Uniform	32	Tropical

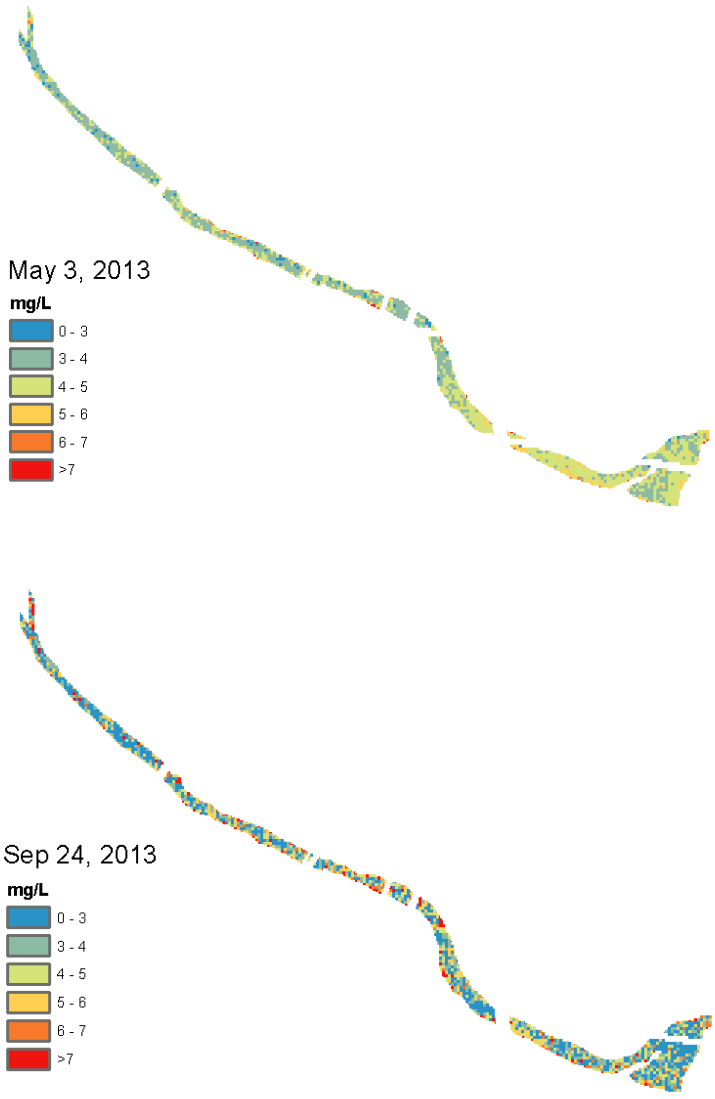

Figure 2.7. TSS concentrations for May 3 and September 24, 2013 in Lady Bird Lake, Austin

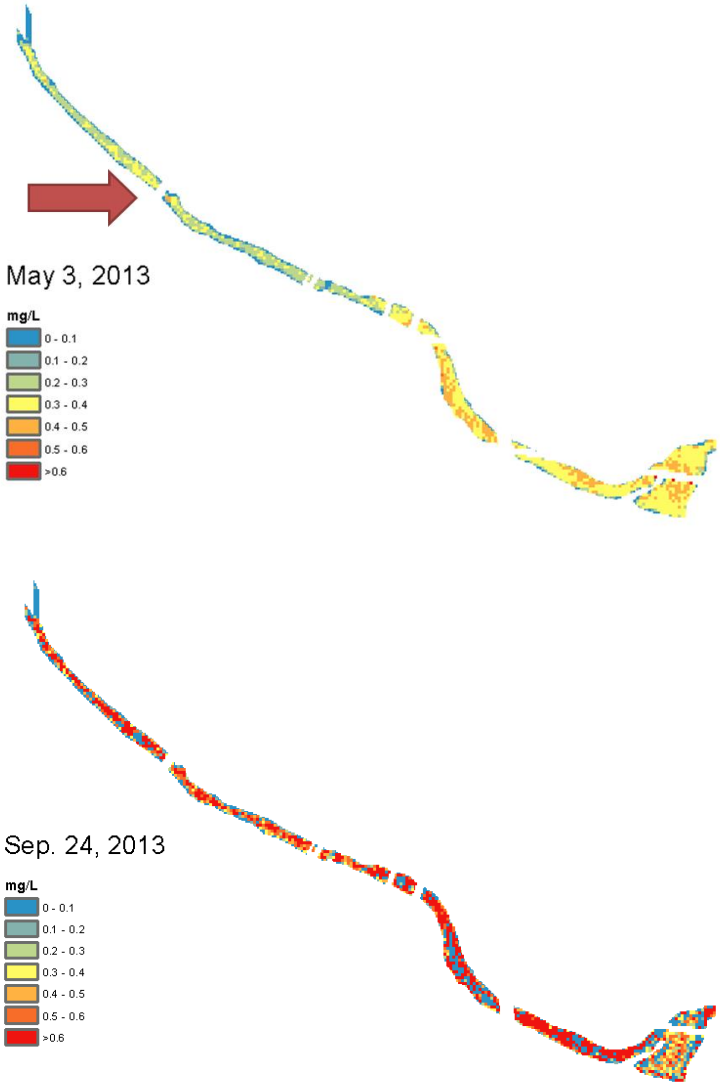

Figure 2.8. TN concentrations for May 3 and September 24, 2013 in Lady Bird Lake, Austin (A hotspot is indicated with the red arrow for the event of May 3)

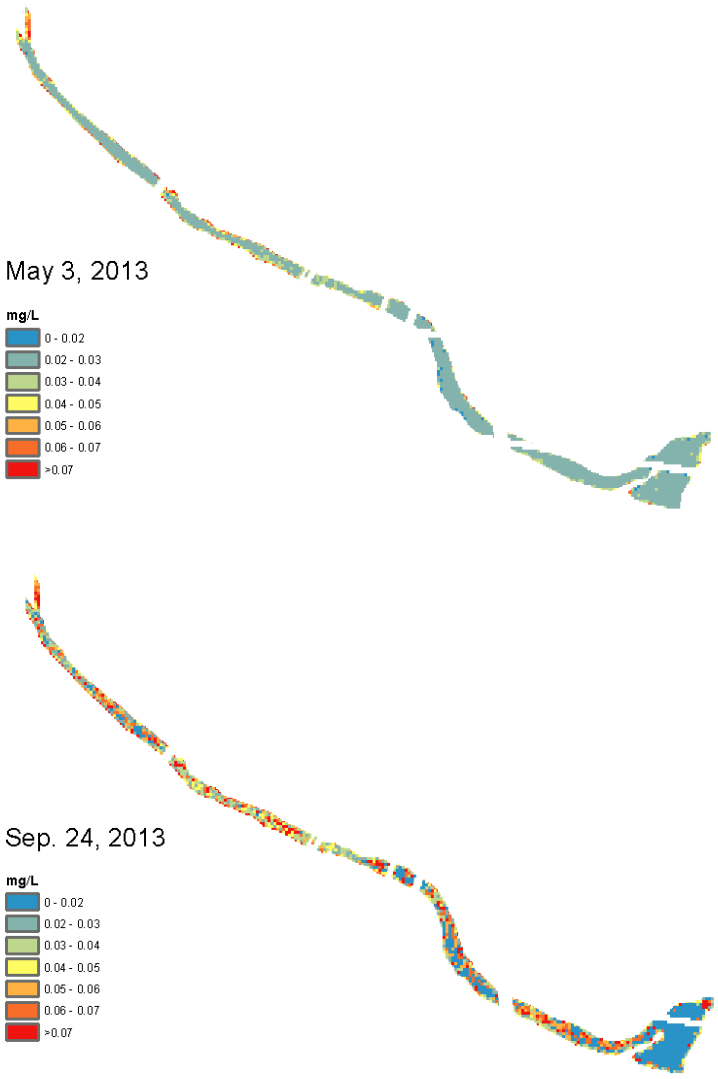

Figure 2.9. TP concentrations May 3 and September 24, 2013 in Lady Bird Lake, Austin

Finally, the following suggestions for future research to improve the accuracy of prediction of water quality using satellites are made:

1. Derive relationships for individual season or month by increasing the temporal resolution of field measurements so it is possible to account for seasonal influence in prediction (McCullough, 2012);

2. For satellite images collected in the 21th century, the available products of atmospheric water content (NASA, 2013a; NOAA, 2013) have good temporal resolution and should be utilized to improve the removal efficiency of atmospheric correction modules;

3. Utilize satellites with cirrus bands (such as Landsat 8) to eliminate the possible influence from thin cirrus cloud that can escape the scrutiny of the naked eye (NASA, 2013b). Bands from Landsat 8 have different wavelength ranges than those used in this study (USGS, 2013c) so results from this study are not applicable to those bands. An additional study is needed to create equations for Landsat 8; and

4. Wind speed and direction can be taken into consideration when comparing scenes for water quality because reflectance can be affected by surface ripples (Doxaran et al., 2002).

CHAPTER III

DETERMINING POLLUTANT BUILDUP AND WASHOFF PARAMETERS FOR SWMM BASED ON LAND USE IN A TEXAS WATERSHED

3.1. Overview

Pollutant buildup and washoff parameters for exponential buildup and washoff equations in SWMM (Storm Water Management Model) were determined for Austin, TX in early 1980s. Early 1980s was chosen in order to examine the native land characteristics before building of BMP (Best Management Practice) became prominent after 1990. 32 parameters were investigated, with 4 parameters for each land use, and 8 land uses under consideration. The built-in exponential buildup and washoff equations in SWMM were used to calibrate the parameters. Land use in early 1980s was created from aerial photography from 1984 and 2006, and GIS land use data from 2006. SWMM was calibrated first for hydraulic parameters and then for pollutant parameters. Parameters for three types of pollutants: TSS (total suspended solids), TN (total nitrogen), and TP (total phosphorus) are calculated. Calibration was performed automatically using SCEUA (Shuffled Complex Evolution – University of Arizona). Confidence intervals of the SCEUA algorithm were calculated and multiple trials with different random seeds were performed in order to get the numerical distribution of 32 buildup and washoff parameters used in the SWMM model. The buildup parameters are clustered in narrow numerical ranges, implying that spatially uniform factors are responsible for pollutant buildup. Washoff parameters did not cluster and are distributed

more evenly, implying a heavier influence of local factors such as topography. Several land uses (bare soil, industrial, single family, and undeveloped) were identified as major sources of non-point source pollution. However, some areas of bare soil may have been wrongly classified as industrial so the parameters for industrial land use might be biased. It is recommended for similar studies in the future watersheds not under rapid transition (less constructions sites and bare soil areas) be used to prevent this problem.

3.2. Introduction

The impact of urban stormwater on water resources, human health, and natural habitats is a major issue in managing urban watersheds (Al Bakri et al., 2008). In cities, the dense population creates ample sources of pollution, and large impermeable surfaces allow pollutants to be washed into nearby water bodies effectively without treatment. Research has focused on the effect of different land use types on the delivery of pollutants to urban streams resulting from the varying densities and types of human activities that occur on these different land uses. The National Urban Runoff Program (NURP) is one of the first programs to determine such differences using field measurements (Urbonas and Stahre, 1993; U.S. EPA, 1983). The NURP concluded that no statistically significant differences exist in pollutant-providing capabilities between different land uses in the U.S. NURP's conclusions were generalized for the entire U.S. but other smaller scale studies based on either event mean concentrations (EMC) (Park et al., 2009) or linear buildup rates from urban surfaces (Wicke et al., 2012; Wang and Li, 2009; Huber and Dickinson, 1988) arrived at different conclusions. For those small-

scale studies, different land uses did generate runoff containing different pollutant concentrations.

SWMM was developed by the U.S. EPA in 1971 (Rossman, 2010), and has been extensively used for diverse purposes. It has been used to simulate flooding in urban areas (Hsu et al., 2000), to evaluate the hydrologic impact from proposed urban developments (Jang et al., 2007), and has been suggested for both TMDL (Total Maximum Daily Load) evaluation (Borah et al., 2006) and for management of urban watersheds (Lee et al., 2010). The popularity of Storm Water Management Model (SWMM) for use in water resources management over the past several decades (Rossman, 2010) has made determination of the parameters for pollutant buildup and washoff equations an important task. The differences in pollutant buildup and washoff for different land uses is important for utilizing the full potential of the (SWMM). SWMM allows the user to choose from several equations to calculate pollutant buildup and washoff.

Three buildup equations (power, exponential, and saturation) and three washoff equations (exponential, rating curve, and event mean concentration) are provided in SWMM (Rossman, 2010). Parameters of exponential buildup and exponential washoff equations are more frequently reported in literature. Therefore, this study considered only parameters of the exponential buildup (Equation 3.1) and washoff (Equation 3.2) equations to address this trend. The equations are:

$$Buildup = C_1 \cdot (1 - \exp(-C_2 \cdot t)) \tag{3.1}$$

$$Washoff = C_3 \cdot Runoff^{C_4} \cdot Buildup' \tag{3.2}$$

In Equation 3.1, the buildup term on the left hand side is the pollutant buildup in mass per unit area or unit curb length, and t on the right hand side is the number of preceding dry weather days. In Equation 3.2, the washoff term on the lefthand side is the washoff load in the unit of mass per hour, the runoff term on the righthand side is runoff rate per unit area (inches/hour or mm/hour), and *Buildup'* is the pollutant buildup in units of total mass. C_1 is the maximum buildup possible (mass per unit area or unit curb length), C_2 is the buildup rate constant controlling the speed of pollutant buildup (1/days), C_3 is the washoff coefficient, and C_4 is the washoff exponent (Rossman, 2010). The unit of C_3 depends on the value of C_4 (unitless). When C_4 is equal to 1, the unit of C_3 is 1/mm or 1/inch.

In the literature, researchers have resorted to either computer modeling or small-scale field measurements in order to determine parameters C_1-C_4. Some of these efforts have been summarized in Table 3.1.

Table 3.1. Parameters for exponential buildup and washoff equations in SWMM from past research

Study	Location	Land use	Pollutant	C_1	C_2	C_3	C_4
Chow et al., 2012	Malaysia	Residential	TSS	0.003 (kg/m curb)	0.8	0.2	1.4
			TP	0.003 (kg/m curb)	0.05	0.41	1.46
		Commercial	TSS	0.015 (kg/m curb)	0.8	1.4	0.9
			TP	0.0005 (kg/m curb)	0.1	0.4	1
		Industrial	TSS	0.013 (kg/m curb)	0.7	3	0.6
			TP	0.0003 (kg/m curb)	0.16	0.8	1.08
Wicke et al., 2012	New Zealand	Urban	TSS (concrete)	27.6 (kg/ha)	0.2	0.24	1
			TSS (asphalt)	13.4 (kg/ha)	0.23	0.27	1
Hossain et al, 2010	Australia	Urban	TSS (road, G)	53 (kg/ha)	0.222	0.0029-0.0135	0.608-0.986
			TSS (road, L)	27.5 (kg/ha)	0.21	0.0015-0.0059	0.945-1.27
			TSS (road, P)	26 (kg/ha)	0.382	0.0062-0.011	0.753-0.914
			TSS (roof, CT)	8.5 (kg/ha)	0.188	0.051-0.202	0.363-0.603
			TSS (roof, CS)	12 (kg/ha)	0.122	0.112-0.213	0.333-0.414

Table 3.1. Continued

Study	Location	Land use	Pollutant	C_1	C_2	C_3	C_4
Hood et al., 2007	Estonia	Urban	TSS*	25 (kg/ha)	1	4.9	1.57
			TN*	0.15 (kg/ha)	0.0015	250	1
			TP*	0.25 (kg/ha)	0.0025	500	2.35
Temprano et al., 2006	Spain	Residential	TSS	0.046 (kg/m curb)	0.3	1.811	1
			TSS	17.5 (kg/ha)	0.3	1.811	1
			COD	0.0027 (kg/m curb)	0.3	3.937	1
			COD	1.02 (kg/ha)	0.3	3.937	1
			TN	0.0001 (kg/m curb)	0.3	8.661	1
			TN	0.039 (kg/ha)	0.3	8.661	1
Barco et al., 2004	Italy	Residential	TSS	18 (kg/ha impervious)	0.3	0.13	1.2

* Unit not given. Presumed to be kg/ha because of its numerical range.

It can be seen in Table 3.1 that the buildup and washoff parameters vary significantly from one location to another, probably due to the difference in environment of each study. There have been no similar studies conducted in Texas. The research presented here will fill this void by investigating the buildup and washoff parameters for total suspended solid (TSS), total nitrogen (TN), and total phosphorus (TP) in a watershed in Austin, Texas. TSS is chosen because it is one of the most commonly measured water quality constituents (USGS, 2014b). Suspended solid load is also responsible for all contaminants of water other than dissolved gases (Tchobanoglous and Schroeder, 1985). TN and TP were selected not only because they are representative nutrients, but also because many states have developed water quality criteria related to them (U.S. EPA, 2014c). In addition, these three water quality constituents are the most frequently reported by USGS thus were chosen by this study.

The phenomenon of "first flush" (i.e. the increase in pollutant concentration in the beginning of a runoff event) was not considered in this study because first flush has been known as a complex process. Its definition and detection has been under debate (Bach et al, 2010). Even though first flush was present at the end of a drainage system, a reliable relation to the pollution input to the drainage system was not found (O'Connor et al., 1999). Therefore, many studies in the literature (such as the ones in Table 3.1) did not consider first flush in their modeling process.

Use of Best Management Practices (BMP), such as stormwater retention ponds, has become prevalent in recent decades (Urbonas and Stahre, 1993). Since 1990, cities in the U.S, have been required to install BMPs as part of their stormwater management

programs under the direction of NPRS (Debo and Reece, 2003). BMPs mitigate stormwater quality, but can also interfere with our determination of pollutant buildup and washoff. This research uses land use determined for the early 1980's in Austin, TX to study the pollutant buildup and washoff parameters for the SWMM model without the interference of BMPs. Land use will first be determined from aerial photographs in 1984. Then SWMM will be calibrated and validated for hydrology followed by calibration of the pollutant buildup and washoff.

3.3. Research Area

As of 2012, the city of Austin, TX had over 7000 BMPs registered in the greater Austin area, up from just over 100 in the early 1980s (City of Austin, 2014b). Unfortunately, land use data prior to 1980 was not available. Nevertheless, the city of Austin kept a detailed record of aerial photographs from March, 1984 (City of Austin, 2014b). In this research, land use data of 1984 is extrapolated primarily from these aerial photographs. To simplify the calculations and test the concept, a subwatershed from the city of Austin was used in this analysis. The Walnut Creek Watershed at Webberville Rd lies in the eastern part of the city with a total area of 13,287 hectares. The elevation change throughout the landscape is gentle, ranging from 285 meters in the north to 132 meters in the south. Most soil types in the watershed are clayey as delineated in the Web Soil Survey (NRCS, 2013).

The climate of Austin is humid subtropical with hot summers and mild winters. It seldom snows in winter. Austin has a bimodal distribution of precipitation, with the

highest monthly rainfall amounts occurring in May and October. Average annual precipitation is around 84 cm (NWS, 2014a). Since stratiform systems are not common in Texas, slow-moving and widespread rainfall is rare in this area. Instead, thunderstorms triggered by the interaction between moist air from the Gulf of Mexico and the dry air from the Rocky Mountains are the main source of precipitation (Norwine et al., 2005). Rainfall from thunderstorms exceeding 13 cm/hr is not uncommon during summer months. The additional tendency to create large amounts of runoff on the thin soil of the Hill Country results in flash flooding as a problem in this area (Texas State Historical Association, 2014; NWS, 2014a)

3.4. Methodology

3.4.1. Data Availability

The sources of the data used in this research are summarized in Table 3.2. The only data source that is not provided in Table 3.2 is land use data, which will be discussed separately. The land use data is based on data from March 1984 for two reasons: 1) the only aerial photos available for the whole watershed is from 1984, and 2) building of BMP (Best Management Practice) was not prominent in 1980s so it is possible to examine the native pollutant buildup / washoff parameters by using data from early 1980s.

In 1980s, this watershed was under rapid development. Land use is supposedly to change significantly from year to year. Even though this watershed has precipitation and runoff data much earlier than 1980s, data from a short period of time (1982-1985)

was used in this study as a compromise between the length of observation data and the accuracy of land use data.

Table 3.2. Data used in the current research

Data	Data date	Format	Source
Elevation	n/a	10-m DEM raster	(USGS, 2014a)
Imperviousness	2001	30-m raster	(MRLC, 2014)
Land use	1984	GIS shape file	Derived in the research
Sewer network	2012	GIS database	(City of Austin, 2012)
River network	n/a	GIS shape file	(USGS, 2014a)
Channel cross-section	1982-1985	Field survey	(USGS, 2014b)
Precipitation	1982-1985	Hourly record	(NCDC, 2014)
Runoff	1982-1985	Daily record	(USGS, 2014b)

3.4.2. Land Use Determination

Land use from 1984 required special attention because no land use data was available for Austin in the early 1980s. Land use in 1984 was therefore derived from three sources: aerial photography from 2006, aerial photography from 1984, and GIS land use data from 2006 (City of Austin, 2014b). Figure 3.1 contains a simple flow chart illustrating the process of land use determination. The process was done piece-wise until the whole watershed was accounted for.

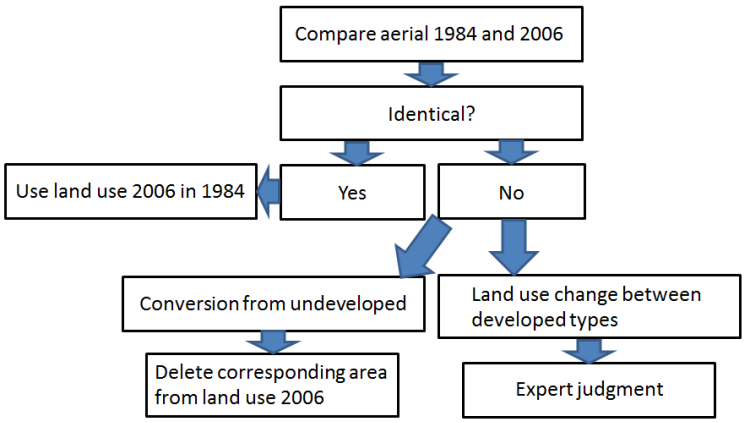

Figure 3.1. Flow chart of land use determination used in this study

First, aerial photographs from 1984 and 2006 were spatially registered and visually compared for each city block. When a difference was found between the photographs, correction was done to the land use image from 2006 to reflect the land use in 1984. The differences were categorized into two types: 1) undeveloped land which was developed (urban expansion), and 2) rezoning or rebuilding of lots. The first type, which is the most common, was easier to handle by simply converting the new urban area to undeveloped land use of 2006 to get the land use of 1984. The second type was more difficult to deal with since rezoning and construction records were not available from 1984. For the second type of correction, determination of land uses from the aerial photography of 1984 was based on subjective determination of similarity to other parts of the 1984 image where land uses had been determined. The 1984 land use distribution of the Walnut Creek Watershed at Webberville Rd is shown in Figure 3.2 and Table 3.3.

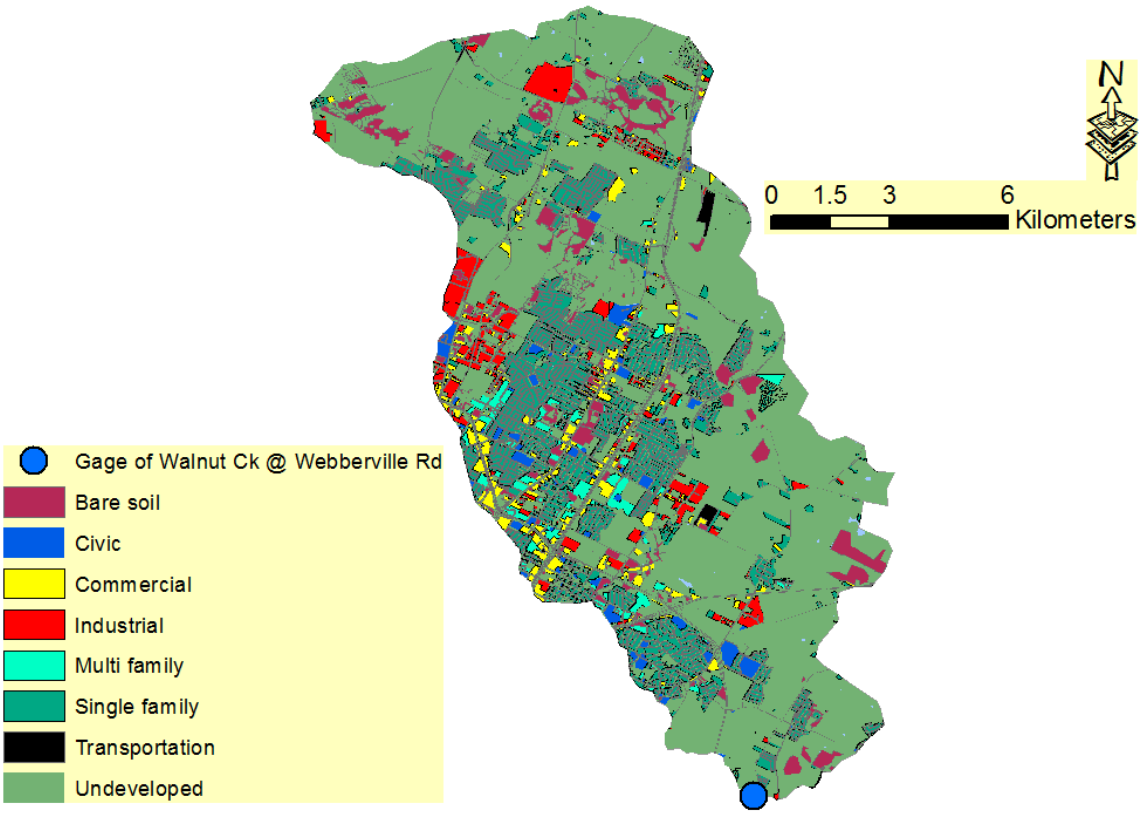

Figure 3.2. Land use distribution in the Walnut Creek Watershed at Webberville Road in 1984 derived from aerial photography and 2006 land use

Table 3.3. Proportions of each land use in the Walnut Creek Watershed

Land use	Area (ha)	% of Total Area
Single family	2181	16.9
Multi-family	310	2.4
Civic	237	1.8
Commercial	472	3.7
Industrial	540	4.2
Transportation	780	6.0
Bare soil	728	5.6
Undeveloped (with water)	7648	59.3
Total	12896	100

3.4.3. Stormwater Management Model (SWMM)

SWMM simulates the quantity and quality of surface water by separating the water cycle into the land surface compartment, the atmosphere compartment, the groundwater compartment, and the transport compartment (Rossman, 2010). The watershed is divided into a number of subcatchments in the land surface compartment based on user-provided watershed delineation for each subcatchment. The atmosphere compartment simulates the distribution of rainfall by a number of rain gages. The values of rainfall at each rain gage are provided by the user. Each subcatchment in the land surface compartment receives rainfall from only one rain gage in the atmosphere compartment (Rossman, 2010).

The land surface compartment calculates surface runoff (inch or mm) by Equation 3.3 as:

$$Runoff = Rainfall - Evaporation - Infiltration \quad (3.3)$$

Evaporation can be a user input or can be calculated by SWMM from daily temperatures. After evaporation is accounted for, infiltration on the pervious part of a subcatchment is calculated by one of the three methods: 1) Horton's equation, 2) Green-Ampt equation, or 3) mass balance using runoff calculated by the Curve Number equation (Huber and Dickinson, 1988). Horton's equation assumes that the infiltration rate decreases as more water enters the soil column by following a relationship of exponential decay. Green-Ampt equation assumes that infiltration is driven by the soil pore suction force and the weight of the infiltrated water column. The Curve Number method is an empirical equation for calculating daily runoff depth. In this study, Horton's equation was used because it allows calculation of sub-daily runoff, and requires fewer parameters than Green-Ampt equation. The Curve Number equation is not considered because it does not allow sub-daily calculation of runoff.

The groundwater compartment separates soil into the unsaturated zone and the saturated zone (i.e. groundwater aquifer). If the groundwater compartment is activated, infiltrated water enters the unsaturated zone of groundwater compartment. The hydrologic connection between the unsaturated saturated zones is calculated using Darcy's Law (Huber and Dickinson, 1988). Darcy's Law is the general rule governing the flow rate in porous media. Flow rate is proportional to the hydraulic conductivity of the media and pressure drop per unit length. If the elevation of saturated zone (i.e. water table) is higher than that of the surface water, the groundwater aquifer can connect with the surface water to provide baseflow, and *vice versa* (Rossman, 2010).

The transport compartment simulates water flow in all conveyance elements (channels, pipes, pumps, regulators, etc.) and storage/treatment devices by link and node objects. Runoff from a subcatchment in the land surface compartment and baseflow from the groundwater compartment enters the corresponding node object in the conveyance network. SWMM provides three options in simulating flow routing (i.e. calculating resultant hydrographs affected by the channel network) in the network: steady flow, kinematic wave, and dynamic wave routing. Steady flow routing is "no routing", which transfers the upstream hydrographs to downstream without changing the hydrographs. It is only suitable in preliminary analysis (Rossman, 2010). Kinematic routing considers only the effect of conduit friction in St. Venant equations and omits inertial and pressure forces and backwater effects. Kinematic routing usually allows moderately large computational time steps in the order of several to more than ten minutes due to its simplicity. Dynamic routing, on the other way, considers all components in the St. Venant equations and is the most realistic routing method. However, it allows only small computational time steps in the order of seconds (Rossman, 2010). Conduit friction is calculated by Manning's equation in most cases. Under pressurized flow, the Hazen-Williams or Darcy-Weisbach equations are used (Rossman, 2010). Quality routing through the conduit network assumes all conduit elements act like a continuous stirring tank reactor (CSTR), which means the pollutant is instantly mixed uniformly in a conduit element (Rossman, 2010).

3.4.4. Model Construction

The building of the SWMM model for this project occurred in two phases. Data

was prepared on an ESRI ArcGIS platform and then used as input to SWMM for simulation. In other words, a loose-coupling technique was used between GIS and SWMM.

On the GIS platform, using the 2012 stormwater sewer network from the city of Austin, all stormwater sewers installed after March, 1984 were deleted. For the remaining manholes, inlets, and junction points, initially all of them were considered in creating subcatchments for the model. Then, only subcatchments larger than 2 ha and their associated manholes, inlets, and junction points were selected. The unselected subcatchments were merged into the selected subcatchments depending on whether they were nested watersheds. This procedure generated 168 subcatchments for use in SWMM simulation.

Ideally, SWMM simulation requires precipitation data with high temporal resolution. Unfortunately, NEXRAD weather radar was not operational until 1991. 15-min precipitation data from the surrounding weather stations covered only a small fraction of dates. For that reason, in this research, 1-hour precipitation data was used for SWMM. Five NCDC (National Climatic Data Center) weather stations (Granger Dam, Georgetown Lake, Spicewood, Red Rock, and Camp Mabry) close to the watershed were used (NCDC, 2014). In order to account for the spatial distribution of precipitation, twelve "rain gages" (as defined in the atmospheric component of SWMM) were created to cover the whole watershed. Precipitation at each rain gage is calculated by inverse distance weighting (IDW) from the four weather stations with a power parameter of two. Farther points dominate the interpolated value when the power

parameter is small. The coefficient of 2 was adopted because it is the most commonly used value in the literature (Lloyd, 2005; Ruelland, 2008).

The conduit network was manually created in SWMM with node objects determined from GIS to simplify the original stormwater sewer network. After the conduit network is created, subcatchment data was associated to corresponding node objects. To accelerate the modeling process (set-up and run time), stormwater sewers were simplified (Leitao et al., 2010). Several methods, including direct pruning/merging, storage node, and storage pipe, have been developed for this purpose (Fischer et al., 2009; Leitao et al., 2010). The storage node (or pipe) method simplifies the network by creating a node (or pipe) reservoir that has an identical storage volume to the pipes it will replace. The node reservoir was selected because direct pruning loses pipe storage and the storage pipe method is only suitable for very flat landscapes (Fischer et al., 2009). Dual conduits were constructed between a flooding node (node that receives more water than it can deliver, so the excess water becomes standing water above the node or is just lost, depending on the user's choice) and its immediate downstream node to mimic the flood plain or surface streets available to transport excess water.

In order to minimize the number of calibrated parameters, no groundwater component was simulated in the SWMM model used in this study. Instead, only direct runoff is simulated. Baseflow separation by the digital filter method (Lim et al., 2005; Eckhardt, 2005) using settings for porous aquifers was used on observed USGS daily flow data from the gage of Walnut Creek @ Webberville Rd (site number: 08158600)

so the simulated and observed data is comparable. The omission of the groundwater component is possible because the SWMM groundwater component does not simulate subsurface stormwater flow, which is the lateral water flow in the unsaturated zone of the soil. The SWMM groundwater component considers only the discharge of water from the saturated zone to the river, which by definition is baseflow. By removing the baseflow from the hydrographs, the system can be simulated using only direct runoff. The initial parameters subject to calibration and the range of allowable parameter values are listed in Tables 3.4 through 3.7. Table 3.4 provides flow-related parameters, and Tables 3.5 through 3.7 provide parameters related to TSS, TN and TP, respectively. The values for assumed conditions in Table 3.4 are from the SWMM User's Manual (Rossman, 2010). Note that SWMM has only one parameter to cover Manning's n for all channels and pipes. The initial values for open channels and closed pipes are chosen to be different and they all change by the same ratio during calibration.

There are no published ranges for pollutant-related parameters C1 to C4 in Tables 3.5 through 3.7. Since no reference is available, the buildup/washoff parameters C1 to C4 were assumed to be proportional to the measured event mean concentrations (EMC) in the NURP report (U.S. EPA, 1983). Precisely, the ratios of maximum value to mean value and the mean value to the minimum value for C1 to C4 were assumed to be identical to those of EMC reported from NURP for the water quality constituent of interest. The mean values of C1to C4 were derived from Table 3.1. If only one value is available for certain type of water quality constituent in Table 3.1, that value is assumed to be the mean value.

Table 3.4. Initial values for SWMM hydraulic-related parameters

Parameter	Initial value	Assumed conditions for initial values	Allowed range
Impervious percentage	Average for each subcatchment from the GIS data layer of imperviousness (MRLC, 2014)	Values derived from GIS layer	0-100
Subcatchment width	Calculated for each subcatchment from 10-m DEM (USGS, 2014a)	Values derived from GIS layer	n/a
Manning's n for impervious area	0.013	Ordinary concrete lining	0.011-0.024
Manning's n for pervious area	0.13	Natural range	0.05-0.40
Storage of impervious surface area	1.27 (mm)	Lower boundary for storage of impervious surface	1.27-2.54 (mm)
Storage of pervious surface area	5 (mm)	Pasture	2.54-7.62 (mm)
Percent of impervious area with no storage	25	Default value	0-100
Maximum infiltration rate	50 (mm/hr)	Dry clayey soil with good vegetation	25.4-152.4
Minimum infiltration rate	0.5 (mm/hr)	Saturated hydraulic conductivity of sandy/silty clay	0.254-10.922
Decay constant for Horton's infiltration equation	4 (1/hr)	Average of suggested range (2 to 7 hr^{-1})	2-7
Drying time	8 (days)	Average of suggested range (2 to 14 days)	2-14
Manning's n for open channels*	0.03	Chosen to cover several types of open channels, including vegetal lined, excavated, and fairly regular natural channels	0.011-0.14
Manning's n for closed pipes	0.013	Chosen to cover several types of pipes including concrete, cast iron, corrugated metal, and plastic	0.011-0.026

Table 3.5. Mean, maximum, and minimum values for buildup/washoff parameters of TSS

TSS (mg/L)	Area-based				Curb length-based			
	C_1 (kg/ha)	C_2 (1/day)	C_3 (hr^{C_4-1}/mm^{C_4})	C_4 (unitless)	C_1 (kg/meter curb)	C_2 (1/day)	C_3 (hr^{C_4-1}/mm^{C_4})	C_4 (unitless)
Mean	18.51	0.24	0.65	0.86	0.019	0.65	0.65	0.86
Maximum	481.29	6.22	16.77	22.44	0.5	16.9	16.77	22.44
Minimum	0.19	0.0024	0.0065	0.0086	0.00019	0.0065	0.0065	0.0086

Table 3.6. Mean, maximum, and minimum values for buildup/washoff parameters of TN

TN (mg/L)	Area-based				Curb length-based			
	C_1 (kg/ha)	C_2 (1/day)	C_3 (hr^{C_4-1}/mm^{C_4})	C_4 (unitless)	C_1 (kg/meter curb)	C_2 (1/day)	C_3 (hr^{C_4-1}/mm^{C_4})	C_4 (unitless)
Mean	0.039	0.3	8.66	1	0.0001	0.3	8.66	1
Maximum	0.39	3	86.61	10	0.001	3	86.61	10
Minimum	0.0027	0.021	0.61	0.07	0.000007	0.021	0.61	0.07

Table 3.7. Mean, maximum, and minimum values for buildup/washoff parameters of TP

TP (mg/L)	Area-based				Curb length-based			
	C_1 (kg/ha)	C_2 (1/day)	C_3 (hr^{C_4-1}/mm^{C_4})	C_4 (unitless)	C_1 (kg/meter curb)	C_2 (1/day)	C_3 (hr^{C_4-1}/mm^{C_4})	C_4 (unitless)
Mean	0.065	0.5	0.54	1.18	0.0038	0.10	0.54	1.18
Maximum	1.11	8.5	9.12	20.06	0.065	1.76	9.12	20.06
Minimum	0.002	0.015	0.016	0.035	0.00011	0.0031	0.016	0.035

A sensitivity analysis was performed to investigate the influence of all flow-related parameters to runoff. The total amount of runoff was monitored at the outlet of the watershed while the parameters were perturbed $\pm$25% and $\pm$50% relative to the initial values. Results of the sensitivity analysis of flow-related parameters are provided in Figures 3.3 and 3.4. To clearly represent the variation of all parameters, parameters with higher sensitivity were displayed in Figure 3.3, and parameters with less sensitivity are displayed in Figure 3.4. The sensitivity analysis showed that the top three parameters that significantly affect runoff are storage of pervious area, maximum infiltration rate and decay constant for Horton's equation. The maximum changes in runoff for those parameters are over 40% in the range of parameter perturbation. On the other hand, the least important parameters are Manning's n for impervious area, minimum infiltration rate, and percent of impervious area with no storage. All of them created only approximately less than 5% change in the range of parameter perturbation.

In SWMM, internal model error can be from two sources: runoff quantity continuity (the difference between precipitation and runoff leaving subcatchments) and flow routing continuity (the difference between water entering and leaving the conveyance network). Even though every trial in the parameter calibration process was not monitored (discussed later), the final calibrated model showed small values in both sources of error, at -0.124% (runoff quantity continuity) and 0.182% (flow routing continuity). Therefore, the error should generally be small in the parameter space where the parameters are calibrated from. The model should be continuously robust throughout the calibration process. Note that negative continuity error indicates that the output is more than input. All parameters in Figures 3.3 and 3.4 were used in the subsequent calibration process in order to achieve higher accuracy. The parameters of "Manning's n for impervious area" and "Storage of impervious area" fluctuate up and down a little bit during the sensitivity analysis but the magnitudes of variation are still less than the magnitude of continuity errors, so they were still included in calibration.

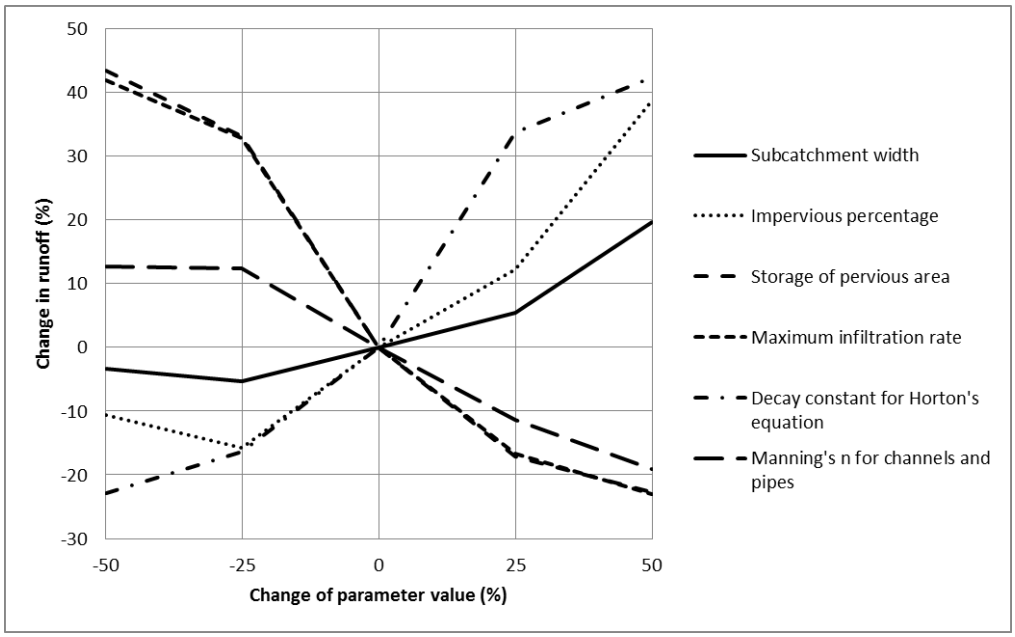

Figure 3.3. Sensitivity analysis for the six hydraulic parameters with higher sensitivities

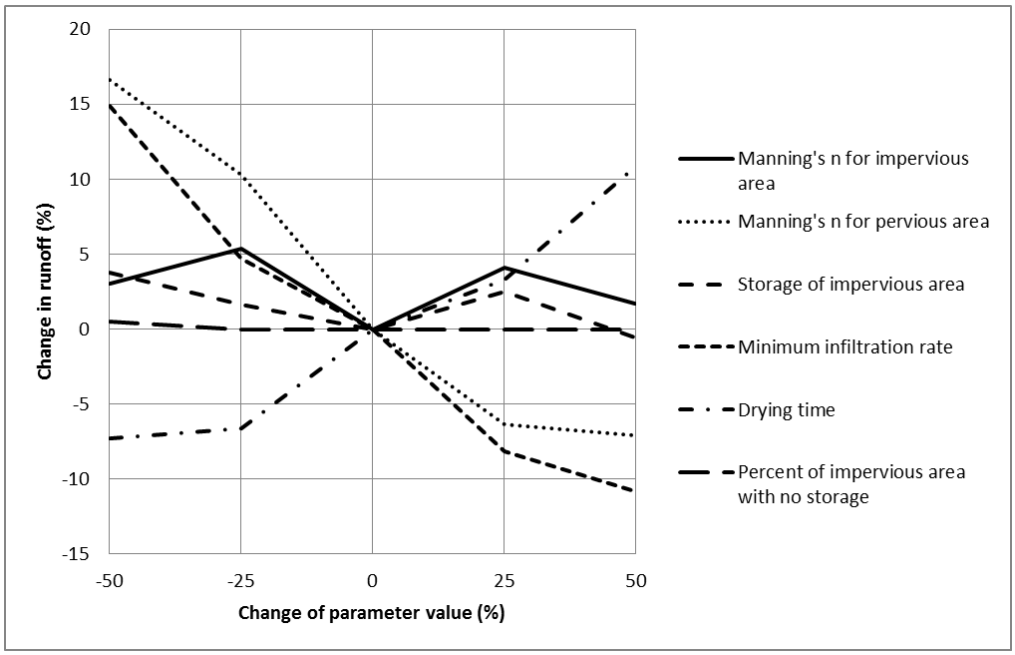

Figure 3.4. Sensitivity analysis for the six hydraulic parameters with lower sensitivities

3.4.5. Model Calibration and Validation

The observed runoff data at the USGS river gage of Walnut Creek at Webberville Road (site number: 08158600) has an average daily direct runoff around 0.3 cms. In order to minimize the impact of error from baseflow separation, relatively large events were chosen to calibrate the model. All events with daily average direct runoff larger than 0.6 cms were selected. Based on this criteria, a total of 36 events were selected between February 1983 and February 1985 (Table 3.8). These 36 events were further split into two groups, calibration and validation respectively, based on the magnitude and duration of events. The calibration and validation groups contain almost the same

distribution in event magnitude and event duration. When the parameters were calibrated, the output of the model was then compared to the events in the validation group in order to show that the calibrated parameters represent the behavior of the real system.

Table 3.8. Events used in calibrating and validating hydraulic related parameters in SWMM

Event beginning date	Duration (days)	Daily mean direct runoff (cms)	Group
March 4, 1983	1	1.755	Calibration
March 9, 1983	1	0.719	Validation
March 15, 1983	2	1.986	Validation
March 23, 1983	2	2.653	Calibration
March 26, 1983	1	4.084	Calibration
May 11, 1983	1	9.313	Validation
May 18, 1983	1	1.059	Validation
May 20, 1983	2	7.933	Validation
June 5, 1983	2	4.942	Calibration
June 14, 1983	1	1.036	Calibration
June 25, 1983	1	1.24	Validation
July 14, 1983	1	1.064	Calibration
July 16, 1983	1	1.823	Calibration
August 8, 1983	1	8.567	Calibration
August 19, 1983	1	5.898	Calibration
September 19, 1983	1	3.063	Validation
October 9, 1983	1	3.512	Calibration
November 4, 1983	2	1.455	Validation

Table 3.8. Continued

Event beginning date	Duration (days)	Daily mean direct runoff (cms)	Group
December 3, 1983	1	1.819	Validation
January 8, 1984	2	1.484	Calibration
March 23, 1984	1	0.839	Validation
July 24, 1984	1	4.374	Validation
September 3, 1984	1	1.085	Validation
October 7, 1984	1	5.362	Validation
October 9, 1984	3	6.212	Validation
October 13, 1984	2	11.59	Validation
October 20, 1984	2	24.12	Calibration
November 18, 1984	1	1.235	Calibration
November 24, 1984	2	2.506	Validation
December 5, 1984	1	0.726	Calibration
December 16, 1984	1	10.27	Calibration
December 31, 1984	1	3.852	Validation
January 16, 1985	1	1.541	Validation
February 10, 1985	2	1.311	Calibration
February 22, 1985	2	7.339	Calibration
February 28, 1985	1	2.34	Calibration

The model was calibrated using the Shuffled Complex Evolution – University of Arizona (SCEUA) module in the model-independent Parameter Estimation and Uncertainty Analysis (PEST) (Doherty, 2010). SCEUA starts with an initial random population of parameter sets. The population is divided into a number of complexes (or

"communities"), and each complex is evolved separately. Then the complexes are combined and the population with the lowest value of the objective function is dropped. Sum of square of the residuals was used as the objective function. This completes a loop and the algorithm enters the next loop by dividing the population into complexes again, as described above. The detailed algorithm is described by Duan et al. (1993).

Accuracy in calibration and validation was assessed using the Nash-Sutcliffe Efficiency (NSE) (Equation 3.4). NSE ranges from -∞ to 1, where a NSE of 1 indicates a perfect fit between measured and predicted values. Q_o^t represents observed flow rate at time t, Q_m^t represents modeled flow rate at time t, and $\overline{Q}_o$ represents the average of observed flow rates. Following calibration the hydraulic model had a NSE of 0.76 and the validation group had a NSE of 0.70. The NSE from calibration and validation are acceptable because the literature suggested NSE to exceed 0.5 (Moriasi et al., 2007). Plots of observed vs. modeled runoff at USGS gage Walnut Ck @ Webberville Rd are shown for calibration (Figure 3.5) and validation (Figure 3.6).

$$NSE = 1 - \frac{\sum_{t=1}^{T}(Q_o^t - Q_m^t)^2}{\sum_{t=1}^{T}(Q_o^t - \overline{Q}_o)^2} \quad (3.4)$$

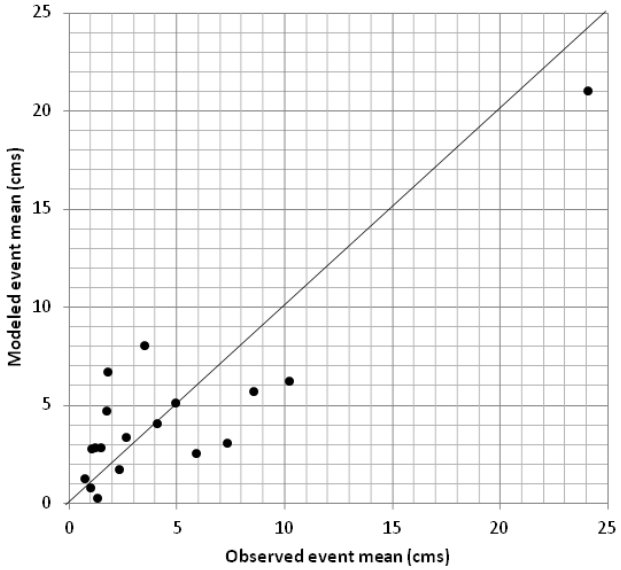

Figure 3.5. Observed and SWMM simulated event mean flow rate for the calibration group of events (NSE=0.76) at USGS Gage Walnut Creek at Webberville Road

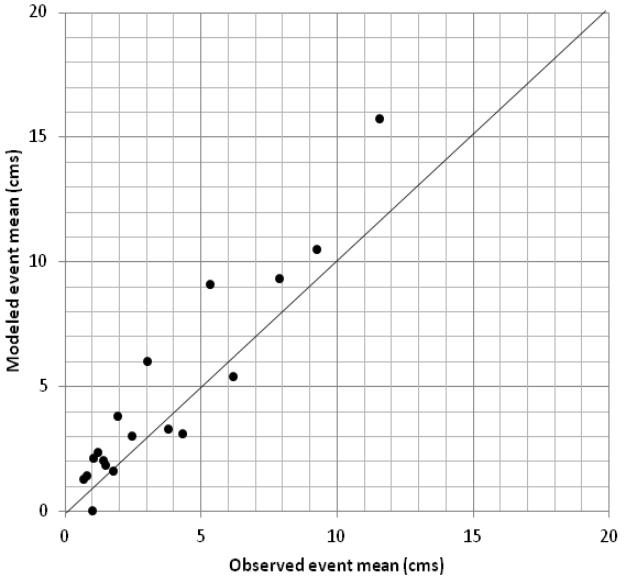

Figure 3.6. Observed and SWMM simulated event mean flow rate for the validation group of events (NSE=0.7) at USGS Gage Walnut Creek at Webberville Road

After flow-related parameters were calibrated and validated, parameters related to TSS, TP and TN were calibrated. In the hydrologic calibration, all twelve flow-related did not differ based on land use of the subcatchments. The pollutant-related parameters, however, were calibrated on a land use basis, i.e. each land use is calibrated independently. Pollutant-related parameters were calibrated based on field observations from two USGS river gages: Walnut Creed at Webberville Road (08158600) and Walnut Creek at Dessau Road (08158200).

The water quality samples contained both direct runoff and baseflow, so pollutant concentrations in baseflow were determined first and isolated from the sample

concentrations to determine the pollutant concentrations in direct runoff by Equation (3.5). In Equation (3.5), C_{dir} indicates the concentration of direct runoff, C_{mix} indicates the mixed concentration in measured runoff, C_{bf} indicates the concentration of base flow, and BFI is base flow index (proportion of baseflow in runoff). Pollutant concentrations in the direct runoff were used in the calibration. When BFI = 1 in Equation (3.5), the concentration in direct runoff has no meaning since no direct runoff exists.

$$C_{dir} = \frac{C_{mix} - C_{bf} \cdot BFI}{(1 - BFI)} \tag{3.5}$$

The baseflow concentrations were calculated by averaging the concentrations from baseflow dominated events ("baseflow dominant" was defined as BFI higher than 0.95 in this study). However, flow-related parameters were calibrated based on daily mean flow rate, which may not be accurate enough to predict the instantaneous flow rate at the time of field observations since the time to peak might be off. Therefore, six events were chosen for which the simulated instantaneous flow rate was close to the observed flow rate (Table 3.9). Events in Table 3.9 were chosen to have low BFI so the possible error in estimating concentration in base flow has lower influence in estimating concentration in direct runoff. Note that concentrations in Table 3.9 are calculated concentrations of direct runoff.

Table 3.9. Events used in water quality parameter calibration

Location	Date	BFI	Observed flow rate (cms)	Simulated flow rate (cms)	TSS (mg/L)	TN (mg/L)	TP (mg/L)
Webberville	10/20/1983	0.3	1.79	5.2	1203	1.88	2.23
Webberville	3/23/1984	0.21	2.79	6.56	1996	1.09	1.20
Webberville	7/24/1984	0.11	16.1	16.25	6976	7.31	4.92
Dessau	11/5/1983	0.19	8.51	8.50	2584	6.32	0.79
Dessau	6/6/1984	0.2	2.22	7.22	1570	2.24	0.48
Dessau	7/24/1984	0.11	13.83	7.17	3336	7.10	2.68

Based on events in Table 3.9, pollutant-related parameters were calibrated. Because of the low number of observations, all six events were used to calibrate and no validation was performed for the pollutant-related parameters. For each water quality constituent, two calibration runs were performed: one for area-based parameters and the other for curb-based parameters. It was noticed that for the watershed of interest, equations based on curb length exhibit significantly worse predictive power than those based on area except for the water quality constituent of TP. Table 3.10 shows a comparison of calibrated NSE for area-based and curb-based parameters. Figures 3.7 and 3.8 show the observed and simulated concentrations for TSS and TN based on area-based parameters, and Figure 3.9 shows the observed and simulated concentrations for TP based on curb length-based parameters. In following analyses in this study, area-based parameters were used for TSS and TN, and curb-length based parameters were used for TP.

Table 3.10. NSE for calibrated area-based vs. curb-based parameters

	TSS	TN	TP
Area-based	0.42	0.74	-0.54
Curb-based	-1.58	-1.73	0.90

The initial random seed in SCEUA affects the final calibration results, so the calibration was performed multiple times with different random seeds to capture the variance of calibrated parameters, discussed below. According to Moriasi et al. (2007) the NSE for TSS is lower than what is considered acceptable (0.5). However, NSE values reported for daily sediment calibration are generally low with few greater than 0.5 (Moriasi et al., 2007). The NSE values from the calibrations for TN and TP are both higher than those generally reported in the literature (Moriasi et al., 2007). Additionally, because the calibration of the water quality parameters in this study are based on instantaneous concentrations at the time of sampling, not daily mean concentrations, the results of the calibration are acceptable.

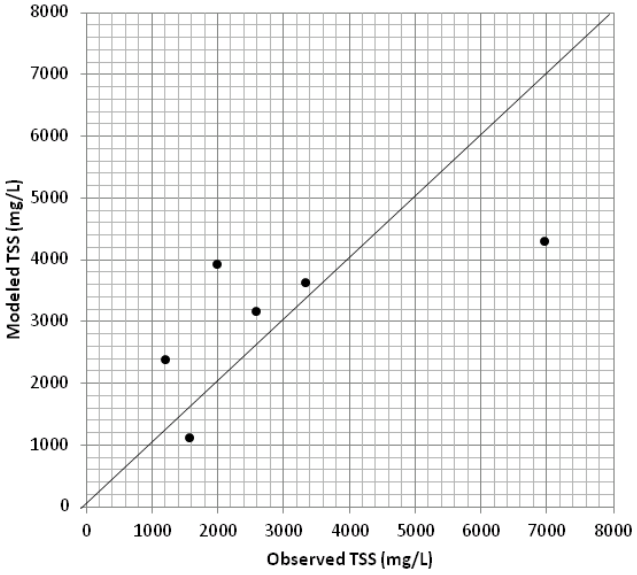

Figure 3.7. Observed and SWMM simulated TSS concentrations for calibrated pollutant-related parameters (NSE=0.42)

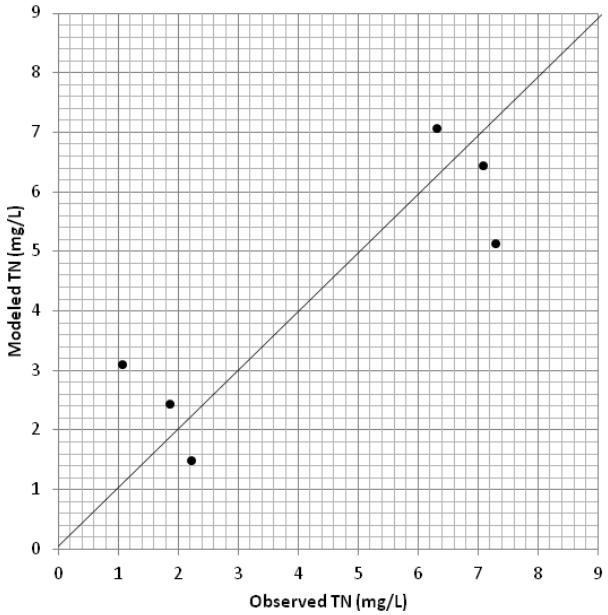

Figure 3.8. Observed and SWMM simulated TN concentrations for calibrated pollutant-related parameters (NSE=0.74)

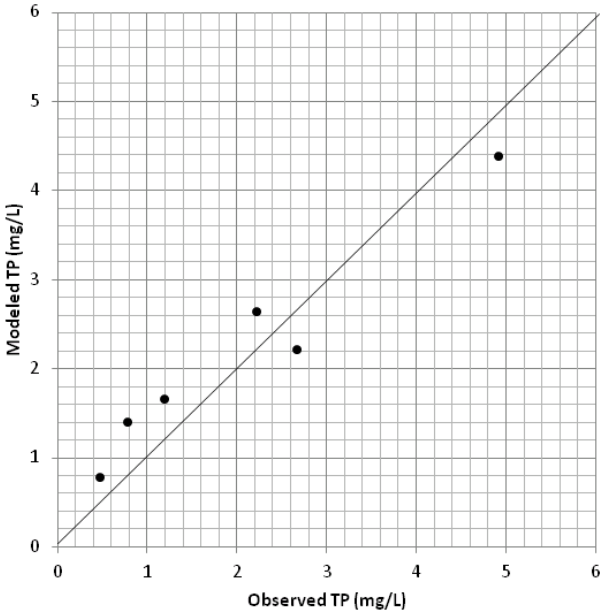

Figure 3.9. Observed and SWMM simulated TP concentrations for calibrated pollutant-related parameters (NSE=0.90)

3.5. Results

The resulting calibrated hydraulic parameters in Table 3.11 are lumped averages for the watershed. A few interesting results are observed. First, the imperviousness area for the watershed decreased from 2001 (original value) to 1984 (calibrated value), indicating that the watershed indeed had been under development. Second, the subcatchment width increased significantly after calibration, indicating that catchment width cannot simply be calculated by dividing the area by the longest path. The second observation indicates that the longest overland flow path increased from 1984 to 2001.

The increased length in overland flow path may indicate that there were less direct routes for overland runoff in 1984 i.e. less gullies and concentrated flow paths.

Table 3.11. Calibrated flow-related parameters

Parameter	Initial value (2001)	Calibrated value (1984)	Change
Impervious percentage	Varies by subcatchment	Varies by subcatchment	-10%
Subcatchment width	Varies by subcatchment	Varies by subcatchment	+246%
Manning's n for impervious area	0.013	0.016	+23%
Manning's n for pervious area	0.13	0.10	-23%
Storage of impervious surface area	1.27 (mm)	1.27 (mm)	n/a
Storage of pervious surface area	5 (mm)	7.62 (mm)	+52%
Percent of impervious area with no storage	25	17.58	-30%
Maximum infiltration rate	50 (mm/hr)	79.58 (mm/hr)	+59%
Minimum infiltration rate	0.5 (mm/hr)	0.66 (mm/hr)	+32%
Decay constant for Horton's infiltration equation	4 (1/hr)	2 (1/hr)	-50%
Drying time	8 (days)	14 (days)	+75%
Manning's n for open channels	0.03	0.031	+3%
Manning's n for closed pipes	0.013	0.026	+100%

The calibrated pollutant-related parameters are provided in Tables 3.12 through 3.14. With 4 parameters for each land use and a total of 8 land uses to be considered, there are a large number of parameters to be calibrated. Under these circumstances, the optimization algorithm does not always give a globally optimal solution possibly a result

of correlation between parameters (Doherty, 2012). After multiple runs of SCEUA, it was observed that some optimized solutions contained sets of parameters quite different from each other even though they resulted in almost identical values of the objective function. Therefore, confidence intervals of each parameter were calibrated rather than a single ”optimal” value for each parameter given the possibility there may be more than one optimal solution.

The method of computing confidence intervals for SCEUA has been described by Van Griensven and Meixner (2007). Based on chi-squared statistics, a confidence interval of objective function values can be obtained using Equation 3.6 (Van Griensven and Meixner, 2007):

$$c = OF \cdot (1 + \frac{\chi^2_{P,CL}}{N-P}) \tag{3.6}$$

Where c is the upper boundary of the confidence interval (the lower boundary is the optimal solution itself), OF is the objective function of the optimal solution, N is the number of observations, P is the number of parameters, and $\chi^2_{P,CL}$ is the chi-squared statistic for P parameter values and CL is the confidence level. SCEUA was run for each water quality constituent fifteen times with different random seeds (Tables 3.12 through 3.14). The “n” value in Tables 3.12 through 3.14 indicates the total number of objective functions (from the fifteen runs) enclosed by the confidence interval. Statistics in Tables 3.12 through 3.14 were derived from all parameter sets associated with objective functions enclosed by the confidence interval. Relative frequency histograms of the parameters are shown in Figures 3.10 through 3.12. The parameters of the objective functions enclosed by the confidence intervals were extracted from the data log file of

SCEUA (sceout.dat), were only recorded to the third digit below the decimal point in that file. Therefore, very small parameters, such as some curb-based parameters in Table 3.14, were not recorded. Those values are marked with an asterisk.

Table 3.12. Summary of TSS sample parameter sets (area-based)

		CL=0.5 (n=763)		CL=0.8 (n=780)		CL=0.95 (n=794)	
Land use	**Parameter**	**Std. Dev.**	**Mean**	**Std. Dev.**	**Mean**	**Std. Dev.**	**Mean**
Bare soil	C_1	121.71	431.21	127.41	425.76	129.35	422.95
	C_2	0.96	0.63	1.02	0.67	1.05	0.69
	C_3	1.95	15.72	2.11	15.60	2.25	15.52
	C_4	0.66	3.59	0.70	3.61	0.73	3.62
Civic	C_1	5.73	1.94	7.46	2.50	9.77	3.12
	C_2	2.14	2.29	2.14	2.30	2.13	2.30
	C_3	5.6	7.69	5.56	7.66	5.54	7.66
	C_4	2.44	7.1	2.43	7.08	2.43	7.05
Commercial	C_1	119.02	38.06	117.85	38.39	117.08	38.89
	C_2	2.18	1.81	2.17	1.81	2.17	1.81
	C_3	5.78	8.28	5.75	8.31	5.71	8.32
	C_4	2.29	4.24	2.27	4.24	2.27	4.24
Industrial	C_1	83.51	452.63	91.80	447.12	96.97	443.26
	C_2	0.73	0.53	0.79	0.56	0.81	0.58
	C_3	3.04	14.98	3.11	14.88	3.17	14.80
	C_4	0.73	6.21	0.77	6.21	0.80	6.23

Table 3.12. Continued

		CL=0.5 (n=763)		CL=0.8 (n=780)		CL=0.95 (n=794)	
Land use	**Parameter**	**Std. Dev.**	**Mean**	**Std. Dev.**	**Mean**	**Std. Dev.**	**Mean**
Multifamily	C_1	18.6	7.52	20.46	8.47	21.96	9.31
	C_2	1.58	1.06	1.59	1.06	1.58	1.07
	C_3	4.7	9.51	4.68	9.55	4.67	9.52
	C_4	2.64	5.41	2.62	5.42	2.61	5.41
Single family	C_1	27.64	188.24	28.52	188.38	29.04	187.84
	C_2	0.03	0.23	0.033	0.23	0.045	0.23
	C_3	0.72	16.5	0.90	16.43	1.06	16.36
	C_4	0.11	2.64	0.11	2.64	0.13	2.64
Transportation	C_1	201.83	130.53	200.07	129.11	198.63	128.05
	C_2	2.08	1.64	2.08	1.65	2.07	1.66
	C_3	5.53	5.99	5.50	6.01	5.48	6.04
	C_4	3.11	5.39	3.10	5.42	3.08	5.44
Undeveloped	C_1	125.36	42.05	124.08	41.31	123.04	40.83
	C_2	2.23	2	2.23	2.02	2.22	2.03
	C_3	4.59	7.59	4.58	7.64	4.56	7.64
	C_4	1.47	7.69	1.48	7.66	1.49	7.65

Table 3.13. Summary of TN sample parameter sets (area-based)

		CL=0.5 (n=518)		CL=0.8 (n=534)		CL=0.95 (n=546)	
Land use	**Parameter**	**Std. Dev.**	**Mean**	**Std. Dev.**	**Mean**	**Std. Dev.**	**Mean**
Bare soil	C_1	0.034	0.37	0.036	0.37	0.042	0.36
	C_2	0.43	0.36	0.47	0.39	0.50	0.41
	C_3	23.45	56.59	23.42	56.18	23.29	55.90
	C_4	1.58	5.40	1.61	5.41	1.63	5.47

Table 3.13. Continued

		CL=0.5 (n=518)		CL=0.8 (n=534)		CL=0.95 (n=546)	
Land use	**Parameter**	**Std. Dev.**	**Mean**	**Std. Dev.**	**Mean**	**Std. Dev.**	**Mean**
Civic	C_1	0.0082	0.0054	0.014	0.0064	0.015	0.0071
	C_2	0.85	0.82	0.84	0.83	0.84	0.84
	C_3	26.27	36.79	26.22	37.11	26.30	37.44
	C_4	3.01	6.01	3.011	5.96	3.01	5.94
Commercial	C_1	0.026	0.010	0.026	0.011	0.027	0.012
	C_2	0.89	0.67	0.91	0.71	0.91	0.72
	C_3	24.47	49.71	24.39	49.85	24.28	49.84
	C_4	2.46	5.85	2.45	5.85	2.45	5.85
Industrial	C_1	0.061	0.36	0.070	0.35	0.077	0.35
	C_2	0.43	0.56	0.45	0.58	0.48	0.60
	C_3	15.97	54.21	16.48	53.53	16.71	53.12
	C_4	1.32	8.89	1.44	8.80	1.46	8.76
Multifamily	C_1	0.016	0.010	0.021	0.012	0.027	0.013
	C_2	0.79	0.60	0.79	0.60	0.80	0.61
	C_3	21.87	43.02	21.99	43.08	21.92	43.21
	C_4	2.26	6.61	2.28	6.56	2.28	6.56
Single family	C_1	0.085	0.36	0.091	0.36	0.096	0.35
	C_2	0.16	0.061	0.19	0.07	0.22	0.079
	C_3	17.57	8.73	18.49	9.62	19.39	10.43
	C_4	2.72	3.66	2.76	3.76	2.78	3.83
Transportation	C_1	0.085	0.030	0.083	0.030	0.083	0.031
	C_2	0.71	0.51	0.71	0.52	0.72	0.54
	C_3	26.10	37.01	25.85	37.00	25.85	37.22
	C_4	3.03	5.51	3.02	5.50	3.01	5.50
Undeveloped	C_1	0.15	0.30	0.15	0.29	0.15	0.29
	C_2	0.99	0.47	0.99	0.47	0.98	0.47
	C_3	8.26	7.94	9.24	8.47	9.73	8.88
	C_4	1.66	7.18	1.66	7.21	1.66	7.24

Table 3.14. Summary of TP sample parameter sets (curb-based)

		CL=0.5 (n=357)		CL=0.8 (n=363)		CL=0.95 (n=378)	
Land use	**Parameter**	**Std. Dev.**	**Mean**	**Std. Dev.**	**Mean**	**Std. Dev.**	**Mean**
Bare soil	C_1	0.020	0.010	0.020	0.010	0.020	0.0097
	C_2	0.084	0.034	0.084	0.033	0.088	0.037
	C_3	2.69	6.66	2.70	6.64	2.66	6.63
	C_4	1.96	2.03	1.94	2.02	1.98	2.05
Civic	C_1*	-	-	-	-	-	-
	C_2	0.65	0.42	0.64	0.41	0.64	0.42
	C_3	2.71	2.12	2.70	2.10	2.70	2.13
	C_4	3.06	4.82	3.04	4.82	3.02	4.87
Commercial	C_1	0.017	0.0050	0.017	0.0048	0.017	0.0048
	C_2	0.27	0.062	0.27	0.062	0.31	0.081
	C_3	2.84	4.73	2.83	4.76	2.83	4.75
	C_4	2.10	2.89	2.09	2.88	2.13	2.91
Industrial	C_1	0.019	0.059	0.019	0.059	0.019	0.059
	C_2	0.0063	0.020	0.0064	0.020	0.0065	0.020
	C_3	1.73	1.05	1.74	1.053	1.71	1.03
	C_4	0.46	0.64	0.47	0.64	0.46	0.64
Multifamily	C_1	0.026	0.016	0.027	0.016	0.026	0.016
	C_2	0.27	0.12	0.28	0.13	0.28	0.14
	C_3	3.56	4.84	3.57	4.77	3.54	4.78
	C_4	2.77	4.03	2.77	4.04	2.79	4.11
Single family	C_1	0.021	0.013	0.021	0.013	0.020	0.012
	C_2	0.0036	0.0054	0.0036	0.0054	0.0040	0.0056
	C_3	2.67	1.74	2.67	1.74	2.65	1.73
	C_4	1.84	2.13	1.85	2.12	1.85	2.15

Table 3.14. Continued

		CL=0.5 (n=357)		CL=0.8 (n=363)		CL=0.95 (n=378)	
Land use	**Parameter**	**Std. Dev.**	**Mean**	**Std. Dev.**	**Mean**	**Std. Dev.**	**Mean**
Transportation	C_1	0.015	0.0040	0.015	0.0040	0.015	0.0038
	C_2	0.28	0.099	0.29	0.10	0.28	0.098
	C_3	3.81	4.79	3.81	4.74	3.79	4.77
	C_4	2.71	2.54	2.70	2.53	2.68	2.51
Undeveloped	C_1*	-	-	-	-	-	-
	C_2	0.14	0.024	0.14	0.024	0.17	0.033
	C_3	2.82	4.43	2.83	4.48	2.80	4.54
	C_4	3.04	4.40	3.04	4.44	3.03	4.47

* Values obtained for each SCEUA loops are too small for PEST to be recorded in the data file.

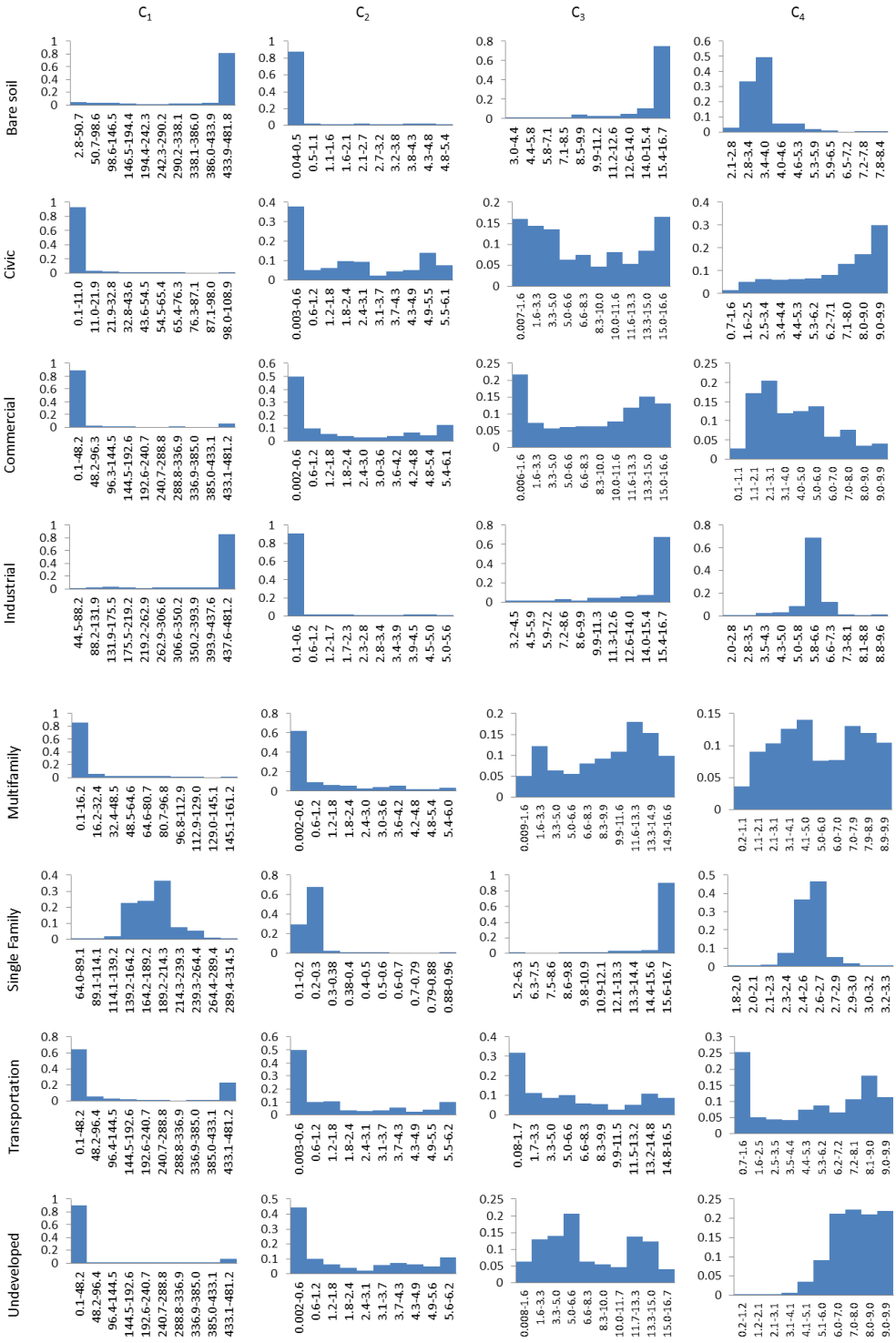

Figure 3.10. Distribution of TSS buildup and washoff parameters with CL=0.95 for different land uses in Table 3.12

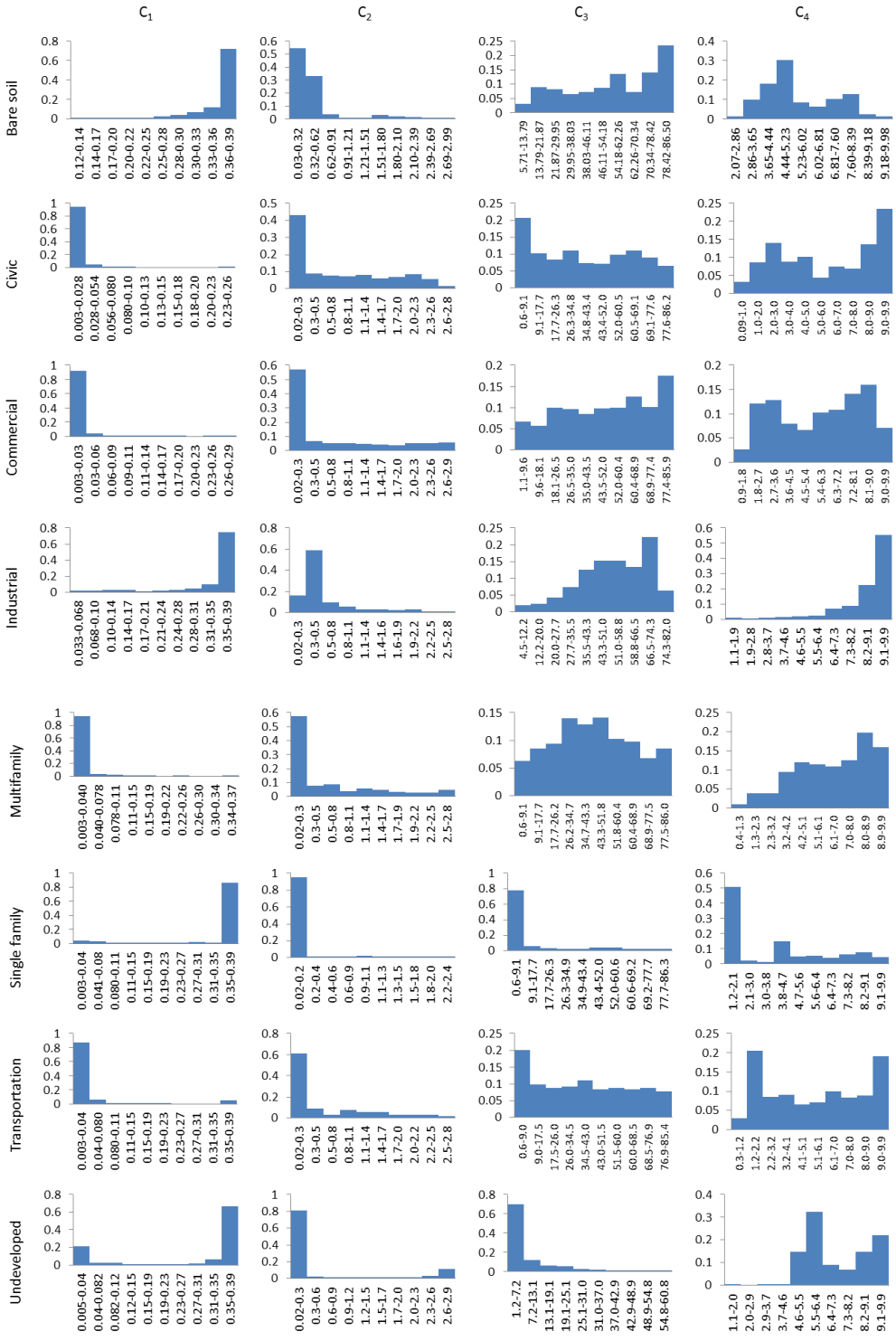

Figure 3.11. Distribution of TN buildup and washoff parameters with CL=0.95 for different land uses in Table 3.13

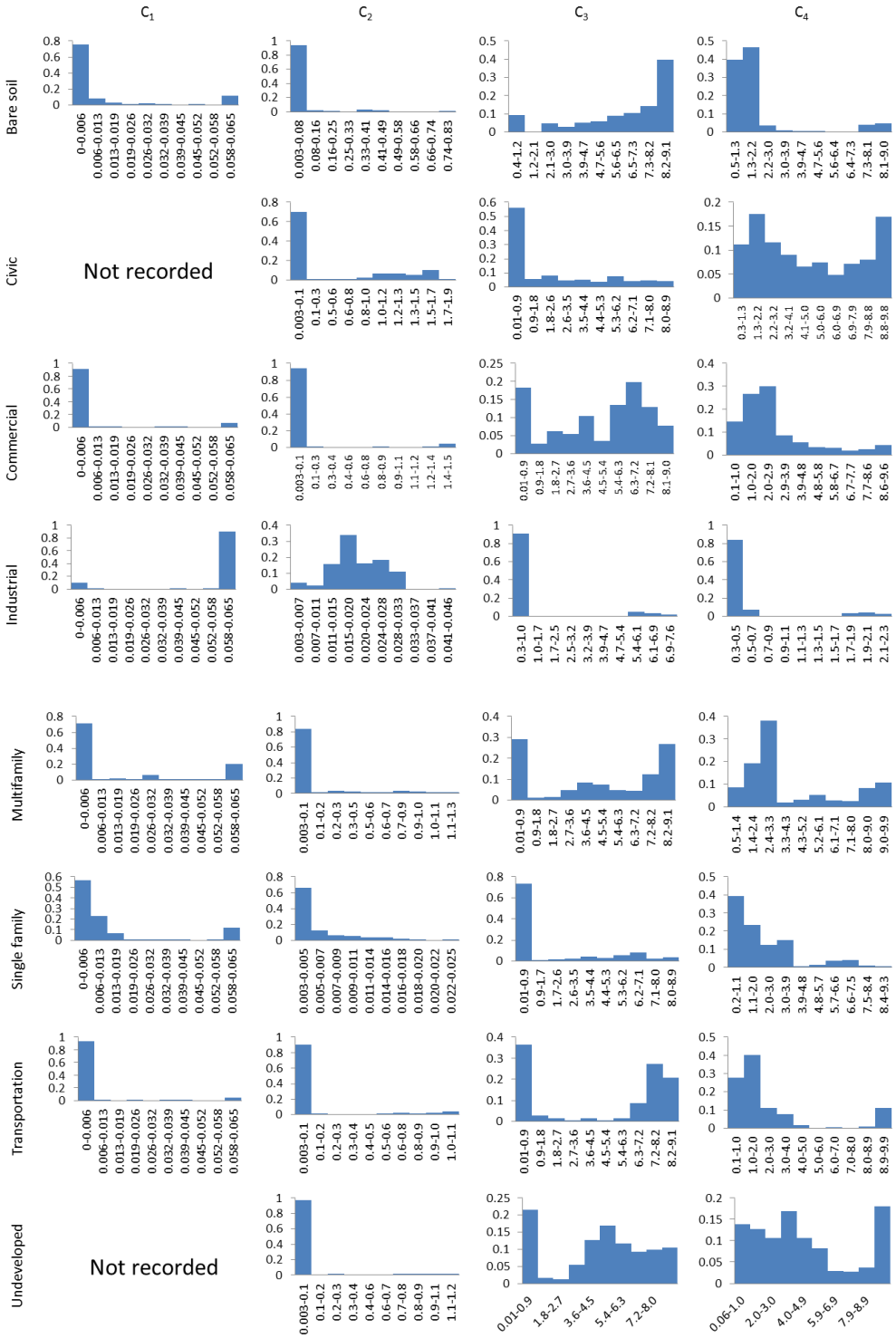

Figure 3.12. Distribution of TP buildup and washoff parameters with CL=0.95 for different land uses in Table 3.14

In Figures 3.10 through 3.12, many of the parameters exhibit bimodal distributions. A Shapiro-Wilkes W Test determined that none of the parameters were normally distributed using a 95% confidence level. Even though Equation (3.6) gave the confidence intervals, the commonly used normal distribution cannot be used to describe the distribution of parameter values within the confidence intervals.

Instead a generalized lambda distribution (GLD), which has been successfully used to fit a range of unimodal and bimodal data, was used (Su, 2009) to describe the distribution of parameters. Compared to ordinary "forward" distribution functions (i.e. the value of variable is the input and the function value is the cumulative probability), GLD is an "inverse" distribution function, in which the input to a GLD is the cumulative probability and the GLD function gives the value of the variable (Karian and Dudewicz, 2000). Therefore, the input values for a GLD equation is always between 0 and 1. There are two parameterizations of the GLD equations (Su, 2009). The first was proposed by Ramberg and Schmeiser (RS, Equation 3.7), and the second was proposed by Freimer, Mudholkar, Kollia, and Lin (FMKL, Equation 3.8). In Equations 7 and 8, the input variable is u, and λ_1, λ_2, λ_3, and λ_4 are coefficients. F(x) means the cumulative probability when the variable value equals to x, so $F^{-1}(u)$ refers to the inverse of cumulative probability function when the cumulative probability u is known.

$$F^{-1}(u) = \lambda_1 + \frac{u^{\lambda_3} - (1-u)^{\lambda_4}}{\lambda_2} \tag{3.7}$$

$$F^{-1}(u) = \lambda_1 + \frac{\frac{u^{\lambda_3 - 1}}{\lambda_3} - \frac{(1-u)^{\lambda_4 - 1}}{\lambda_4}}{\lambda_2} \tag{3.8}$$

The RS GLD has a simpler form but it requires $\frac{\lambda_2}{\lambda_3 u^{\lambda_3-1}-\lambda_4(1-u)^{\lambda_4-1}} \geq 0$. The FMKL GLD only requires that λ_2 is positive. The statistical package GLDEX (Su, 2007) for the software R (Vienna University of Economics and Business, 2014) was used to fit GLD to obtain the confidence intervals of the parameters in Tables 3.15 through 3.17. In GLDEX (Su, 2007), sets of low discrepancy quasi random "initial" coefficients λ_1, λ_2, λ_3, and λ_4 will first be generated. Then, for every observation, u in either Equation 3.7 or 3.8 is solved by Newton-Raphson Method. Once values of u are obtained, Maximum Likelihood estimation was used to derive the "final" coefficients λ_1, λ_2, λ_3, and λ_4. Multiple runs of such calculations were done to see if the sets of initial coefficients converge to the same sets of "final" coefficients.

Recall that parameter sets enclosed by the confidence intervals for TP parameters were not recorded due to insufficient numerical accuracy of the log file. In Tables 3.15 through 3.17, their confidence intervals were calculated from final calibrated parameters of the 15 calibration runs assuming normal distribution of the population. Note that the final parameter file of SCEUA (.par file) has higher numerical precision than the data log file (sceout.dat) does.

Table 3.15. Confidence interval for TSS parameters with 50%, 80%, and 95% confidence levels

Land use	Para-meter	Calibration range		Best solution	95% Mean	Confidence level=50%		Confidence level=80%		Confidence level=95%	
		Low	High			Low	High	Low	High	Low	High
Bare soil	C_1	0.19	481.29	481.25	429.74	429.66	443.32	392.89	457.49	337.96	465.13
	C_2	0.0024	6.22	0.33	0.70	0.55	0.71	0.49	0.83	0.30	1.03
	C_3	0.0065	16.77	16.76	15.83	15.41	16.38	14.48	16.43	12.58	16.61
	C_4	0.0086	22.44	2.73	3.46	3.36	3.60	3.25	4.05	2.98	6.84
Civic	C_1	0.19	481.29	0.19	1.42	0.28	1.12	0.19	5.59	0.03	16.49
	C_2	0.0024	6.22	0.003	2.11	1.47	2.99	1.07	3.77	0.21	5.54
	C_3	0.0065	16.77	15.49	7.51	5.78	9.65	4.49	10.80	3.27	12.53
	C_4	0.0086	22.44	8.30	7.22	6.29	8.07	5.26	8.70	4.06	8.98
Commercial	C_1	0.19	481.29	0.76	32.9	31.32	40.08	28.91	51.72	20.92	92.50
	C_2	0.0024	6.22	0.007	1.76	1.26	2.24	0.89	2.82	0.45	3.65
	C_3	0.0065	16.77	6.83	8.24	6.74	10.22	4.72	10.17	3.42	13.39
	C_4	0.0086	22.44	2.22	4.11	3.36	4.94	2.55	6.16	1.87	7.42
Industrial	C_1	0.19	481.29	480.72	448.91	448.04	464.22	426.15	469.56	380.72	470.46
	C_2	0.0024	6.22	0.37	0.59	0.42	0.62	0.40	0.67	0.32	1.05
	C_3	0.0065	16.77	16.59	15.18	14.42	15.93	13.31	16.35	11.24	16.25
	C_4	0.0086	22.44	6.00	6.28	6.18	6.40	5.68	6.73	4.54	7.48
Multifamily	C_1	0.19	481.29	0.29	6.84	3.00	8.92	2.71	16.12	1.00	32.35
	C_2	0.0024	6.22	0.01	0.88	0.62	1.33	0.32	2.36	0.09	2.58
	C_3	0.0065	16.77	1.69	9.59	7.66	11.46	5.98	13.17	4.15	14.12
	C_4	0.0086	22.44	1.11	5.49	4.29	6.51	3.58	7.08	2.31	8.05
Single family	C_1	0.19	481.29	137.55	181.40	177.17	188.40	173.19	208.08	159.55	329.00
	C_2	0.0024	6.22	0.222	0.22	0.22	0.24	0.21	0.25	0.20	0.31
	C_3	0.0065	16.77	16.76	16.49	16.41	16.68	16.09	16.71	15.32	16.73
	C_4	0.0086	22.44	2.48	2.62	2.60	2.66	2.56	2.72	2.51	2.85

Table 3.15. Continued

Land use	Para-meter	Calibration range		Best solution	95% Mean	Confidence level=50%		Confidence level=80%		Confidence level=95%	
		Low	High			Low	High	Low	High	Low	High
Transportation	C_1	0.19	481.29	481.16	117.29	113.10	136.81	102.52	165.40	89.28	232.61
	C_2	0.0024	6.22	0.036	1.55	1.10	2.06	0.64	2.80	0.29	3.77
	C_3	0.0065	16.77	0.215	5.46	4.16	7.62	2.86	9.62	1.64	13.39
	C_4	0.0086	22.44	1.427	5.52	4.07	6.50	3.16	7.13	1.76	7.96
Undeveloped	C_1	0.19	481.29	425.89	37.54	33.10	45.34	24.31	51.98	14.39	83.98
	C_2	0.0024	6.22	0.002	2.09	1.41	2.49	0.98	3.11	0.58	4.55
	C_3	0.0065	16.77	5.40	7.68	6.40	8.85	4.96	10.26	3.54	11.43
	C_4	0.0086	22.44	6.66	7.78	7.12	8.29	6.49	8.72	5.37	9.16

Table 3.16. Confidence interval for TN parameters with 50%, 80%, and 95% confidence levels

Land use	Para-meter	Calibration range		Best solution	95% Mean	Confidence level=50%		Confidence level=80%		Confidence level=95%	
		Low	High			Low	High	Low	High	Low	High
Bare soil	C_1	0.0027	0.39	0.39	0.37	0.36	0.38	0.35	0.38	0.30	0.39
	C_2	0.021	3	0.033	0.36	0.25	0.45	0.17	0.63	0.12	0.84
	C_3	0.61	86.61	66.02	56.59	47.69	66.24	36.65	73.56	26.88	77.68
	C_4	0.07	10	8.10	5.40	4.94	5.87	4.45	6.42	3.78	7.13
Civic	C_1	0.0027	0.39	0.003	0.0054	0.0037	0.0061	0.0036	0.014	0.0035	0.02
	C_2	0.021	3	0.022	0.82	0.52	1.07	0.37	1.37	0.26	1.78
	C_3	0.61	86.61	61.72	36.79	26.98	46.89	21.34	53.62	13.47	69.12
	C_4	0.07	10	2.15	6.01	5.15	7.02	4.20	7.60	2.97	8.34

Table 3.16. Continued

Land use	Para-meter	Calibration range		Best solution	95% Mean	Confidence level=50%		Confidence level=80%		Confidence level=95%	
		Low	High			Low	High	Low	High	Low	High
Commercial	C_1	0.0027	0.39	0.003	0.010	0.0043	0.011	0.0029	0.020	0.0022	0.050
	C_2	0.021	3	0.024	0.67	0.36	0.88	0.29	1.19	0.17	1.62
	C_3	0.61	86.61	41.59	49.71	39.02	61.38	28.29	69.33	24.68	73.09
	C_4	0.07	10	7.52	5.85	4.96	6.78	4.22	7.44	3.05	8.13
Industrial	C_1	0.0027	0.39	0.39	0.36	0.35	0.38	0.31	0.38	0.26	0.38
	C_2	0.021	3	0.41	0.56	0.37	0.64	0.34	0.85	0.23	1.28
	C_3	0.61	86.61	69.60	54.21	48.65	61.60	38.94	65.53	25.69	68.86
	C_4	0.07	10	9.84	8.89	8.58	9.47	7.70	9.66	5.32	9.89
Multifamily	C_1	0.0027	0.39	0.003	0.010	0.0056	0.011	0.0047	0.021	0.0038	0.045
	C_2	0.021	3	0.023	0.60	0.29	0.82	0.23	1.07	0.12	1.53
	C_3	0.61	86.61	34.45	43.02	31.49	54.38	22.08	62.30	13.24	68.07
	C_4	0.07	10	8.72	6.61	5.87	7.59	4.80	8.12	3.59	8.58
Single family	C_1	0.0027	0.39	0.39	0.36	0.36	0.37	0.34	0.38	0.30	0.38
	C_2	0.021	3	0.038	0.061	0.046	0.068	0.039	0.10	0.034	0.17
	C_3	0.61	86.61	0.61	8.73	4.37	10.44	3.30	16.79	2.46	27.84
	C_4	0.07	10	1.38	3.66	3.07	4.52	2.47	5.08	2.00	6.17
Transportation	C_1	0.0027	0.39	0.03	0.030	0.021	0.032	0.018	0.048	0.016	0.087
	C_2	0.021	3	0.022	0.51	0.25	0.71	0.21	0.89	0.21	1.35
	C_3	0.61	86.61	12.64	37.01	26.71	46.95	17.77	58.76	11.38	66.56
	C_4	0.07	10	9.91	5.51	4.64	6.44	3.33	7.66	2.29	8.91
Undeveloped	C_1	0.0027	0.39	0.39	0.30	0.29	0.31	0.27	0.32	0.22	0.34
	C_2	0.021	3	0.021	0.47	0.42	0.53	0.33	0.60	0.19	0.79
	C_3	0.61	86.61	3.80	7.94	5.46	9.05	4.95	12.95	4.25	19.48
	C_4	0.07	10	5.59	7.18	6.79	7.72	6.27	8.04	5.40	8.57

Table 3.17. Confidence interval for TP parameters with 50%, 80%, and 95% confidence levels

Land use	Para-meter	Calibration range		Best solution	95% Mean	Confidence level=50%		Confidence level=80%		Confidence level=95%	
		Low	High			Low	High	Low	High	Low	High
Bare soil	C_1	1.1e-4	0.065	1.6e-4	0.013	6.9e-3	0.011	5.4e-3	0.016	2.3e-3	0.024
	C_2	3.1e-3	1.76	3.3e-3	0.061	0.019	0.037	0.014	0.057	0.011	0.11
	C_3	0.016	9.12	2.61	5.95	5.78	7.82	4.24	8.74	3.16	8.74
	C_4	0.035	10	1.18	2.00	1.70	2.24	1.49	2.48	0.80	3.20
Civic	C_1	1.1e-4	0.065	1.2e-4	1.4e-4	1.3e-4*	1.4e-4*	1.2e-4*	1.5e-4*	1.1e-4*	1.6e-4*
	C_2	3.1e-3	1.76	3.3e-3	0.44	0.35	0.48	0.28	0.53	0.21	0.66
	C_3	0.016	9.12	0.017	2.70	0.97	2.99	0.83	3.56	0.46	4.94
	C_4	0.035	10	1.17	4.82	3.84	5.80	2.90	6.68	1.58	8.06
Commercial	C_1	1.1e-4	0.065	1.8e-4	3.9e-3	4.7e-3	5.6e-3	4.3e-3	5.4e-3	2.5e-3	5.2e-3
	C_2	3.1e-3	1.76	5.6e-3	0.077	0.052	0.075	0.037	0.087	0.024	0.13
	C_3	0.016	9.12	0.045	4.68	3.70	5.76	2.92	6.75	1.96	7.40
	C_4	0.035	10	1.37	3.41	1.77	3.86	1.27	4.76	0.95	5.87
Industrial	C_1	1.1e-4	0.065	0.065	0.058	0.058	0.059	0.054	0.06	0.049	0.067
	C_2	0.0031	1.76	0.012	0.019	0.018	0.023	0.015	0.024	0.011	0.027
	C_3	0.016	9.12	0.35	1.01	0.99	1.12	0.94	1.19	0.77	1.25
	C_4	0.035	10	0.75	0.67	0.56	0.67	0.56	0.74	0.51	0.83
Multifamily	C_1	1.1e-4	0.065	0.031	0.021	0.012	0.018	0.010	0.024	6e-3	0.035
	C_2	3.1e-3	1.76	0.90	0.20	0.064	0.10	0.052	0.23	0.028	0.37
	C_3	0.016	9.12	0.016	2.00	3.94	5.97	2.57	6.62	1.99	7.60
	C_4	0.035	10	3.01	4.16	3.30	4.55	2.69	5.53	1.76	6.55
Single family	C_1	1.1e-4	0.065	0.012	0.031	8.8e-3	0.016	6.8e-3	0.020	3.9e-3	0.027
	C_2	3.1e-3	1.76	3.1e-3	7.2e-3	4.2e-3	6e-3	3.8e-3	7.4e-3	3.4e-3	0.011
	C_3	0.016	9.12	0.43	1.83	1.34	2.04	1.05	2.41	0.76	2.90
	C_4	0.035	10	0.67	2.70	1.30	2.69	0.99	3.37	0.60	4.80

Table 3.17. Continued

Land use	Para-meter	Calibration range		Best solution	95% Mean	Confidence level=50%		Confidence level=80%		Confidence level=95%	
		Low	High			Low	High	Low	High	Low	High
Transportation	C_1	1.1e-4	0.065	4.2e-4	3e-3	3.4e-3	4.4e-3	3e-3	5.2e-3	1.6e-3	4.3e-3
	C_2	3.1e-3	1.76	0.034	0.12	0.097	0.15	0.078	0.13	0.067	0.18
	C_3	0.016	9.12	0.020	4.73	4.44	5.15	3.92	5.55	3.05	6.40
	C_4	0.035	10	1.17	2.92	1.98	2.95	1.69	3.56	1.38	4.46
Undeveloped	C_1	1.1e-4	0.065	1.1e-4	1.3e-4	1.2e-4*	1.3e-4*	1.1e-4*	1.4e-4*	1.1e-4*	1.4e-4*
	C_2	3.1e-3	1.76	3.2e-3	0.036	0.018	0.029	0.012	0.041	0.018	0.053
	C_3	0.016	9.12	0.028	4.78	3.34	5.42	2.74	6.39	2.37	7.18
	C_4	0.035	10	2.88	4.77	3.14	5.40	2.49	6.36	1.38	8.15

* Confidence interval calculated from final calibrated parameters of multiple runs assuming normal distributions.

3.6. Discussion and Conclusion

This study calibrated 32 buildup and washoff parameters (4 for each land use) for each of the water quality constituent of interest (TSS, TN, and TP) from the Austin area. Due to the large number of parameters considered, equifinality (multiple models are all acceptable to represent the system) is likely to happen. The direct effect of equifinality is the increased uncertainty in parameter estimation (Beven, 2006). In this study, the calibrated model did reach similar final optimal objective functions but quite different calibrated parameter sets. Some prior studies also encountered similar problems, particularly water balance models at large scales (Wilby, 2005; Widen-Nilsson et al., 2009). Usually, a Monte Carlo process is used to explore the parameter space and

uncertainty. In this study, a similar approach was used by using different random seeds and considered the confidence intervals of SCEUA. As shown in Figures 3.10 through 3.12, this approach provided satisfactory estimates for most parameters.

The results showed that values of most buildup parameters (C_1 and C_2) concentrate in narrow numerical regions. However, it is not the case for washoff parameters (C_3 and C_4). Many washoff parameters have values distributed evenly in the whole calibrated numerical interval. This phenomenon may indicate that pollutant buildup is controlled by factors that are spatially uniform, such as land use, temperature or climate. On the other hand, washoff is controlled by local factors such as topography and slope, so the values are diversified. The uniform effect of climate on pollutant buildup has been studied by field experiments (Wang and Li, 2009). As for pollutant washoff, runoff rate is likely the dominant factor as supported by many pollutant washoff models (Soonthornnonda et al., 2008; Rossman, 2010), thus local factors such as topography and slope can play a significant role.

The water quality record of Walnut Creek Watershed showed particularly high concentrations in water quality constituents. TSS from the USGS gage at the outlet of the Walnut Creek for example, frequently reached concentrations of more than 6000 mg/L (USGS, 2014b), which is much higher than anything found in literature (Barco et al., 2004; Hood et al., 2007; Temprano et al., 2006). One would expect that this watershed has a tremendous capability to generate pollutants. Nevertheless, the results from this study showed that C_1 (representing the maximum amount of pollutant per unit area or unit curb length that can possibly be deposited) of many land uses is actually

quite low and is close to the numbers from literature (Table 3.1). However, there are exceptions with extremely high values of C_1. C_1 is extremely high for bare soil, industrial, and single family land uses for TSS, bare soil, industrial, single family, and undeveloped land uses for TN, and industrial land use for TP (as shown in Table 3.18).

Table 3.18. Land uses with high capacity to provide pollutants for non-point pollution

	TSS	TN	TP
Bare soil	x	x	
Industrial	x	x	x
Single family	x	x	
Undeveloped		x	

These land uses are potentially the major pollutant sources and plans of watershed non-point source pollution control need to address them. For future plans of controlling non-point pollution, watershed managers should consider these land uses as the first targets. Bare soil, single family, and undeveloped land uses all have large portions of pervious surface. Without proper care, the soil can be easily eroded and provide large quantity of pollutants. That undeveloped land provides a large quantity of TN but not TSS may indicate the existence of manure sources. As for TP, literature showed that urbanized river basins (compared to rural ones) have high phosphorus

concentration in the fluvial sediment (Owens and Walling, 2002). However, among land uses in urbanized region, industrial land use should not have particularly higher capability in TP generation than commercial land use does (Chow et al., 2013). In fact, pollutant generating capability for commercial and industrial land uses should be similar, according to Show et al. (2013). The disparity in pollutant generating capability for commercial and industrial land uses, and the high TP generating capability for industrial land use, is worth investigating.

After further examination, this phenomenon can be contributed the following reasons: 1) a sand and gravel mining pit (approximate location: (-97.7169^{o}, 30.4564^{o})) exists in the northern edge of the watershed, and part of it was categorized as industrial land use, and/or 2) from the aerial photos, many industrial sites were newly built or under construction in 1984 (particularly the large industrial lots in the western part of the watershed), but were not identified as "bare soil" as was done for many residential construction sites.

Both reasons explained the disparity in pollutant generating capability of commercial and industrial land uses. However, they do not directly explain why industrial land use has high TP generating capability. Since most TP is associated with particulate and sediment in water, TP generating capability should be similar to TSS generating capability for most land uses. Therefore, TP generating capability should also be high for bare soil and residential land uses in Table 3.18. The reasons why TP generating capability is not high for bare soil and residential land uses are probably the follows:

1. Bare soil usually can be found in construction sites. In construction sites, sand and gravel is more likely to be found. Phosphorus is meager in such soil texture (Young et al., 2012), thus bare soil is a significant source for sediment but not phosphorus; and

2. Residential land use has the highest curb length per unit area among all types of land use. Recall that the pollutant equations for TP are curb-base. Single family land use can actually a major source of TP per unit area since it is a significant source of TSS, but the high curb density makes the maximum amount of pollutant per unit curb length extremely low.

Because the parameters for industrial land use might not reflect actual characteristics, it may be appropriate to ignore parameters for industrial land use, and instead use the parameters of commercial land use for industrial areas.

The parameter C_2 governs the speed of pollutant buildup. For each water quality constituent, the values of C_2 for most land uses stay in the same numerical range. For TSS, C_2 stays in the range of approximately 0 - 0.6. For TN, C_2 stays in the range of approximately 0 - 0.3. For TP, C_2 stays in the range of approximately 0-0.1 except for the land uses of industrial and single family. This indicates that pollutant buildup is mainly controlled by factors that are spatially distributed, such as land use, temperature or climate.

The parameters C_3 and C_4 both control the washoff rates of water quality constituents, with C_3 the coefficient and C_4 the exponent of the equation. Distributions of these parameters are more diverse and can be related to local factors that control

runoff rates. It is interesting to compare the results with the equation (Equation 3.9) of shear stress along a channel (Knighton, 1998) calculated as:

$$\tau = \gamma R s \tag{3.9}$$

Where τ is the shear stress at the bottom of the channel (N/m), γ is the specific weight of water (9.81 kN/m^3), R is the hydraulic radius (m^2/m), and s is slope (m/m). For overland flow where width is much larger than depth, the hydraulic radius R is close to the depth of runoff. Given the same shear stress, pollutant washoff can be assumed to be proportional to the amount of available pollutant buildup on the surface. Therefore, Equation 3.9 can be linked to Equation 3.2 as shown in Equation 3.10.

$$\tau = \gamma R s \propto (\gamma s) \cdot Runoff \propto C_3 \cdot Runoff^{C_4} \tag{3.10}$$

Recall that the unit of runoff is depth/hr. Equation 3.10 implies that the value of C_4 should be close to 1 theoretically. This agrees with studies found in the literature that took the value of C_4 as 1 (Wicke et al., 2012; Temprano et al., 2006). However, this study found that C_4 is not close to 1 for many land uses. For a few land uses, for example the land use of transportation, the value of C_4 is indeed close to 1, but many land uses have very large C_4. The use of the conventional value of 1 for C_4 can result in large errors in calculations.

This study still leaves space for improvements. Since bare soil is one of the main contributors in non-point pollution, it is crucial to identify it as an individual land use as was done in this study. However, it is sometimes difficult to distinguish whether a lot under construction should be identified as bare soil. Many new industrial sites under construction were identified as industrial instead of bare soil. That greatly distorted the

derived parameters for industrial land use. Therefore, it was suggested to use the parameters of commercial land use for industrial land use, since they showed similar pollutant loadings in field observations (Chow et al., 2013). For future applications in deriving buildup and washoff parameters, it was also suggested not to use urban watersheds under rapid transition (like the Walnut Creek watershed used in this study) because identification of bare soil can be a problem.

The next problem that this study encountered is the numerical accuracy for some water quality constituents. Identification of confidence intervals for parameters derived by SCEUA requires that parameters from every step in SCEUA to be recorded. However, some parameters of TP are too small to be recorded for this purpose. The fact that TP is based on curb length further exacerbates this problem since parameter values are much smaller based on curb length. For future applications in deriving buildup and washoff parameters, researchers should be cautious about the problems of numerical accuracy for water quality constituents with low concentrations, particularly if they are curb-based.

CHAPTER IV

DERIVING POLLUTANT-REDUCING EFFICIENCIES OF BMPS BASED ON ENVIRONMENTAL FACTORS

4.1. Overview

A modeling approach is utilized to derive pollution-removing efficiency of BMP (Best Management Practice) and the relationship between environmental factors (the ratio of BMP area/catchment area, dominant land use type, the ratio of the dominant land use area/catchment area, slope, and BMP type) and the removal efficiency. A SWMM (Storm Water Management Model) model was built for an urban watershed in Austin, TX in order to simulate direct runoff. The change of water quality in Lady Bird Lake detected by Landsat imagery due to water discharged from the Austin watershed during base flow dominant dates was used to determine mean pollutant concentrations in base flow. Using the base flow concentrations, USGS water quality measurements at the outlet of the Austin watershed were converted to concentrations in direct runoff, which were used to calibrate the SWMM model. BMPs with similar environmental factors are grouped together and assumed to have the same removal efficiency. The whole model is then calibrated for BMP removal efficiency and Monte Carlo Simulations are performed to account for uncertainties in the model. After removal efficiency of each BMP group is derived, a multiple regression analysis is utilized to derive the relationship between BMP removal efficiency and environmental factors. The overall coefficient of determination (R squared) tends to be low due to the fact that Monte Carlo Simulations

took account for all variations in the model. By considering only the mean removal efficiency for each BMP group, the R squared number is 0.57 for TSS (total suspended solids), 0.34 for TN (total nitrogen), and 0.51 for TP (total phosphorous).

The predictive equations can provide guides for precise planning of BMPs. Two planning criteria were tried for different time frames (10-40 years). One criterion is goal concentrations in runoff, and the other is a combination of goal concentration and the budget constraint. It was found that the optimal area for different types of BMPs was different for each criterion. It was also found that the Austin watershed of interest does not have enough BMPs built compared with the optimal plans.

4.2. Introduction

Control of non-point urban stormwater pollution usually involves the use of Best Management Practices (BMPs). In a broader context, BMPs can be non-structural (educational programs) or structural (e.g. detention basins). While it is difficult to quantify the effect of non-structural BMPs (Urbonas and Stahre, 1993), efficiencies of structural BMPs can be measured. Predicting BMP removal efficiency reliably is essential in creating urban Stormwater Management Plans (SWMPs), which are part of the requirements from the National Pollutant Discharge Elimination System (NPDES) (Debo and Reece, 2003) under the Clean Water Act (33 U.S.C. §1251 et seq. (1972)). Compliance is usually evaluated by the number of applied BMPs (U.S. EPA, 2012a) because NPDES permits for non-point stormwater do not specify the limits of pollutants; rather, they require a reduction in the discharge of pollutants to the “maximum extent

practicable" (U.S. EPA, 2000; Roesner and Traina, 1994) through the use of BMPs. Therefore, it is desirable to have SWMPs designed to reduce as much pollution as possible within a given budget and construction area. It is challenging to predict the integrated effects of multiple BMPs in a large watershed due to the uncertainty of BMP removal efficiency under untested field conditions (Edwards et al., 1997). The term "removal efficiency" in this study is correlated to portion of pollutant removed by the BMP, thus a removal efficiency of 1 indicates total removal of pollutants.

Barrett (2005) in a study of a small set of BMPs selected from the International BMP Database (Moeller and Connor, 2014) found that the traditional definition of removal efficiency (percent reduction) may not be a satisfactory indicator of effectiveness because the reduction varies with the quantity of runoff. The use of regression analysis for event-based influence and effluence concentrations (EMC) was proposed. Such methods yield good linear regression equations for various types of BMPs.

The reliability of BMPs is not well established (Urbonas and Stahre, 1993). Data from the International BMP Database (Moeller and Connor, 2014), show that efficiencies of BMPs can vary by an order of two. Part of the reason for the variation is that removal efficiency is affected not only by the design of the BMP, but also by various physical parameters including parameters affecting sedimentation (temperature, particle size distribution, density, electric charge associated with clay particles), parameters affecting removal of nitrogen (temperature, pH, bacterial community, dissolved oxygen (DO)) and parameters affecting removal of phosphorous (particulate

association, pH and oxidation reduction potential, cation exchange coefficient/P-index, and temperature). There are two problems linking these physical parameters to the removal efficiency of BMPs. First and the most important, these physical parameters are typically not measured in situ at the locations of BMPs. Second, analytical evaluation of BMP removal efficiency has not taken these parameters into consideration to this point (Chen and Adams, 2006).

To refine the studies of BMP efficiencies, several researchers have proposed that environmental parameters such as watershed area, slope, imperviousness, average storm runoff volume, average intervals between runoff events, water temperature, etc. be considered (Urbonas, 1994; Strecker et al., 2001). However, no comprehensive studies have been done to determine the effect of environmental parameters on BMP removal efficiency. Thus, there exists the need to find a new method to quantify the removal efficiency of BMPs by taking the impact of the environment into consideration, and using the results to optimize urban SWMPs.

Storm Water Management Model (SWMM) was developed by the U.S. EPA in 1971 (Rossman, 2010), and has been extensively used for diverse purposes. It has been used to simulate flooding in urban areas (Hsu et al., 2000), to evaluate the hydrologic impact from proposed urban developments (Jang et al., 2007), and has been suggested for both Total Maximum Daily Load (TMDL) evaluation (Borah et al., 2006) and for management of urban watersheds (Lee et al., 2010). This study utilized SWMM to quantify the removal efficiency of BMPs, particularly their removal efficiency in reducing total suspended solids (TSS), total nitrogen (TN), and total phosphorus (TP).

After determing BMP removal efficiency, the statistical relationship between several environmental factors and the BMP removal efficiency were derived. In the end, scenarios were tested to show that availability of these environmental relationships is important in planning BMP installation in a developing watershed.

4.3. Research Site

An urban watershed near the heart of the city of Austin, Texas was used in this research (Figure 4.1). The watershed is monitored at Shoal Creek at West 12th St (USGS 08156800) (USGS, 2014b) for stream flow and water quality. The effluent from the watershed enters Lady Bird Lake (a.k.a. Town Lake approximately 300 m below the Shoal Creek gage. The landscape is relatively flat, with elevation ranging from 145 to 276 meters above sea level (City of Austin, 2014b). The watershed has an area of 3244 ha and is approximately 36.6% impervious in 2006 (EROS, 2014b). The soil types in the watershed are mostly clayey and in hydrologic soil groups C or D. The major soil map units (areal percentage $\geq$ 5%) are shown in Table 4.1 (USDA, 2013). The types of BMPs and the number of each in the Shoal Creek Watershed of 2012 are provided in Table 4.2 (City of Austin, 2014b) to show the building trend of different types of BMPs.

Table 4.1. Details of main soil map units in the research watershed

Map Unit Name	% of Total Watershed Area	Soil Type	Hydrological Soil Group
Urban land and Austin soils, 0 to 5% slopes	34%	Silty clay	C
Urban land, Austin, and Whitewright soils, 1 to 8 % slopes	21%	Silty clay	C
Houston black soils and urban land, 0 to 8% slopes	10%	Clay	D
Tarrant soils and urban land, 0 to 2 % slopes	7%	Variable	D
Tarrant soils and urban land, 5 to 18% slopes	5%	Variable	D
San Saba soils and urban lands, 0 to 2% slopes	5%	Clay	D
Urban land, 0 to 6% slopes	5%	Variable	D

Table 4.2. Types (with mean area) and number of BMPs installed in Shoal Creek Watershed as of 2012

BMP Type	Number installed	Mean area (square meter)
Biofiltration	13	838.3
Filtration Only	4	356.5
Flood Detention	521	1636.2
Infiltration / Detention	3	2622.5
Infiltration Basin	1	233.3
Infiltration Trench	3	1149.1
Parking Lot Detention	140	693.4
Rain Garden	9	92.9
Rainwater Harvesting	5	216.0
Retention / Irrigation	6	1366.8
Sedimentation / Sand Filtration	94	795.4
Sedimentation Only	3	1758.9
Vegetative Filter Strip	19	3721.8
Wet Pond	14	10531.9

The climate of Austin is humid subtropical with hot summers and mild winters. Austin has a bimodal distribution of precipitation, with the highest monthly rainfall totals in May and October. Average annual precipitation is around 84 cm compared to a U.S. national average of 94 cm (NWS, 2014a). Since stratiform systems are not common in Texas, slow-moving and widespread rainfall is rare in this area. Instead, thunderstorms triggered by the interaction between moist air from the Gulf of Mexico and the dry air from the Rocky Mountains are the main source of precipitation (Norwine

et al., 2005). Rainfall from thunderstorms exceeding 13 cm/hr is not uncommon during summer months.

Land use in this watershed is shown in Figure 4.1 and Table 4.3 (City of Austin, 2014b). The main land use is single family residential (36.2%), followed by transportation (23.5%). The smallest land use is undeveloped land (4.6%).

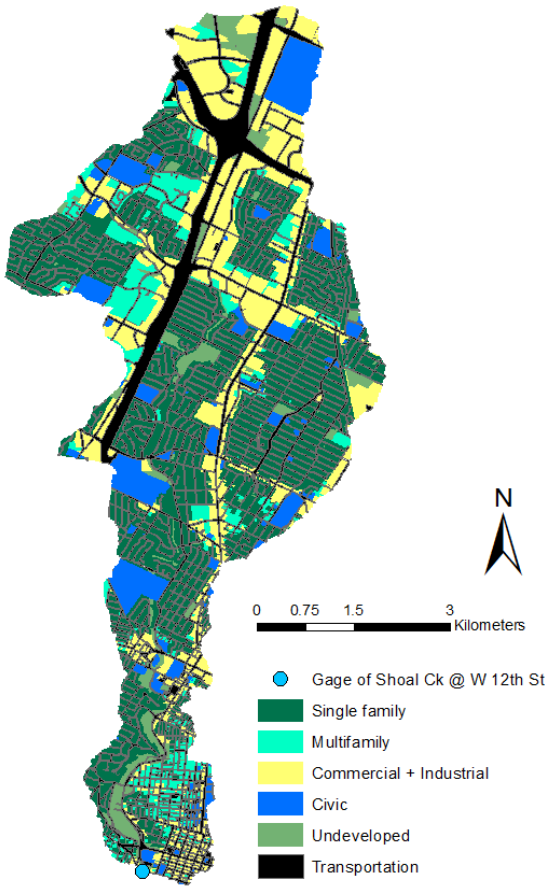

Figure 4.1. Land use in the Shoal Creek Watershed, Austin, TX

Table 4.3. Land use of Shoal Creek Watershed, Austin, TX

Land use	Area (ha)	% of Watershed Area
Single family	1173.9	36.2
Multi family	259.7	8.0
Civic	295.1	9.1
Commercial + Industrial	602.3	18.6
Transportation	762.2	23.5
Undeveloped (with water)	150.6	4.6
Total	3243.8	100

4.4. Methodology

The proposed methodology can be divided into three steps:

Step 1: Use SWMM to determine upstream BMP efficiencies based on measured pollutant concentrations at the outlet of a test watershed;

Step 2: Use multiple regression analysis, to determine the relationship between selected environmental factors and BMP efficiencies calculated in Step 1. BMP removal efficiency was the independent variable and environmental factors were the dependent variables; and

Step 3: Use the predictive equations from Step 2, estimate optimal BMP placement.

4.4.1. Determining BMP Removal Efficiency

Model construction

SWMM was used to construct a model for the Shoal Creek Watershed. The sources for the inputs needed for SWMM are shown in Table 4.4. The SWMM hydrological and hydraulic parameters (Table 4.5) from the study on the Walnut Creek Watershed at Webberville Rd (USGS site # 08158600) in Chapter 3 were used because of the proximity of the two watersheds to each other and their similar attributes (i.e. imperviousness, slope, and area). More importantly the hydrological parameters from the earlier study were used because that study was conducted using data from the early 1980s prior to most BMP establishment, so the parameters represent "native" characteristics of the watershed without interference from BMPs. The construction of BMPs became significant after the 1990s due to the NPDES requirements (U.S. EPA, 2000; City of Austin, 2014b). SWMM-simulated BMP removal efficiency is calculated directly from arithmetic operations of concentrations so it is independent from flow rate in the SWMM model. Omitting the impact of BMP to hydrology does not affect determination of BMP removal efficiency in the SWMM model.

Table 4.4. Data sources for the SWMM model of the research watershed

Data	Data date	Format	Source
Elevation	n/a	10-m DEM raster	(USGS, 2013a)
Imperviousness	2006	30-m raster	(MRLC, 2013)
Land use	2010	GIS shape file	(City of Austin, 2014b)
Sewer network	2012	GIS database	(City of Austin, 2012)
River network	n/a	GIS shape file	(USGS, 2013a)
Precipitation	2008-2009	Hourly record	(NWS, 2014a)
	2010-2013	Hourly shape file	(NWS, 2014c)
Runoff	2008-2013	Daily record	(USGS, 2013b)

Table 4.5. The hydrological / hydraulic parameters found in the Walnut Creek Study (Chapter 3)

Parameter	Calibrated value
Imperviousness	Varies by subcatchment
Width	Varies by subcatchment
Manning's n for impervious	0.016
Manning's n for pervious	0.10
Storage of impervious surface	1.27 (mm)
Storage of pervious surface	7.62 (mm)
Max infiltration rate	79.58 (mm/hr)
Min infiltration rate	0.66 (mm/hr)
Decay constant	2 (1/hr)
Drying time	14 (days)
Manning's n for open channels	0.031
Manning's n for closed pipes	0.026

SWMM simulates hydrological responses across the entire watershed by simulating individual subcatchments. The subcatchments were determined by merging drainage areas of manholes, inlets, and junction points so that no subcatchment is smaller than 2 hectares. A total of 264 subcatchments were created and simulated in SWMM. Then, conduits (including natural channels and storm water sewers) were simplified using the storage node method (Fischer et al., 2009; Leitao et al., 2010) which creates a node reservoir that has a storage volume identical to that of the pipes it will replace. Chapter 3 provided the detailed procedure.

For each pollutant, SWMM defines the transportation of pollutants using four parameters. Two parameters are used to simulate the buildup of a pollutant when there is no runoff, and two parameters simulate the washoff of that pollutant when runoff occurs. Exponential buildup and washoff equations (Rossman, 2010) were used in this study because the parameters are reported frequently in literature. In this study, two sets of buildup and washoff parameters were tested. The first set are parameters reported in the literature (Table 4.6), and the second set are parameters derived from the study conducted on the Walnut Creek Watershed at Webberville Rd (Table 4.7), summarized from Chapter 3). For the list of research studies used to create Table 4.6, please refer to Chapter 3, Table 3.1. In the literature, buildup and/or washoff parameters were not reported for every type of land use, so land use is not distinguished in Table 4.6. On the other hand, the Walnut Creek Study did distinguish these parameters by land use (Table 3.7). Note that the units of C1 for TSS and TN are different from that of TP since the

Walnut Creek Study found that TSS and TN have higher prediction accuracy when using area-based C1 values, while TP has higher accuracy with curb length-based C1 values.

Table 4.6. Surface pollutant buildup / washoff parameters summarized from literature

	TSS		**TN**		**TP**	
	Mean	**Std. Dev.**	**Mean**	**Std. Dev.**	**Mean**	**Std. Dev.**
C1	33.2 (kg/ha)	19.8	0.0433 (kg/ha)	0.0189	0.00165 (kg/meter curb)	0.00135
C2	0.291 (1/day)	0.091	0.311 (1/day)	0.0830	0.105 (1/day)	0.055
C3	0.906 (hr^{C_4-1}/mm^{C_4})	0.905	10.82 (hr^{C_4-1}/mm^{C_4})	6.485	0.750 (hr^{C_4-1}/mm^{C_4})	0.449
C4	0.939 (unitless)	0.331	1.046 (unitless)	0.307	1.287 (unitless)	0.378

Table 4.7. Surface pollutant buildup / washoff parameters for individual land use from the Walnut Creek Watershed (summarized from Chapter 3)

TSS														
	Bare soil		Civic		Com+Ind		Multifamily		Single Family		Transportation		Undeveloped	
	Mean	Std. Dev.	Mean	Std. Dev.	Mean	Std. Dev	Mean	Std. Dev.	Mean	Std. Dev.	Mean	Std. Dev	Mean	Std. Dev.
C1	423.0	129.4	3.1	9.8	38.9	117.1	9.3	22.0	187.8	29.0	128.1	198.6	40.8	123.0
C2	0.7	1.1	2.3	2.1	1.8	2.2	1.1	1.6	0.2	0.05	1.7	2.1	2.0	2.2
C3	15.5	2.3	7.7	5.5	8.3	5.7	9.5	4.7	16.4	1.1	6.0	5.5	7.6	4.6
C4	3.6	0.7	7.1	2.4	4.2	2.3	5.4	2.6	2.6	0.1	5.4	3.1	7.7	1.5
TN														
	Bare soil		Civic		Com+Ind		Multifamily		Single Family		Transportation		Undeveloped	
	Mean	Std. Dev.	Mean	Std. Dev.	Mean	Std. Dev	Mean	Std. Dev.	Mean	Std. Dev.	Mean	Std. Dev	Mean	Std. Dev.
C1	0.4	0.04	0.005	0.01	0.01	0.03	0.01	0.02	0.4	0.09	0.03	0.08	0.3	0.2
C2	0.4	0.5	0.8	0.8	0.7	0.9	0.6	0.8	0.06	0.2	0.5	0.7	0.5	1.0
C3	56.6	23.4	36.8	26.2	49.7	24.4	43.0	22.0	8.7	18.5	37.0	25.9	7.9	9.2
C4	5.4	1.6	6.0	3.0	5.9	2.5	6.6	2.3	3.7	2.8	5.5	3.0	7.2	1.7
TP														
	Bare soil		Civic		Com+Ind		Multifamily		Single Family		Transportation		Undeveloped	
	Mean	Std. Dev.	Mean	Std. Dev.	Mean	Std. Dev	Mean	Std. Dev.	Mean	Std. Dev.	Mean	Std. Dev	Mean	Std. Dev.
C1	0.01	0.02	1e-4	4e-5	0.005	0.02	0.02	0.03	0.01	0.02	0.004	0.02	1e-4	3e-5
C2	0.03	0.08	0.4	0.6	0.06	0.3	0.1	0.3	0.005	0.004	0.1	0.3	0.02	0.1
C3	6.7	2.7	2.1	2.7	4.7	2.8	4.8	3.6	1.7	2.7	4.8	3.8	4.4	2.8
C4	2.0	1.9	4.8	3.0	2.9	2.1	4.0	2.8	2.1	1.9	2.5	2.7	4.4	3.0

Eight runoff events measured at the outlet of the Shoal Creek Watershed over the period July 2008 to December 2013 were selected from the USGS archive (USGS,

2014b) (Table 4.8). The associated base flow index (BFI), a measure of the proportion of stream flow that is baseflow (ranging from 0 to 1), and water quality data of the measured runoff (direct runoff plus base flow) are also provided in Table 4.8. July 2008 was selected as the simulation starting point because the last recorded BMP in the GIS database for the Shoal Creek Watershed was dated May 12, 2008 (City of Austin, 2014b).

Table 4.8. Runoff events chosen for SWMM calibration

From		To		Mean flow rate (cms)	BFI	TSS (mg/L)	TN (mg/L)	TP (mg/L)
07/24/2008	18:10	07/24/2008	21:40	0.45	0.39	466	3.2	0.59
02/09/2009	7:40	02/09/2009	14:25	0.42	0.17	214	2.2	0.4
01/09/2011	2:45	01/09/2011	23:30	3.77	0.52	244	1.9	0.44
11/15/2011	10:40	11/15/2011	18:15	0.28	0.25	82	2.3	0.32
11/22/2011	4:25	11/22/2011	11:15	1.20	0.54	444	2.5	0.58
03/09/2012	14:20	03/10/2012	3:10	1.02	0.13	320	1.9	0.41
07/09/2012	19:15	07/10/2012	2:05	0.29	0.11	176	2.1	0.33
10/30/2013	21:10	10/31/2013	13:55	13.75	0.09	762	2.5	0.97

Calculation of direct runoff concentration

In Table 4.8, the BFIs were used to calculate the proportion of the measured TSS, TN and TP concentrations in direct runoff because SWMM models only direct runoff, omitting the groundwater module for simplicity (see Chapter 3 for details).

Concentrations were calculated for direct runoff using Equation 3.5 assuming uniform mixing of base flow and direct runoff for the water quality constituents. In Equation 3.5, C_{dir} indicates the concentration of direct runoff, C_{mix} indicates the mixed concentration in USGS-measured runoff in streamflow, C_{bf} indicates the concentration of base flow, and BFI is base flow index.

$$C_{dir} = \frac{C_{mix} - C_{bf} \cdot BFI}{(1 - BFI)} \tag{3.5}$$

Two sources of data were used to estimate base flow concentrations of TSS, TN and TP. The first source was satellite-derived water quality in Lady Bird Lake. By choosing dates when only baseflow was present in Shoal Creek (BFI = 1) any change of water quality in Lady Bird Lake between the locations before and after the confluence of Shoal Creek is solely influenced by baseflow of Shoal Creek. The second source is groundwater samples in or close to the watershed. Base flow concentration is calculated primarily based on the first source, with the second source as a backup.

Satellite imagery has been used to determine water quality in numerous studies (Liu et al., 2003; Bukata, 2005). Each water quality constituent exhibits a specific spectral response that can be observed by satellites (Liu et al., 2003). Studies have indicated that multispectral satellite imagery can be used to estimate water quality using a variety of methods, with the majority using either multiple regression analysis or artificial neural networks (ANN) (Kloiber et al., 2002; Liu et al., 2003; Kishino et al., 2005). An earlier study on Lady Bird Lake determined the relationship between reflectance of each band and the concentration of total suspended solids (TSS), total nitrogen (TN), and total phosphorous (TP). Please refer to Chapter 2 for details.

The satellite derived relationships for TSS, TN and TP from the study in Chapter 2 was used to determine concentrations of these constituents at two points in Lady Bird Lake. Six Landsat images (Table 4.9) with BFI = 1 in Shoal Creek around the dates of the images were selected for the procedure. Point A was before the confluence of Shoal Creek and Lady Bird Lake and represented the original concentrations of these constituents in the lake. Point B was approximately 130 meters downstream from the confluence point and had negligible lateral offset from the mixing point of Shoal Creek and Lady Bird Lake. Therefore, the changes in water quality constituent concentrations from point A to point B were assumed to be only a result of inflow from Shoal Creek. Equation 4.1 was used to determine the concentration change of TSS, TN and TP by the inflow from Shoal Creek measured at Point B (Socolofsky and Jirka, 2005). Equation 4.1 assumes two no-flux boundaries. The first one is the free surface of the Lady Bird Lake. The second is the nearest bank of Lady Bird Lake, which is approximately 15 meters from point B. The bottom and the far bank of Lady Bird Lake are not considered boundaries. Only the first reflectance from the boundary was considered for simplicity of application of the equation.

Table 4.9. Landsat images used in deriving TSS, TN and TP concentrations in Lady Bird Lake

Date	Remote sensor
April 22, 2009	Landsat 7 ETM+
October 15, 2009	Landsat 7 ETM+
July 30, 2010	Landsat 7 ETM+
September 16, 2010	Landsat 7 ETM+
January 22, 2011	Landsat 7 ETM+
February 26, 2012	Landsat 7 ETM+

$$C(x,y,z) = \frac{\dot{m}}{4\pi x\sqrt{D_z D_y}}\left(2 \cdot \exp\left(-\frac{z^2 U}{4D_z x} - \frac{y^2 U}{4D_y x}\right) + \exp\left(-\frac{z^2 U}{4D_z x} - \frac{(y-30)^2 U}{4D_y x}\right)\right) \quad (4.1)$$

Where C(x,y,z) represents the change in concentration of a particular constituent from point A to point B in Lady Bird Lake (with point B at position (x, y, z) relative to the confluence point, which is (0, 0, 0)), $\dot{m}$ is the mass flux of the point source (at the confluence point) (mass/sec), D_z and D_y are the vertical and lateral diffusion coefficients estimated as 0.0061 (m^2/s) and 0.1364 (m^2/s) respectively from equations derived by Fischer et al. (1979), and U is the mean flow velocity. The monthly mean flow velocities from 1985 to 2010 of Lady Bird Lake are provided in Table 4.10 and were used to determine U (Bob Huber of Lower Colorado River Authority, personal communication, 20 August 2012). The flow velocity in Table 4.10 corresponding to the month of each image in Table 4.9 is chosen for U.

In this study, z is 0.3 meter (1 foot) to represent the fact that the satellite-derived water quality was calibrated by the 1-foot deep USGS water quality samples, as

described in Chapter 2. The value of y in this study is zero since there is little lateral offset between the confluence point and point B. The value of x is 130 m. Using Equation 4.1, the mass flux $\dot{m}$ can be calculated at the confluence point (i.e. outlet of the Shoal Creek Watershed). Since the chosen image dates contain only base flow (BFI = 1), the base flow concentration can be calculated by dividing the mass flux (mass/sec) by flow rate (volume/sec), which is the daily mean flow rate from USGS (USGS, 2014b). The mean of the six base flow estimates derived from images listed in Table 4.9 was used in calculation of concentrations of direct runoff by Equation 3.5.

Table 4.10. Monthly average flow velocities in Lady Bird Lake

	Jan	Feb	Mar	Apr	May	Jun	Jul	Aug	Sep	Oct	Nov	Dec
m/s	0.027	0.029	0.047	0.052	0.073	0.092	0.072	0.059	0.055	0.023	0.013	0.020

There was only one groundwater sampling station (YD-58-35-701) with water quality samples in the Shoal Creek Watershed (USGS, 2014b). The average groundwater concentrations, assumed to be close to the baseflow concentrations in Shoal Creek, of silica after filtration (USGS water quality constituent # 00955, the water quality constituent closest to TSS for groundwater samples), TN (# 00600), and TP (# 00665) are provided in Table 4.11. Depending on soil and bedrock imperviousness, the ratio of nitrate concentration in groundwater and in base flow generally ranges from 1:10

to 10:1 (USGS, 2010). For regions with impervious soil like the Shoal Creek Watershed, the concentration in base flow is higher than that in groundwater (USGS, 2010). As for phosphorous, a few studies showed that the ratio of TP concentrations in base flow and in groundwater is also in that range (CSIRO, 2009). Therefore, if a satellite derived baseflow concentration for a particular constituent was ten times higher than the groundwater value, the satellite-derived value was discarded and the groundwater concentration was used instead.

Table 4.11. Mean values for TSS (used "silica after filtration" instead), TN, and TP in groundwater

	Silica after filtration	TN	TP
Baseflow concentration (mg/L)	12.07	0.42	0.02

Grouping of BMPs

It is impractical to calibrate removal efficiency for individual BMPs due to the large number of BMPs in the Shoal Creek Watershed. Therefore, a three-phase simplification/grouping process was performed to merge individual BMPs into a smaller number of "BMP categories". BMPs grouped into a common category were assumed to have identical efficiencies. The term "removal efficiency" in this study is defined as the

proportion of pollutant removed by the BMP where a value of 1 means total removal and a value of 0 means no removal. The factors considered in categorization were:

1. Type of BMP,

2. Dominant land use type in the BMP catchment,

3. The areal ratio of the dominant land use in the catchment (dominant land use area / BMP catchment area),

4. Slope at the BMP location ,

5. The ratio of BMP area / BMP catchment area,

BMP type is the most essential categorization factor because form defines function in this case. The other factors were chosen primarily because they can be easily quantified using readily available GIS data. Some studies have hinted that land use can affect BMP removal efficiency (ASCE, 2001), but no comprehensive study has been conducted. Therefore, this study hypothesizes that land use is one of the main influences on BMP removal efficiency resulting in the selection of dominant land use type and its areal ratio as grouping factors. Slope has also been found to be a controlling factor in removal efficiency for some types of BMPs (Yu et al., 2001; Liu et al., 2008). There were three reasons that BMP area rather than BMP holding capacity was selected as a factor. First, the ratio of area of the BMP to the area of the entire catchment has been found important for BMP removal efficiency (Liu et al., 2008). Second, using available data in the city of Austin GIS database (City of Austin, 2014b), it was found that the area of BMPs had a strong linear correlation to the holding capacity (Figure 4.2). Lastly

holding capacity is not commonly available in GIS databases. Therefore, the ratio of BMP area to total watershed area was selected.

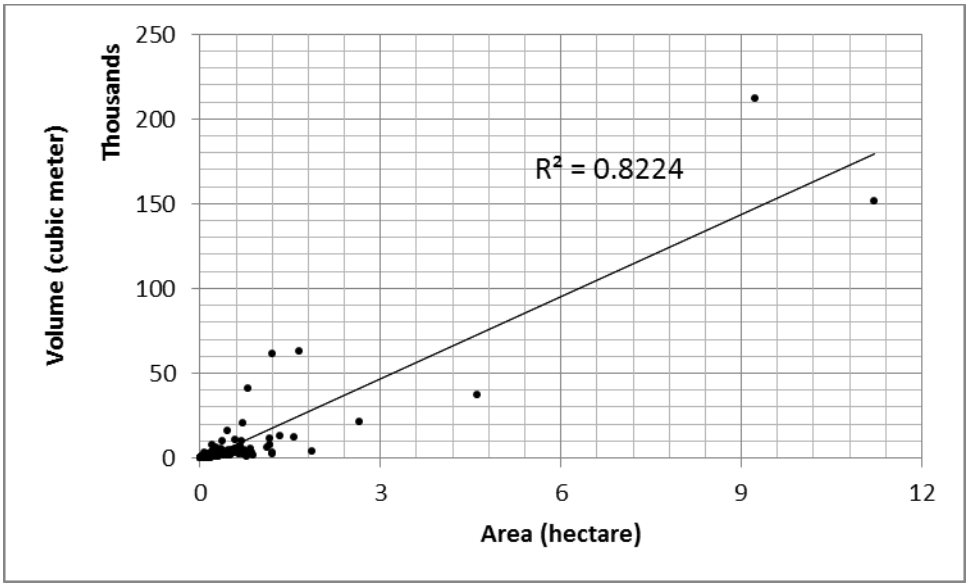

Figure 4.2. Scatter plot of BMP area and BMP holding capacity

Fourteen types of BMPs have been installed in the Shoal Creek Watershed (Table 4.2). In the first phase of categorization, these 14 types of BMPs were simplified into four basic types: detention with impervious bottom, detention with pervious bottom, infiltration, and retention. These categories were based on three attributes of BMPs: how water was stored in the BMP, whether the bottom is pervious or impervious, and

whether significant infiltration/filtration is facilitated based on significant vegetative cover, as illustrated in Figure 4.3.

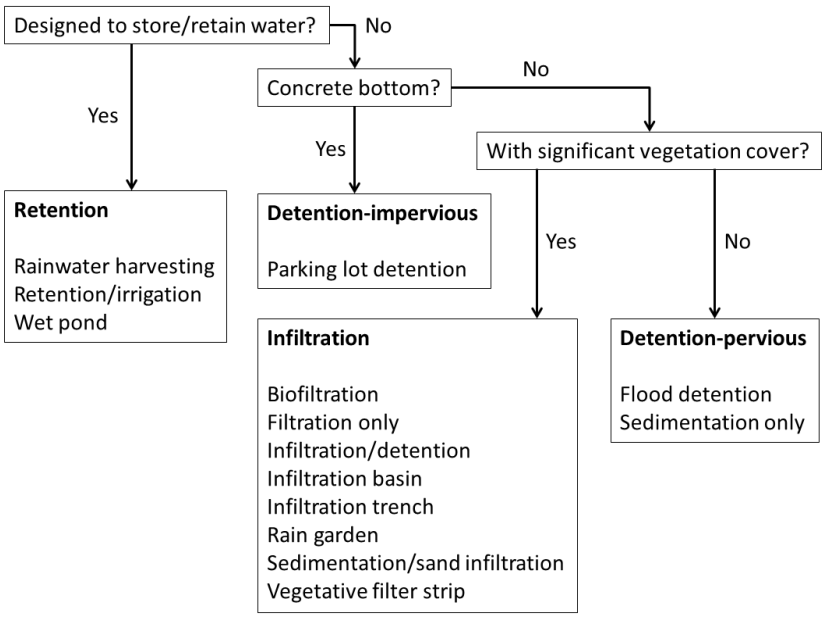

Figure 4.3. Methodology for grouping BMPs in the city of Austin

In the second phase, BMPs within the same category in individual subcatchments were merged into a single BMP device, following a method proposed by Elliot et al. (2009). Elliot et al. aggregated multiple BMP devices into fewer devices in an urban watershed with negligible loss of model accuracy. Travel time from the aggregated device to the watershed outlet is the median of the travel times of all devices. Other

attributes were summed up for the aggregated device. In the end of this phase, each subcatchment had at most four BMP devices, potentially one of each category.

After the initial merging in the second phase, the last phase further categorized BMPs in the watershed by considering all five categorization factors. Table 4.12 (a)-(d) show the detailed definition of categories. The mean value of continuous factors for each category is also provided in Table 4.12, which is discussed in a later section. The numerical ranges of each category were deliberately created to result in similar numbers of BMPs in each category at the end of the process. A total of 142 distinct BMP categories were identified, down from the 835 individual actual BMPs.

Table 4.12. Definition and mean value of continuous factors of each BMP category ("com+ind" means the land use of commercial plus industrial)

(a) Detention-impervious

Definition					Values used in statistical analysis (only continuous variables listed)		
Type of BMP	**Dominant Land use**	**Dominant LU area / catchment area**	**BMP area / catchment area**	**Slope (%)**	**Dominant LU area / catchment area**	**BMP area / catchment area**	**Slope (%)**
Detention-impervious	Single family	0.53-0.7	0.01-0.07	1.5-3	0.61	0.03	2.2
Detention-impervious	Single family	0.53-0.7	0.01-0.07	>3	0.61	0.03	6
Detention-impervious	Single family	0.7-0.82	0-0.01	0-1.5	0.8	0.005	1

Table 4.12. Continued

Definition					Values used in statistical analysis (only continuous variables listed)		
Type of BMP	**Dominant Land use**	**Dominant LU area / catchment area**	**BMP area / catchment area**	**Slope (%)**	**Dominant LU area / catchment area**	**BMP area / catchment area**	**Slope (%)**
Detention-impervious	Single family	0.7-0.82	0.01-0.07	0-1.5	0.8	0.03	1
Detention-impervious	Multifamily	0.25-0.55	0-0.01	0-1.5	0.38	0.005	1
Detention-impervious	Multifamily	0.25-0.55	0.01-0.07	0-1.5	0.38	0.03	1
Detention-impervious	Multifamily	0.25-0.55	0.01-0.07	>3	0.38	0.03	6
Detention-impervious	Multifamily	0.25-0.55	>0.07	0-1.5	0.38	0.2	1
Detention-impervious	Multifamily	0.55-0.67	0-0.01	0-1.5	0.63	0.005	1
Detention-impervious	Multifamily	0.55-0.67	>0.07	0-1.5	0.63	0.2	1
Detention-impervious	Multifamily	0.55-0.67	>0.07	>3	0.63	0.2	6
Detention-impervious	Multifamily	0.67-1	>0.07	0-1.5	0.81	0.2	1
Detention-impervious	Com + Ind*	0.17-0.55	0-0.01	0-1.5	0.4	0.005	1
Detention-impervious	Com + Ind	0.17-0.55	0-0.01	>3	0.4	0.005	6
Detention-impervious	Com + Ind	0.17-0.55	0.01-0.07	1.5-3	0.4	0.03	6
Detention-impervious	Com + Ind	0.17-0.55	0.01-0.07	>3	0.4	0.03	6

Table 4.12. Continued

Definition					Values used in statistical analysis (only continuous variables listed)		
Type of BMP	**Dominant Land use**	**Dominant LU area / catchment area**	**BMP area / catchment area**	**Slope (%)**	**Dominant LU area / catchment area**	**BMP area / catchment area**	**Slope (%)**
Detention-impervious	Com + Ind	0.17-0.55	>0.07	0-1.5	0.4	0.2	1
Detention-impervious	Com + Ind	0.17-0.55	>0.07	1.5-3	0.4	0.2	2.2
Detention-impervious	Com + Ind	0.55-0.77	0-0.01	1.5-3	0.67	0.005	2.2
Detention-impervious	Com + Ind	0.55-0.77	0.01-0.07	0-1.5	0.67	0.03	1
Detention-impervious	Com + Ind	0.55-0.77	0.01-0.07	1.5-3	0.67	0.03	2.2
Detention-impervious	Com + Ind	0.55-0.77	0.01-0.07	>3	0.67	0.03	6
Detention-impervious	Com + Ind	0.55-0.77	>0.07	0-1.5	0.67	0.2	1
Detention-impervious	Com + Ind	0.55-0.77	>0.07	>3	0.67	0.2	6
Detention-impervious	Com + Ind	0.77-1	0-0.01	0-1.5	0.9	0.005	1
Detention-impervious	Com + Ind	0.77-1	0-0.01	1.5-3	0.9	0.005	2.2
Detention-impervious	Com + Ind	0.77-1	0.01-0.07	1.5-3	0.9	0.03	2.2
Detention-impervious	Com + Ind	0.77-1	0.01-0.07	>3	0.9	0.03	6
Detention-impervious	Com + Ind	0.77-1	>0.07	0-1.5	0.9	0.2	1

Table 4.12. Continued

Definition					Values used in statistical analysis (only continuous variables listed)		
Type of BMP	**Dominant Land use**	**Dominant LU area / catchment area**	**BMP area / catchment area**	**Slope (%)**	**Dominant LU area / catchment area**	**BMP area / catchment area**	**Slope (%)**
Detention-impervious	Com + Ind	0.77-1	>0.07	1.5-3	0.9	0.2	2.2
Detention-impervious	Com + Ind	0.77-1	>0.07	>3	0.9	0.2	6
Detention-impervious	Transportation	0.38-0.55	0.01-0.07	1.5-3	0.46	0.03	2.2
Detention-impervious	Transportation	0.38-0.55	0.01-0.07	>3	0.46	0.03	6
Detention-impervious	Transportation	0.55-0.77	>0.07	1.5-3	0.62	0.2	2.2
Detention-impervious	Transportation	0.77-0.85	>0.07	>3	0.78	0.2	6

(b) Detention-pervious

Definition					Values used in statistical analysis (only continuous variables listed)		
Type of BMP	**Dominant Land use**	**Dominant LU area / catchment area**	**BMP area / catchment area**	**Slope (%)**	**Dominant LU area / catchment area**	**BMP area / catchment area**	**Slope (%)**
Detention - pervious	Single Family	0.33-0.45	0-0.01	0-1.5	0.39	0.005	1
Detention - pervious	Single Family	0.33-0.45	0-0.01	1.5-3	0.39	0.005	2.2
Detention - pervious	Single Family	0.33-0.45	0-0.01	>3	0.39	0.005	6

Table 4.12. Continued

Definition					Values used in statistical analysis (only continuous variables listed)		
Type of BMP	**Dominant Land use**	**Dominant LU area / catchment area**	**BMP area / catchment area**	**Slope (%)**	**Dominant LU area / catchment area**	**BMP area / catchment area**	**Slope (%)**
Detention - pervious	Single Family	0.33-0.45	0.01-0.07	1.5-3	0.39	0.03	2.2
Detention - pervious	Single Family	0.33-0.45	0.01-0.07	>3	0.39	0.03	6
Detention - pervious	Single Family	0.33-0.45	>0.07	0-1.5	0.39	0.2	1
Detention - pervious	Single Family	0.45-0.6	0-0.01	0-1.5	0.52	0.005	1
Detention - pervious	Single Family	0.45-0.6	0-0.01	1.5-3	0.52	0.005	2.2
Detention - pervious	Single Family	0.45-0.6	0-0.01	>3	0.52	0.005	6
Detention - pervious	Single Family	0.45-0.6	0.01-0.07	1.5-3	0.52	0.03	2.2
Detention - pervious	Single Family	0.45-0.6	0.01-0.07	>3	0.52	0.03	6
Detention - pervious	Single Family	0.6-0.85	0-0.01	0-1.5	0.73	0.005	1
Detention - pervious	Single Family	0.6-0.85	0-0.01	1.5-3	0.73	0.005	2.2
Detention - pervious	Single Family	0.6-0.85	0-0.01	>3	0.73	0.005	6
Detention - pervious	Single Family	0.6-0.85	0.01-0.07	0-1.5	0.73	0.03	1
Detention - pervious	Single Family	0.6-0.85	0.01-0.07	>3	0.73	0.03	6

Table 4.12. Continued

Definition					Values used in statistical analysis (only continuous variables listed)		
Type of BMP	**Dominant Land use**	**Dominant LU area / catchment area**	**BMP area / catchment area**	**Slope (%)**	**Dominant LU area / catchment area**	**BMP area / catchment area**	**Slope (%)**
Detention - pervious	Multifamily	0.19-0.45	0-0.01	0-1.5	0.38	0.005	1
Detention - pervious	Multifamily	0.19-0.45	0-0.01	>3	0.38	0.005	6
Detention - pervious	Multifamily	0.19-0.45	0.01-0.07	>3	0.38	0.03	6
Detention - pervious	Multifamily	0.45-0.8	0-0.01	1.5-3	0.62	0.005	2.2
Detention - pervious	Multifamily	0.45-0.8	0-0.01	>3	0.62	0.005	6
Detention - pervious	Multifamily	0.45-0.8	0.01-0.07	0-1.5	0.62	0.03	1
Detention - pervious	Multifamily	0.45-0.8	0.01-0.07	1.5-3	0.62	0.03	2.2
Detention - pervious	Multifamily	0.45-0.8	0.01-0.07	>3	0.62	0.03	6
Detention - pervious	Multifamily	0.45-0.8	>0.07	>3	0.62	0.2	6
Detention - pervious	Multifamily	0.8-1	0.01-0.07	0-1.5	0.98	0.03	1
Detention - pervious	Multifamily	0.8-1	>0.07	0-1.5	0.98	0.2	1
Detention - pervious	Multifamily	0.8-1	>0.07	>3	0.98	0.2	6
Detention - pervious	Civic	0.29-0.55	0-0.01	1.5-3	0.4	0.005	2.2

Table 4.12. Continued

Definition					Values used in statistical analysis (only continuous variables listed)		
Type of BMP	**Dominant Land use**	**Dominant LU area / catchment area**	**BMP area / catchment area**	**Slope (%)**	**Dominant LU area / catchment area**	**BMP area / catchment area**	**Slope (%)**
Detention - pervious	Civic	0.29-0.55	0-0.01	>3	0.4	0.005	6
Detention - pervious	Civic	0.29-0.55	0.01-0.07	1.5-3	0.4	0.03	2.2
Detention - pervious	Civic	0.29-0.55	0.01-0.07	>3	0.4	0.03	6
Detention - pervious	Civic	0.29-0.55	>0.07	1.5-3	0.4	0.2	2.2
Detention - pervious	Civic	0.55-0.9	0.01-0.07	0-1.5	0.68	0.03	1
Detention - pervious	Civic	0.55-0.9	0.01-0.07	1.5-3	0.68	0.03	2.2
Detention - pervious	Civic	0.55-0.9	>0.07	1.5-3	0.68	0.2	2.2
Detention - pervious	Civic	0.9-1	0-0.01	1.5-3	0.97	0.005	2.2
Detention - pervious	Civic	0.9-1	0.01-0.07	>3	0.97	0.03	6
Detention - pervious	Civic	0.9-1	>0.07	1.5-3	0.97	0.2	2.2
Detention - pervious	Com + Ind	0.18-0.4	0-0.01	0-1.5	0.31	0.005	1
Detention - pervious	Com + Ind	0.18-0.4	0-0.01	1.5-3	0.31	0.005	2.2
Detention - pervious	Com + Ind	0.18-0.4	0-0.01	>3	0.31	0.005	6

Table 4.12. Continued

Definition					Values used in statistical analysis (only continuous variables listed)		
Type of BMP	**Dominant Land use**	**Dominant LU area / catchment area**	**BMP area / catchment area**	**Slope (%)**	**Dominant LU area / catchment area**	**BMP area / catchment area**	**Slope (%)**
Detention - pervious	Com + Ind	0.18-0.4	0.01-0.07	0-1.5	0.31	0.03	1
Detention - pervious	Com + Ind	0.18-0.4	0.01-0.07	1.5-3	0.31	0.03	2.2
Detention - pervious	Com + Ind	0.18-0.4	0.01-0.07	>3	0.31	0.03	6
Detention - pervious	Com + Ind	0.18-0.4	>0.07	0-1.5	0.31	0.2	1
Detention - pervious	Com + Ind	0.4-0.7	0-0.01	0-1.5	0.54	0.005	1
Detention - pervious	Com + Ind	0.4-0.7	0-0.01	1.5-3	0.54	0.005	2.2
Detention - pervious	Com + Ind	0.4-0.7	0.01-0.07	0-1.5	0.54	0.03	1
Detention - pervious	Com + Ind	0.4-0.7	0.01-0.07	1.5-3	0.54	0.03	2.2
Detention - pervious	Com + Ind	0.4-0.7	0.01-0.07	>3	0.54	0.03	6
Detention – pervious	Com + Ind	0.4-0.7	>0.07	0-1.5	0.54	0.2	1
Detention - pervious	Com + Ind	0.4-0.7	>0.07	1.5-3	0.54	0.2	2.2
Detention - pervious	Com + Ind	0.7-1	0-0.01	0-1.5	0.87	0.005	1
Detention - pervious	Com + Ind	0.7-1	0-0.01	1.5-3	0.87	0.005	2.2

Table 4.12. Continued

Definition					Values used in statistical analysis (only continuous variables listed)		
Type of BMP	**Dominant Land use**	**Dominant LU area / catchment area**	**BMP area / catchment area**	**Slope (%)**	**Dominant LU area / catchment area**	**BMP area / catchment area**	**Slope (%)**
Detention - pervious	Com + Ind	0.7-1	0-0.01	>3	0.87	0.005	6
Detention - pervious	Com + Ind	0.7-1	0.01-0.07	1.5-3	0.87	0.03	2.2
Detention - pervious	Com + Ind	0.7-1	0.01-0.07	>3	0.87	0.03	6
Detention - pervious	Com + Ind	0.7-1	>0.07	0-1.5	0.87	0.2	1
Detention - pervious	Com + Ind	0.7-1	>0.07	1.5-3	0.87	0.2	2.2
Detention - pervious	Com + Ind	0.7-1	>0.07	>3	0.87	0.2	6
Detention - pervious	Transportation	0.18-0.35	0-0.01	0-1.5	0.26	0.005	1
Detention - pervious	Transportation	0.18-0.35	0-0.01	1.5-3	0.26	0.005	2.2
Detention - pervious	Transportation	0.18-0.35	>0.07	>3	0.26	0.2	6
Detention - pervious	Transportation	0.35-0.52	0-0.01	1.5-3	0.46	0.005	2.2
Detention - pervious	Transportation	0.35-0.52	0.01-0.07	1.5-3	0.46	0.03	2.2
Detention - pervious	Transportation	0.35-0.52	0.01-0.07	>3	0.46	0.03	6
Detention - pervious	Transportation	0.35-0.52	>0.07	0-1.5	0.46	0.2	1

Table 4.12. Continued

Definition					Values used in statistical analysis (only continuous variables listed)		
Type of BMP	**Dominant Land use**	**Dominant LU area / catchment area**	**BMP area / catchment area**	**Slope (%)**	**Dominant LU area / catchment area**	**BMP area / catchment area**	**Slope (%)**
Detention - pervious	Transportation	0.52-0.8	0-0.01	>3	0.63	0.005	6
Detention - pervious	Transportation	0.52-0.8	0.01-0.07	0-1.5	0.63	0.03	1
Detention - pervious	Transportation	0.52-0.8	0.01-0.07	>3	0.63	0.03	6
Detention - pervious	Undeveloped	0.56-0.65	0-0.01	1.5-3	0.58	0.005	2.2
Detention - pervious	Undeveloped	0.56-0.65	0.01-0.07	1.5-3	0.58	0.03	2.2
Detention - pervious	Undeveloped	0.65-0.78	>0.07	1.5-3	0.73	0.2	2.2
Detention - pervious	Undeveloped	0.65-0.78	>0.07	>3	0.73	0.2	6

(c) Infiltration

Definition					Values used in statistical analysis (only continuous variables listed)		
Type of BMP	**Dominant Land use**	**Dominant LU area / catchment area**	**BMP area / catchment area**	**Slope (%)**	**Dominant LU area / catchment area**	**BMP area / catchment area**	**Slope (%)**
Infiltration	Single Family	0.51-0.75	0-0.01	>3	0.64	0.005	6
Infiltration	Single Family	0.51-0.75	>0.07	1.5-3	0.64	0.2	2.2
Infiltration	Single Family	0.51-0.75	>0.07	>3	0.64	0.2	6
Infiltration	Multifamily	0.99	>0.07	1.5-3	0.99	0.2	2.2

Table 4.12. Continued

Definition					Values used in statistical analysis (only continuous variables listed)		
Type of BMP	**Dominant Land use**	**Dominant LU area / catchment area**	**BMP area / catchment area**	**Slope (%)**	**Dominant LU area / catchment area**	**BMP area / catchment area**	**Slope (%)**
Infiltration	Multifamily	1	>0.07	>3	1	0.2	6
Infiltration	Civic	0.5-0.89	0.01-0.07	>3	0.68	0.03	6
Infiltration	Civic	0.5-0.89	>0.07	1.5-3	0.68	0.2	2.2
Infiltration	Civic	0.89-1	>0.07	1.5-3	0.99	0.2	2.2
Infiltration	Com + Ind	0.54-0.7	0.01-0.07	1.5-3	0.62	0.03	2.2
Infiltration	Com + Ind	0.54-0.7	0.01-0.07	>3	0.62	0.03	6
Infiltration	Com + Ind	0.54-0.7	>0.07	1.5-3	0.62	0.2	2.2
Infiltration	Com + Ind	0.7-0.87	0.01-0.07	>3	0.8	0.03	6
Infiltration	Com + Ind	0.7-0.87	>0.07	0-1.5	0.8	0.2	1
Infiltration	Com + Ind	0.7-0.87	>0.07	>3	0.8	0.2	6
Infiltration	Com + Ind	0.87-1	0.01-0.07	>3	0.99	0.03	6
Infiltration	Com + Ind	0.87-1	>0.07	1.5-3	0.99	0.2	2.2
Infiltration	Com + Ind	0.87-1	>0.07	>3	0.99	0.2	6
Infiltration	Transportation	0.52	0.01-0.07	0-1.5	0.52	0.03	1
Infiltration	Transportation	0.62	>0.07	1.5-3	0.62	0.2	2.2
Infiltration	Transportation	0.75	0.01-0.07	0-1.5	0.75	0.03	1
Infiltration	Undeveloped	0.2	>0.07	>3	0.2	0.2	6
Infiltration	Undeveloped	0.6-0.99	>0.07	1.5-3	0.8	0.2	2.2

Table 4.12. Continued

(d) Retention

Definition					Values used in statistical analysis (only continuous variables listed)		
Type of BMP	**Dominant Land use**	**Dominant LU area / catchment area**	**BMP area / catchment area**	**Slope (%)**	**Dominant LU area / catchment area**	**BMP area / catchment area**	**Slope (%)**
Retention	Multifamily	0.69	0.01-0.07	>3	0.69	0.03	6
Retention	Multifamily	0.9	0.01-0.07	0-1.5	0.9	0.03	1
Retention	Civic	0.42	0.01-0.07	1.5-3	0.42	0.03	2.2
Retention	Com + Ind	0.98	>0.07	1.5-3	0.98	0.2	2.2
Retention	Transportation	0.36-0.5	0.01-0.07	0-1.5	0.43	0.03	1
Retention	Transportation	0.36-0.5	0.01-0.07	1.5-3	0.43	0.03	2.2
Retention	Transportation	0.5-0.65	0.01-0.07	1.5-3	0.59	0.03	2.2
Retention	Transportation	0.5-0.65	>0.07	0-1.5	0.59	0.2	1
Retention	Undeveloped	0.56	>0.07	0-1.5	0.56	0.2	1
Retention	Undeveloped	0.83	0.01-0.07	1.5-3	0.83	0.03	2.2

Calibrating for BMP removal efficiency

Barrett (2005) determined that a linear equation with an intercept can be a good approach to describe the relationship of influence and effluence concentrations. However, a single-coefficient equation without the intercept term was used in this study in order to reduce the number of parameters being calibrated. The single-coefficient equation can be described by Equation 4.2:

$$C_{eff} = (1 - E) \cdot C_{inf} \quad (4.2)$$

Where E is the removal efficiency of the BMP (an E of 1 means complete removal of pollutant, and an E of 0 indicates no removal), C_{eff} is the concentration of the constituent of interest (mg/L) as it leaves the BMP, C_{inf} is the concentration of the constituent of interest (mg/L) as it enters the BMP. Note that the definition of removal efficiency in equation (1) is different from that of SWMM (Rossman, 2010), which is percent reduction.

The concept of calibrating BMP removal efficiency is to use BMP removal efficiency of each "BMP category" as parameters being calibrated in the SWMM model (from "model construction" in Step 1), and make the simulated and observed pollutant concentrations at the outlet of Shoal Creek Watershed to be as close to each other as possible. BMP devices belonging to the same category have the same removal efficiency during calibration. Removal efficiency of BMPs was calibrated automatically using the Shuffled Complex Evolution – University of Arizona (SCEUA) module (Duan et al., 1993) of PEST (Doherty, 2010).

If multiple BMP devices occur to be in the same subcatchment, the subcatchment is further divided for each BMP device according to the area of catchment of each BMP device. Attributes such as slope and dominant land use of each BMP catchment are assumed to be identical of the original subcatchment.. The goal of such action is to have only one BMP device in a subcatchment so the pollutant removal efficiency of the device can be individually examined. After such adjustments, the number of subcatchments increased from 264 (in "model construction") to 390. These adjustments could not be done in the "model construction" of Step 1 because the BMP devices

merged by the method proposed by Elliot et al. (2009) are not considered to be at any specific location, so physical catchments cannot be created specifically for any merged BMP device. Attributes of catchments for each BMP device must be created from an existing "blue print", which is the subcatchments in "model construction" of Step 1.

In order to facilitate calibration of the removal efficiency, modification to the original SWMM engine was required. The original SWMM model assigns BMP removal efficiency based on land use and does not consider removal efficiency of individual BMPs. The function of Low Impact Development (LID) in SWMM deals only with the hydrology, not water quality. Thus, sections of the SWMM engine were rewritten to allow removal efficiency in water quality improvements to be calibrated for individual BMP devices. Please refer to Appendix A for details of the modified SWMM. In Appendix A, only modified source code files are shown. Deleted parts are shown with a strikethrough, and added parts are shown with an underline.

Monte Carlo Simulations were performed to take account for two sources of uncertainty in calibration, as Table 4.13 shows:

1. The uncertainty of the parameters of pollutant buildup/washoff; and

2. The uncertainty of base flow concentrations from coefficients of predictive equations for satellite-derived water quality.

Table 4.13. Sources of uncertainty considered in Monte Carlo Simulation

Parameters varies in Monte Carlo Simulations	Source	Probability distribution
pollutant buildup/washoff used in SWMM	From Chapter 3	General Lambda Distribution
	From literature	Normal distribution
coefficients of predictive equations for satellite-derived water quality	From Chapter 3	Normal distribution

Two Monte Carlo Simulations (100 calibrations each) were performed for each water quality constituent. One of them used pollutant buildup/washoff parameters from the literature (Table 4.6) and the other used buildup/washoff parameters based on land use (Table 4.7). The flow chart of Monte Carlo Simulations in this study is provided in Figure 4.4.

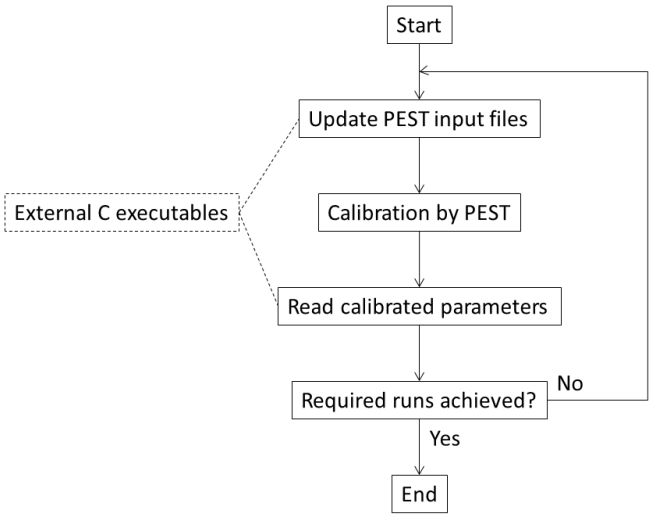

Figure 4.4. Monte Carlo Simulations used in the research to account for the uncertainty in parameters

4.4.2. Determine the Relationship between Environmental Factors and BMP Removal Efficiency

Multiple linear regression analysis was used to analyze the relationships between BMP removal efficiency (dependent variable) and the categories used to group them (independent variables) from all available Monte Carlo Simulation results. Since these categories represent the influence of the environment in which each BMP is installed, they will be termed "environmental factors" hereafter. Mean values were used in the analysis for each of the factors that was numerical in nature i.e. ratio of BMP area/catchment area, slope of the BMP and ratio of dominant land use area/catchment area, as shown in Table 4.12. For categorical factors (type of BMP, and dominant land

use), dummy variables were created in multiple regression analysis. If a categorical factor has n possible outcomes, (n-1) dummy variables were created. Each dummy variable was one-to-one associated to one outcome, leaving one "reference outcome" without an associated dummy variable. For each of the outcomes (excluding the reference outcome), a value of 1 for corresponding dummy variable means appearance of such outcome, and a value of 0 means no such outcome. Values of -1 for all dummy variables indicate the existence of the reference outcome. This system is used by the statistical software JMP (SAS, 2014), used for the multiple regression analysis of this study.

An example of the assignment of dummy variables is illustrated for the factor "type of BMP". There are four possible outcomes: detention-impervious, detention-pervious, infiltration, and retention. Three dummy variables were created: DV[detention-impervious], DV[detention-pervious], and DV[infiltration]. DV[retention] was assigned as the "reference outcome" for this group. Table 4.14 shows the four possible combinations in value assignment of dummy variables for different types of BMPs.

Table 4.14. Example of assigning values of dummy variables to different outcomes of a categorical variable

Type of BMP	DV[detention-impervious]	DV[detention-pervious]	DV[infiltration]
Detention-impervious	1	0	0
Detention-pervious	0	1	0
Infiltration	0	0	1
Retention	-1	-1	-1

In addition to individual independent variables, the combinations (equivalent to arithmetical multiplication, symbol: *) of (BMP type * BMP/catchment areal ratio), (BMP type * slope), and (dominant land use * dominant land use/catchment areal ratio) were also included in the analysis in order to investigate the factors affecting BMP removal efficiency. The combination terms are indicators for the interactions between the included terms (Aiken and West, 1991).

Two factors are considered in selecting the best set of dependent variables in the final multiple regression equations: the p value (indicating significance of the variable) and Variance Inflation Factor (VIF) (to avoid multicollinearity). First, the dependent variable with the highest p value ($p > 0.05$) is removed, the regression is redone and the process is repeated until no dependent variable has a p value greater than 0.05. Next, the dependent variable with the highest VIF (VIF > 10 (Chatterjee and Simonoff, 2013)) is removed and the regression is redone. The process is repeated until no dependent variable has a p value > 0.05 and a VIF > 10. The same procedure was used in Chapter 2.

In the last substep of step 1 above, two sets of BMP removal efficiency data were generated. One is based on the pollutant buildup/washoff parameters derived from literature (Table 4.6), and the other is based on the pollutant buildup/washoff parameters from the Webberville study in Chapter 3 (Table 4.7). Multiple regression analysis was applied to both sets of BMP removal efficiency data, and only the equations yielding the best R^2 were reported. That is, equations for TSS and TP were derived based on pollutant buildup/washoff parameters from the Webberville study (Table 4.7), and the equation for TN was derived based on pollutant buildup/washoff parameters derived from literature (Table 4.6).

4.4.3. Estimating Optimal BMP Building Plans

The purpose of Step 3 is to illustrate that optimal BMP installation plans can be significantly influenced by predicted BMP removal efficiency. To demonstrate such an application, a program "Bmp LOcatioN Designator (BLONDE) was created for this study by C to draw a general conceptual plan for each subcatchment in the watershed of interest. The process taken by BLONDE is:

1. Convert spatial information of area, slope and land use on ArcGIS to a text file, and then process the text file by each subcatchment;

2. Based on a characteristic storm event provided by the user in the input files, generate runoff for each subcatchment using the SCS Curve Number method (SWMM is not used by BLONDE in order to accelerate the simulation);

3. Calculate pollutant concentration based on the pollutant buildup/washoff parameters;

4. Calculate pollutant reduction based on the predictive equations derived in Step 2; and then

5. Using area of each type of BMPs as variables under calibration, use PEST to optimize BMP installation based on each subcatchment.

Optimization was achieved by either one of two criteria:

1. Goal concentrations: Under this criterion, the outlet concentrations of the three water quality constituents must be as close to "goal concentrations" as possible. For TSS, there is neither legal limitations on concentrations for urban streams nor NPDES limitations for overland runoff; therefore, the value pertaining to the subjective perception of "cloudy" water, 60 mg/L (State of Michigan, 2014), was used. For TN and TP, Texas does not have any plan to set numerical criteria for these two pollutants in the near future. However, the state of Florida has had established limits, which are 2 mg/L for TN and 0.5 mg/L for TP (U.S. EPA, 2014b). Florida was selected from the three states (Wisconsin and New Jersey being the other two) with TN and TP criteria because the climate conditions in Florida are the closest to Texas.

Optimization is based on a "comprehensive rating" that encompasses all three water quality constituents (TSS, TN, and TP). Before calculation of the comprehensive rating, the difference (as a proportion of the goal concentration) between current and goal concentration for each water quality constituent was calculated. Then, a weight was given to each water quality constituent based on the accuracy of predictive equations for each water quality constituent. Water quality constituent with higher predictive accuracy is given a higher weight. The weights for TSS, TN, and TP are 0.40, 0.24, and

0.36, respectively. The comprehensive rating was then calculated by summing the products of weight and difference for each water quality constituent. The goal is to create a BMP installation plan with the lowest possible comprehensive rating.

2. Combined (goal + cost) criteria: This criterion takes financial constraints into consideration. Similar to the previous criterion, a comprehensive rating decides which BMP installation plan is optimal. The difference is that the combined comprehensive rating considers both the difference in cost (building cost plus maintenance cost) and the difference in concentration.

After the comprehensive rating from the "goal criterion" was calculated, it was averaged with a budget rating. The budget rating is the difference (as proportion of the goal cost) between the current cost and the goal cost. The goal cost was determined from the number of years under consideration and the current number of BMPs in the Shoal Creek Watershed, which is provided in Table 4.15 (City of Austin, 2014b). The goal of this criterion was also to have a BMP installation plan with the lowest possible comprehensive rating.

Note that optimizing cost alone (i.e. achieving the maximum value of pollutant reduction per unit cost) will not yield meaningful results, since the optimal plan for such a criterion is to build nothing.

The cost and maintenance for each type of BMP is given in Table 4.15, which is approximated from literature in dollars of year 1990 (EPA, 1999; ASCE, 2001).

Table 4.15. The installation and maintenance costs used in BLONDE

	Installation ($/ha)	Maintenance ($/ha/yr)	Actual area installed (ha)
Detention-impervious	10,000	100	6.29
Detention-pervious	10,000	200	25.83
Infiltration	25,000	2,500	3.45
Retention	30,000	1,500	6.35

4.5. Results and Discussion

The predictive equations for BMP removal efficiency from multiple regression analysis are given in Equations 4.3, 4.4, and 4.5. Note that the dependent variables were transformed by either square or natural logarithm in Equations 4.3 through 4.5 in order to yield better R^2 accuracy (Allen, 2004). The parameter "BMP_rto" means the areal ratio of BMP/catchment. The parameter "slp" means slope of BMP. The parameter of "LU_rto" means the areal ratio of dominant land use in the whole catchment. "DV1[X]" means the dummy variables created for the variable "type of BMP" with the outcome "X", which could be detention_impervious, detention_pervious, or infiltration. "DV2[Y]" means the dummy variables created for the variable "dominant land use" with outcome "Y", which could be civic, com+ind (i.e. commercial plus industrial land use), multifamily, single family, or transportation.

The 95% confidence intervals of coefficients in Equations 4.3 to 4.5 are reported in Table 4.16.

$$(\text{BMP removal efficiency for TSS})^2 = 0.61 - 0.32 \cdot BMP\_rto - 0.0089 \cdot slp - 0.09 \cdot DV1[detention\_impervious] + 0.12 \cdot DV1[detention\_pervious] - 0.04 \cdot DV1[infiltration] - 0.066 \cdot DV2[civic] + 0.04 \cdot DV2[com+ind] - 0.07 \cdot DV2[multifamily] + 0.26 \cdot DV2[single\ family] - 0.027 \cdot DV2[transportation] - 0.13 \cdot LU\_rto + 0.4 \cdot BMP\_rto \cdot DV1[detention\_impervious] - 0.71 \cdot BMP\_rto \cdot DV1[detention\_pervious] + 0.11 \cdot BMP\_rto \cdot DV1[infiltration] + 0.0047 \cdot slp \cdot DV1[detention\_impervious] + 0.0041 \cdot slp \cdot DV1[detention\_pervious] - 0.009 \cdot slp \cdot DV1[infiltration] \quad (4.3)$$

$$\ln(\text{BMP removal efficiency for TN}) = -2.22 + 1.92 \cdot BMP\_rto + 0.062 \cdot slp + 0.63 \cdot DV1[detention\_impervious] - 0.077 \cdot DV1[detention\_pervious] + 0.049 \cdot DV1[infiltration] + 0.058 \cdot DV2[civic] - 0.15 \cdot DV2[com+ind] + 0.22 \cdot DV2[multifamily] - 0.64 \cdot DV2[single\ family] + 0.3 \cdot DV2[transportation] + 0.65 \cdot LU\_rto - 2.54 \cdot BMP\_rto \cdot DV1[detention\_impervious] + 0.79 \cdot BMP\_rto \cdot DV1[detention\_pervious] - 0.25 \cdot BMP\_rto \cdot DV1[infiltration] - 0.031 \cdot slp \cdot DV1[detention\_impervious] - 0.037 \cdot slp \cdot DV1[detention\_pervious] + 0.01 \cdot slp \cdot DV1[infiltration] \quad (4.4)$$

$$(\text{BMP removal efficiency for TP})^2 = 0.49 - 0.35 \cdot BMP\_rto - 0.0048 \cdot slp - 0.12 \cdot DV1[detention\_impervious] + 0.15 \cdot DV1[detention\_pervious] - 0.074 \cdot DV1[infiltration] - 0.11 \cdot DV2[civic] + 0.043 \cdot DV2[com+ind] - 0.049 \cdot DV2[multifamily] + 0.16 \cdot DV2[single\ family] - 0.016 \cdot DV2[transportation] + 0.67 \cdot BMP\_rto \cdot DV1[detention\_impervious] - 1.04 \cdot BMP\_rto \cdot DV1[detention\_pervious] +$$

$$0.17 \cdot BMP\_rto \cdot DV1[infiltration] + 0.012 \cdot slp \cdot DV1[detention\_impervious] + 0.0091 \cdot slp \cdot DV1[detention\_pervious] - 0.0012 \cdot slp \cdot DV1[infiltration]] \quad (4.5)$$

Table 4.16. 95% confidence interval of coefficients in predictive equations for TSS, TN, and TP

Variable and/or dummy variable		TSS (Eq. (3))	TN (Eq. (4))	TP (Eq. (5))
intercept	**Upper 95% CI**	0.637	-2.135	0.510
	Mean	0.614	-2.223	0.494
	Lower 95% CI	0.592	-2.311	0.477
BMP_rto	**Upper 95% CI**	-0.242	2.238	-0.264
	Mean	-0.323	1.917	-0.346
	Lower 95% CI	-0.404	1.596	-0.429
slp	**Upper 95% CI**	-0.00514	0.0771	-0.00093
	Mean	-0.00891	0.0622	-0.00484
	Lower 95% CI	-0.0127	0.0472	-0.00875
DV1[detention_impervious]	**Upper 95% CI**	-0.0688	0.714	-0.102
	Mean	-0.0904	0.628	-0.125
	Lower 95% CI	-0.112	0.543	-0.147
DV1[detention_pervious]	**Upper 95% CI**	0.142	-0.00601	0.172
	Mean	0.124	-0.0773	0.154
	Lower 95% CI	0.106	-0.149	0.135

Table 4.16. Continued

Variable and/or dummy variable		TSS (Eq. (3))	TN (Eq. (4))	TP (Eq. (5))
DV1[infiltration]	Upper 95% CI	-0.0115	0.162	-0.0448
	Mean	-0.04	0.0494	-0.0743
	Lower 95% CI	-0.0684	-0.0635	-0.104
DV2[civic]	Upper 95% CI	-0.054	0.107	-0.0928
	Mean	-0.0662	0.0583	-0.105
	Lower 95% CI	-0.0784	0.00981	-0.118
DV2[com+ind]	Upper 95% CI	0.0492	-0.117	0.0521
	Mean	0.0403	-0.153	0.0429
	Lower 95% CI	0.0313	-0.188	0.0337
DV2[multifamily]	Upper 95% CI	-0.0584	0.263	0.0606
	Mean	-0.0698	0.218	0.0489
	Lower 95% CI	-0.0811	0.173	0.0371
DV2[single family]	Upper 95% CI	0.275	-0.599	0.169
	Mean	0.263	-0.644	0.157
	Lower 95% CI	0.252	-0.689	0.145
DV2[transportation]	Upper 95% CI	-0.0146	0.344	-0.00396
	Mean	-0.0267	0.296	-0.0161
	Lower 95% CI	-0.0388	0.249	-0.0283
LU_rto	Upper 95% CI	-0.108	0.756	n/a
	Mean	-0.135	0.652	n/a
	Lower 95% CI	-0.161	0.547	n/a
BMP_rto · DV1[detention_impervious]	Upper 95% CI	0.505	-2.107	0.782
	Mean	0.397	-2.537	0.67
	Lower 95% CI	0.288	-2.966	0.558

Table 4.16. Continued

Variable and/or dummy variable		TSS (Eq. (3))	TN (Eq. (4))	TP (Eq. (5))
BMP_rto · DV1[detention_pervious]	Upper 95% CI	-0.618	1.17	-0.939
	Mean	-0.715	0.787	-1.0387
	Lower 95% CI	-0.812	0.404	-1.139
BMP_rto · DV1[infiltration]	Upper 95% CI	0.243	0.254	0.304
	Mean	0.115	-0.254	0.172
	Lower 95% CI	-0.0133	-0.762	0.0394
slp · DV1[detention_impervious]	Upper 95% CI	0.00939	-0.012	0.0171
	Mean	0.00466	-0.0307	0.0123
	Lower 95% CI	-6.58e-5	-0.0495	0.00737
slp · DV1[detention_pervious]	Upper 95% CI	0.00832	-0.0204	0.0134
	Mean	0.00414	-0.037	0.00911
	Lower 95% CI	-4.06e-5	-0.0535	0.00478
slp · DV1[infiltration]	Upper 95% CI	-0.00348	0.0318	0.00452
	Mean	-0.00895	0.0101	-0.00115
	Lower 95% CI	-0.01443	-0.0116	-0.00683

The predictive accuracy of Equations 4.3, 4.4 and 4.5 were assessed by comparing the BMP efficiencies derived from the Monte Carlo simulations in Step 1 and the BMP efficiencies derived from the multiple regression equations. The overall R^2 in Table 4.17 showed low R^2 accuracy because for each BMP category, all 100 Monte Carlo simulation results are included in the accuracy assessment. The Monte Carlo simulations were performed by randomizing all pollutant buildup / washoff parameters,

and all coefficients in predictive equations for satellite-derived water quality, as summarized by Table 4.13. Such variation in parameters and coefficients makes the derived BMP efficiencies scatter a great deal. This can be evaluated by the standard error for each predictive equation. The values of standard error are all around 0.3, meaning the average distance from a data point derived by Monte Carlo simulation to the fitted line is 0.3.

Nevertheless, if the mean BMP removal efficiency value for each BMP category is used to correlate with predicted BMP removal efficiency for that BMP category, the accuracy increased significantly, as shown in Table 4.17. Figures 4.5 through 4.7 show the prediction accuracy based on category-averaged removal efficiency.

Table 4.17. R^2 accuracy and standard error of predictive equations (under "all Monte Carlo Results" rows) with the accuracy to predict mean removal efficiency of each BMP category given.

		TSS (Eq. (4.3))	TN (Eq. (4.4))	TP (Eq. (4.5))
All Monte Carlo Results	**R^2**	0.23	0.13	0.19
	Standard error of regression	0.30	0.33	0.30
BMP category mean	**R^2**	0.57	0.34	0.51

The mean removal efficiency of each BMP category was averaged from Monte Carlo Simulation results, and was used as "observed removal efficiency" in the figures.

The "predicted removal efficiency" in each figure is the predicted BMP removal efficiency (by Equations 4.3, 4.4, or 4.5) for each BMP category. Since there is no BMP removal efficiency measured by field experiments in this study, the BMP efficiencies derived from the Monte Carlo simulations were considered the closest data to observed data because the Monte Carlo simulations were performed based on observed pollutant concentrations at the outlet of the Shoal Creek Watershed.

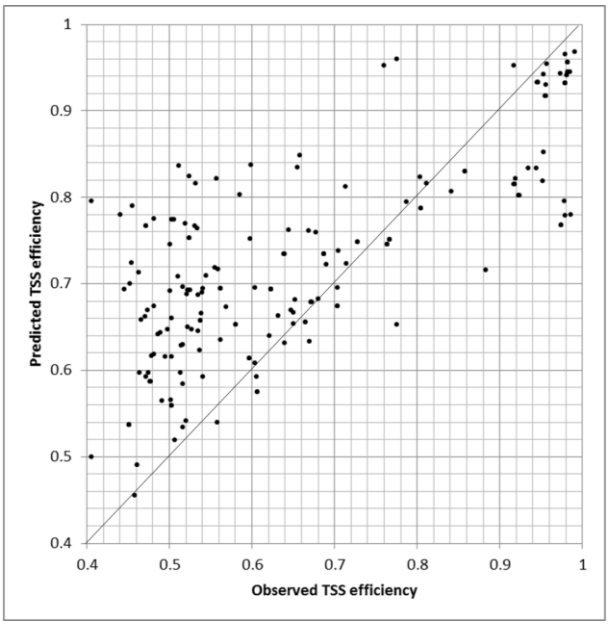

Figure 4.5. Scatter plot of observed and predicted BMP removal efficiency for TSS, R^2=0.57

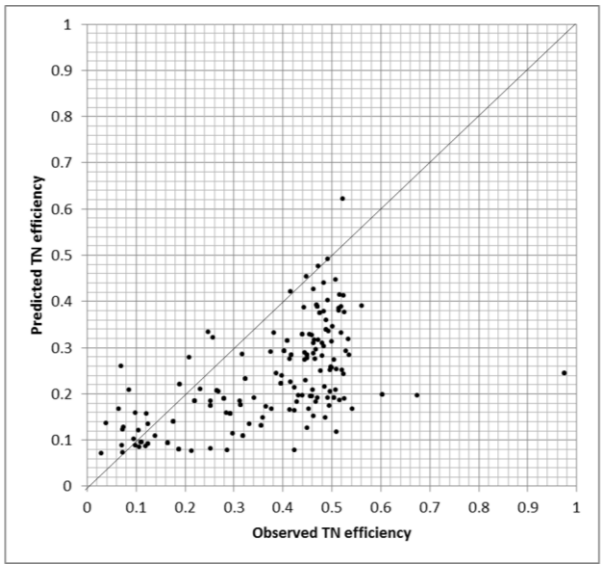

Figure 4.6. Scatter plot of observed and predicted BMP removal efficiency for TN, R^2=0.34

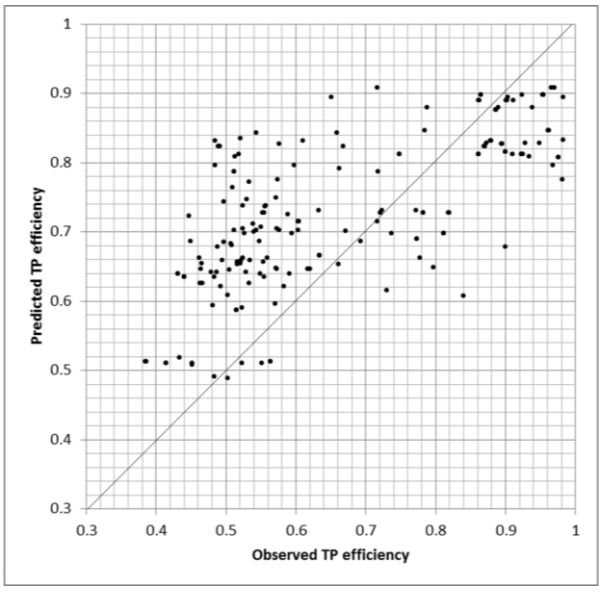

Figure 4.7. Scatter plot of observed and predicted BMP removal efficiency for TP, R^2=0.51

A sensitivity analysis of each environmental factor to BMP removal efficiency is shown in Table 4.18. Table 4.18 shows the change in BMP removal efficiency when the environmental factor of interest increases 10% in possible numerical range, represented qualitatively. For BMP_rto, slp, and LU_rto, the change were 0.1 (ratio), 10 (percentage), and 0.1 (ratio), respectively.

For the effect of land use, a separate table (Table 4.19) was created by assuming negligible BMP_rto (i.e. the catchment is sufficiently large), flat surface, and only one land use in the watershed. The purpose of this analysis is to isolate the influence of land use.

Table 4.18. Qualitative representation of BMP removal efficiency with a 10% increase in environmental factors ("n/a" indicates that such environmental factor is not in the predictive equation)

		Environmental factors		
		BMP_rto	**slp**	**LU_rto**
TSS	**Detention-impervious**	0.0061	-0.033	-0.01
	Detention-pervious	-0.067	-0.030	-0.0081
	Infiltration	-0.015	-0.144	-0.0094
	Retention	-0.0082	-0.062	-0.009
TN	**Detention-impervious**	-0.018	0.107	0.020
	Detention-pervious	0.045	0.041	0.0098
	Infiltration	0.030	0.17	0.011
	Retention	0.041	0.20	0.0058
TP	**Detention-impervious**	0.026	0.057	n/a
	Detention-pervious	-0.093	0.027	n/a
	Infiltration	-0.014	-0.049	n/a
	Retention	-0.010	-0.020	n/a

Table 4.19. BMP efficiencies for an imaginary watershed with zero slope, negligible ratio of BMP/catchment, and only one type of land use

		Civic	Commercial/ industrial	Multifamily	Single family	Transportation	Undeveloped	Average
Removal efficiency with TSS	Detention-impervious	0.568	0.655	0.565	0.807	0.602	0.624	0.637
	Detention-pervious	0.733	0.802	0.731	0.931	0.76	0.777	0.789
	Infiltration	0.611	0.693	0.608	0.838	0.643	0.663	0.676
	Retention	0.651	0.728	0.648	0.866	0.68	0.594	0.695
Removal efficiency with TN	Detention-impervious	0.413	0.335	0.484	0.205	0.524	0.389	0.392
	Detention-pervious	0.204	0.165	0.239	0.101	0.259	0.192	0.193
	Infiltration	0.232	0.187	0.271	0.115	0.294	0.218	0.220
	Retention	0.117	0.095	0.138	0.058	0.149	0.137	0.116
Removal efficiency with TP	Detention-impervious	0.514	0.642	0.647	0.725	0.594	0.607	0.622
	Detention-pervious	0.736	0.831	0.834	0.897	0.794	0.804	0.816
	Infiltration	0.56	0.613	0.608	0.759	0.635	0.647	0.637
	Retention	0.651	0.760	0.696	0.833	0.720	0.711	0.729

Based on Tables 4.18 and 4.19, several observations can be drawn:

1. Land use does have an influence on BMP removal efficiency by comparing the mean removal efficiency from each land use in Table 4.19. For TSS, BMPs will have the most removal efficiency with single family and the least removal efficiency with multifamily or civic. For TN, BMPs will have the most removal efficiency with

transportation and the least removal efficiency with single family. For TP, the land uses with the highest and lowest with civic. The influence from land use is probably due to the composition of pollutant, such as the particle size distribution, is different from different land uses.

2. Certain types of BMP are particularly efficient for certain types of pollutants by comparing mean removal efficiency from each type of BMP in Table 4.19. Detention basin with pervious bottom is the most efficient in removing TSS and TP, while detention basin with impervious bottom is the most efficient in removing TN.

3. The average efficiencies are similar for TSS and TP, which are in the order of 0.8, while the removal efficiency with TN tends to be low, which is in the order of 0.2-0.3. These findings (in Table 4.19) generally conform to results from studies based on several field experiments (Yu et al., 2001; Liu et al., 2008; Limouzin et al., 2011), which are summarized in Table 4.20.

Table 4.20. Summary of BMP removal efficiency from literature ("n/a" indicates that the specific pollutant is not studied)

Study	Type of BMP	Mean TSS removal efficiency	Mean TN removal efficiency	Mean TP removal efficiency
Yu et al., 2001	Swale	0.72	0.19	0.62
Liu et al., 2008	Vegetated buffer	0.87	n/a	n/a
Limouzin et al., 2011	Biofiltration	0.94	0.53	0.82

4. The reaction of TSS and TP to the same type of BMP and land use is similar while TN seems to react in the opposite way. For example, the trend of increasing BMP_rto makes removal efficiency of detention-impervious to increase but makes removal efficiency of other types of BMP to decrease is the same for both TSS and TP in Table 4.18. The land use or BMP type that has maximum and minimum of BMP removal efficiency in Table 4.19 is also similar for TSS and TP, but opposite for TN.

The similarity in response for TSS and TP might due to the fact that most soluble and particulate phosphorous is adsorbed to soil particles (Leisenring et al., 2010).

5. It was surprising to find that decreasing BMP_rto (increasing the catchment size) has low influence to most BMP efficiencies from Table 4.18, and only moderately decreases TSS and TP efficiencies with detention basins with pervious bottom. This does not conform to the literature, which showed that the area ratio (of BMP to the catchment) is influential to BMP removal efficiency of at least certain types of BMP,

such as vegetated buffer (Liu et al., 2008). This phenomenon might be due to the fact that all catchments used in the research are of moderate sizes and do not "overfill" BMPs. In other words, as long as the BMP size is properly designed according to expected design storms, moderately changing the size of BMP will not have significantly impact to the removal efficiency.

6. As expected, slope has significant impact to removal efficiency of infiltration BMPs, as Table 4.18 shows. Increasing slope significantly decreases the removal efficiency of infiltration BMPs to handle TSS, which is also confirmed with studies in literature (Yu et al., 2001; Liu et al., 2008) because the retention time is shortened. The same trend is also true for TP but not as significant. The intriguing part is that increasing slope significantly increases the removal efficiency of infiltration BMPs to handle TN. The only possible explanation is that higher slope increases sunlight heating of the surface, and higher temperature encourages most nitrogen removal mechanisms such as ammonification, volatilization, nitrification and denitrification (Leisenring et al., 2010). The Shoal Creek Watershed is a south-facing watershed (the northern part of the watershed has higher elevation) and this encourages sunlight heating for steeper slopes. This explanation is supported in this study by examining the removal efficiency of the BMP type of detention impervious. From Table 4.19, the BMP type of detention impervious has the highest TN removal efficiency among all types of BMP. Note that by definition the BMP type of detention impervious is detention basins with concrete surface (such as parking lot detention). Concrete surface usually has higher

temperature than natural surface (e.g. soil), and this might contribute to the higher TN removal removal efficiency of this particular type of BMP.

7. The ratio of dominant LU to the whole catchment has negligible influence to BMP efficiencies, as shown in Table 4.18. This phenomenon might indicate that the effect of increasing land use area only has negligible impact to BMP efficiencies when the land use becomes dominant. The "tapering off" nonlinear assumption can also explain why the areal ratio of dominant land use is not selected for TP.

BLONDE was used for each of the goal and mixed criterion with different scenario time frames. The time frames under consideration were 10 years, 20 years, 30 years, and 40 years. For each run, 100 Monte Carlo Simulations are performed to take account for the uncertainty in parameters of predictive equations. In response to each of the criterion mentioned above (goal or combined), the optimal annual cost (building plus maintenance, in dollar of 1990) and optimal installed area for each type of BMP are shown in Figures 4.8 and 4.9. In Figures 4.8 and 4.9, "det_imp" means the total area of the BMP of detention-impervious, "det_per" means the total area of the BMP of detention-pervious, "inf" means the total area of the BMP of infiltration, and "ret" means the total area of the BMP of retention. Cost is in dollars (1990) and area is in hectares.

In Figure 4.8 (goal criterion), it is not a surprise to see that the optimal area of BMPs does not change with the duration of scenarios since cost is not an issue for this criterion. The decreasing trend of annual cost reflects the fact that the initial cost is dominant in this criterion up to 40 years and possibly beyond. Even though the goal criterion was set strictly so that the optimal total cost and optimal total area of BMP are

too high to be realistic, Figure 4.8 shows the ideal ratio of each type of BMPs. Under the presumption that the budget is not a concern, the optimal ratio in area of the four types of BMPs (detention-impervious : detention-pervious : infiltration : retention) should be around 4 : 1 : 2 : 2 if only TSS, TN, and TP are considered and the goal concentrations are similar to what was chosen.

Figure 4.9 (combined criterion) showed a more realistic outcome of optimization. In addition to the more "realistic" annual cost and BMP area from this criterion, the first thing worth discussing is that initial cost is no longer the dominant factor in annual cost. After 30 years, the maintenance cost starts to play a role and the annual cost increases accordingly. Total area of the four types of BMPs fluctuates up and down along with the annual cost. However, the areal ratio of the four types of BMPs is not the same like what is in the previous criterion. The area of infiltration and retention BMPs takes a much smaller ratio to reflect their higher initial and maintenance cost. The optimal ratio of the four types of BMPs (detention-impervious : detention-pervious : infiltration : retention) should be around 4 : 3 : 1 : 1 for watersheds with similar budget and goal concentrations. Compared with what is from the previous criterion, the most significant change is that the BMP type of detention-pervious takes a much higher weight for this criterion.

The 95% confidence intervals of the optimal annual cost and installed area are provided in Tables 4.21 and 4.22.

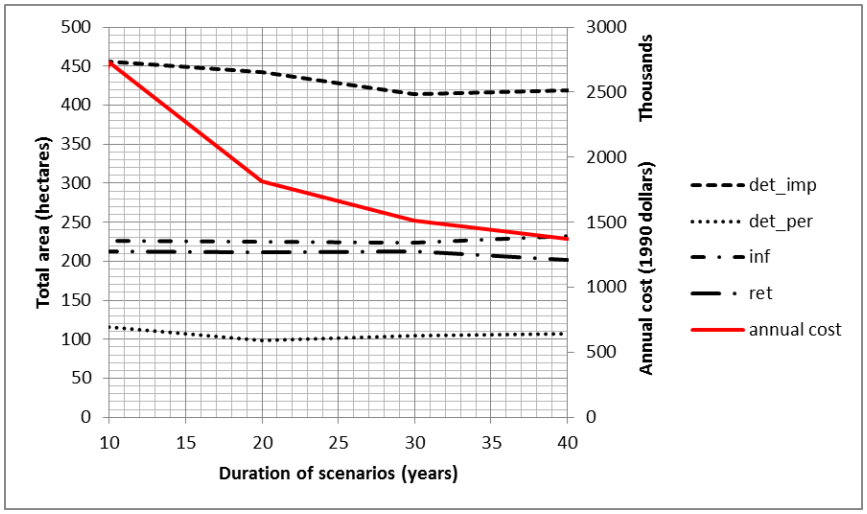

Figure 4.8. Annual total cost and total area for the four types of BMPs at different time frames under the "goal" criterion

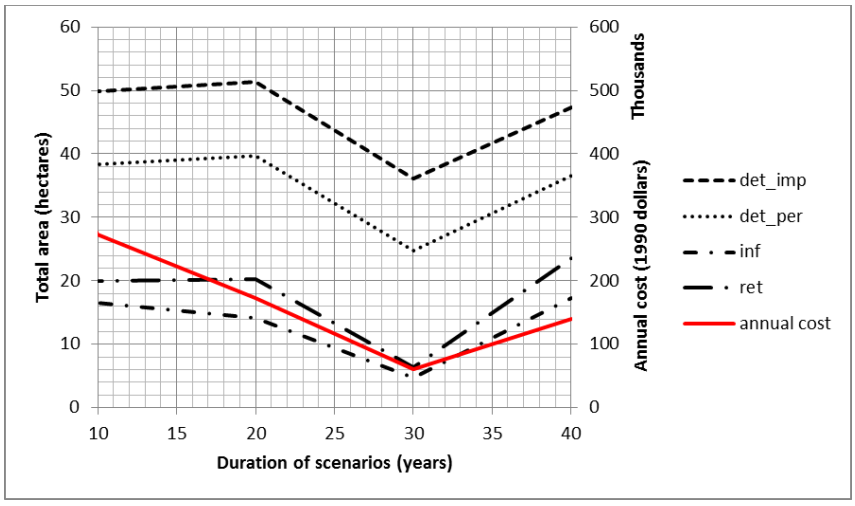

Figure 4.9. Annual total cost and total area for the four types of BMPs at different time frames under the "combined" criterion

Table 4.21. The mean and 95% confidence intervals for annual total cost and total area for the four types of BMPs at different time frames under the "goal" criterion

Scenarios		Annual cost	Total area (hectares)			
			Detention-impervious	Detention-pervious	Infiltration	Retention
10 year	lower	2,607,597.08	422.87	98.83	211.60	200.91
	mean	2,729,242.35	455.82	115.53	226.40	212.70
	upper	2,850,887.62	488.77	132.23	241.20	224.48
20 year	lower	1,746,144.51	410.66	93.16	210.83	201.76
	mean	1,811,795.89	442.32	98.80	224.89	211.29
	upper	1,877,447.28	473.97	104.44	238.96	220.82
30 year	lower	1,435,380.19	381.42	93.71	210.27	197.76
	mean	1,514,490.65	414.32	104.37	224.05	212.98
	upper	1,593,601.11	447.22	115.02	237.82	228.19
40 year	lower	1,305,423.84	389.69	94.59	217.64	187.13
	mean	1,373,644.31	419.17	107.44	231.79	201.88
	upper	1,441,864.79	448.64	120.30	245.93	216.62

Table 4.22. The mean and 95% confidence intervals for annual total cost and total area for the four types of BMPs at different time frames under the "goal" criterion

		Annual cost	Total area (hectares)			
			Detention-impervious	Detention-pervious	Infiltration	Retention
10 years	lower	147,767.59	40.32	28.97	6.81	7.28
	mean	273,220.82	49.85	38.33	16.46	20.00
	upper	398,674.05	59.38	47.69	26.12	32.73
20 years	lower	80,510.78	36.56	25.56	5.30	6.32
	mean	172,262.08	51.41	39.62	14.08	20.28
	upper	264,013.37	66.26	53.69	22.87	34.23
30 years	lower	59,864.25	34.61	23.67	4.48	6.16
	mean	60,537.69	36.07	24.76	4.68	6.43
	upper	61,211.12	37.53	25.86	4.87	6.69
40 years	lower	48,275.38	33.81	22.80	4.07	5.64
	mean	139,903.88	47.35	36.53	17.26	23.52
	upper	231,532.37	60.90	50.26	30.46	41.39

For the combined criterion, if the optimal area for the 20-year scenario (to reflect the time passed since Phase I NPDES) is compared with the actual installation area (Table 4.15), it is clear that building of BMPs are currently less than what is required by the optimal plan in Austin (at least in the Shoal Creek Watershed), and the area of detention-impervious, infiltration, and retention BMPs should be significantly increased (particularly detention-impervious type of BMP) to match the optimal plan. The comparison is shown in Table 4.23.

Table 4.23. Comparison of actual and optimized (under the combined criterion) area of BMP installed

	Detention-impervious	Detention-pervious	Infiltration	Retention
Actual (ha)	6.29	25.83	3.45	6.35
Optimized for 20 years (ha)	51.41	39.62	14.08	20.28

4.6. Conclusion and Recommendation

The results showed that the modelling approach used by this study is effective in deriving BMP efficiencies and the relationship between BMP efficiencies and environmental factors. The results showed that most BMPs have considerably high removal efficiency in removing pollutants, but the removal efficiency can also vary significantly. Some of the trends of BMP efficiencies and relationships can be verified by field experiments in the literature (Yu et al., 2001; Liu et al., 2008; Limouzin et al., 2011).

The responses of environmental factors seem quite different (sometimes opposite) for TN, as compared to those of TSS and TP. That indicates that it might be a difficult task to consider TN while in the same time consider TSS or TP, because environmental factors in favor of lowering TN might work the opposite way to TSS or TP.

Besides, scenarios were studied to show what the optimal BMP installation plans can change under different criteria. The optimal ratio between the four main types of BMPs (detention-impervious, detention-pervious, infiltration, and retention) can be quite

different whether cost is considered. When cost is considered, it was also found that the optimal plan can noticeably vary according to the length of time frame considered. The current installation of BMPs in Austin (at least in Shoal Creek Watershed) is not optimized and more detention-impervious, infiltration, and retention BMPs should be built (particularly detention-impervious type of BMP).

This study showed that optimal plans can be determined if BMP removal efficiency can be determined. This study provided equations to predict BMP efficiencies from the size of BMP, slope of BMP, and land use of the watershed. The equations given in Equations 4.3 through 4.5 are only the beginning. To better fine-tune the approach used in this research, the following approaches were proposed in order to enhance similar studies in the future:

1. Data deficiency:

This study lacked several key data items. For example, there was no volume data for BMPs from GIS datasets, and surface area was used as a surrogate. It was also preferred to have more entries of water quality data, too.

Field work is possible for watersheds of similar size to measure the actual capture size of at least a portion of all BMPs. Therefore, the first suggestion is to perform a comprehensive field work to measure the capture volume of at least a significant portion of all BMPs. Even though it may be very challenging to measure all BMPs, measuring a significant portion of BMPs can improve the correlation estimate between surface area and capture volume.

This study adopts USGS data, and water quality measurements were very limited. The second suggestion is also about field work. It is suggested to increase the size of water quality data in order to get more reliable calibration results.

2. Deficiency in variable selection:

One of the most significant deficiencies in this study is the missing of several important variables. For example, BMPs are categorized by principle of functioning, not actual designs. Due to the lack of data regarding design details, this is a necessary compromise. Nevertheless, it is still suggested to have detailed data about each BMP and categorize BMPs based on actual designs attributes in the future. One problem with such detailed information is that the initial number of BMP types will be likely high. It would be more difficulty to combine types of BMPs.

For sensible environmental factors (little change makes big difference in removal efficiency), it might be good to reduce the numerical range of each category so that each BMP category will have less scattered removal efficiency. To the contrary, the numerical range can be larger for insensitive environmental factors.

As for the future, the following two directions were recommend to continue the direction of this study:

1. Improving BLONDE:

The optimization was performed by BLONDE, which can only optimize BMP installation based on subcatchments, and does not directly couple to a GIS platform (currently BLONDE can only read GIS files, but cannot display results on GIS yet).

Coupling BLONDE to a GIS platform and cell-based optimizing will be the next steps for BLONDE improvement.

2. Multi-city correlation:

In addition to the environmental factors examined by this study, it is possible to link BMP removal efficiency further to geographic locations of cities. Some factors such as average intervals between runoff events were not considered by this study because they only matter when multiple geographic locations are considered. The next goal for the methodology used by this study is to apply the same procedure to other cities and derive predictive equations for BMP removal efficiency not only based on the environmental factors chosen by this study, but also other environmental factors (such as climate, elevation, average income, etc.) involving multiple locations. The ultimate goal is to provide a set of equations that can predict BMP efficiencies for not only one city, but any city in the world.

CHAPTER V

SUMMARY

Based on the objectives set forth in Chapter 1, this study achieved the following goals:

5.1. Derive the Relationship between BMP Pollutant Removal Efficiency and the Environmental Factors

Inverse modeling was used to calibrate BMP removal efficiency of each BMP category from the measured pollutant concentration at the outlet of the Shoal Creek Watershed. A SWMM model, which simulates only direct runoff for sake of simplicity, was constructed for inverse modeling.

Since only direct runoff was simulated by SWMM, mean pollutant concentration in base flow has to be known in order to convert measured concentration to the concentration in direct runoff. Statistical relationship of band reflectance and pollutant concentration was derived for Lady Bird Lake. The difference in pollutant concentration during base flow dominant dates before and after confluence of the Shoal Creek Watershed was considered to be solely influenced by the base flow. An advective diffusion equation was utilized to calculate pollutant provided by the Shoal Creek Watershed at its outlet.

Pollutant buildup and washoff parameters are required by SWMM. The technique of inverse modeling was also applied to Webberville Watershed in order to

obtain parameters of pollutant buildup and washoff of the water quality constituents of choice in this study: TSS, TN, and TP. Observed hydrological and water quality data at the outlet of Webberville Watershed in 1980s was used in inverse modeling in order to avoid the influence of BMP to model parameter estimates. Before 1990, the construction of BMPs is not mandatory so the number of BMP was negligible. This part of the study revealed that land uses of bare soil, industrial, single family, and undeveloped are found as major pollutant sources in Austin, TX. Pollutant buildup parameters were controlled by large-scale factors such as climate, and washoff parameters were controlled locally by factors such as local topography.

Putting all information together, the removal efficiency of all BMP categories was derived by inverse modeling for the Shoal Creek Watershed. Multiple regression analysis was applied to derive the statistical relation of removal efficiency and associated environmental factors. The derived equations were found to show the same behaviors in pollutant reduction found in field studies.

Land use was proven to be one of the important factors in deciding BMP removal efficiency. For TSS, BMPs will have the most removal efficiency with single family and the least removal efficiency with multifamily or civic. For TN, BMPs will have the most removal efficiency with transportation and the least removal efficiency with single family. For TP, the land uses with the highest and lowest with civic.

Among the five environmental factors, areal ratio of dominant land use in the BMP catchment and areal ratio of BMP area in the BMP catchment were found to the two weakest factors in controlling BMP removal efficiency.

It was also found that for a certain pollutant, the removal efficiency is not equal to all types of BMPs. Detention basin with pervious bottom is the most efficient in removing TSS and TP, while detention basin with impervious bottom is the most efficient in removing TN.

Increasing slope was found to increase removal efficiency of TN, probably due to the increased surface temperature from heating by sunlight. To the contrary, decreasing slope increases the removal efficiency for TSS and TP due to increased retention time.

The influence of environmental factors is similar for BMP removal efficiency of TSS and TP, but quite different to that of TN. Therefore, it is a difficult task to control TSS, TN, and TP in the same time because environmental factors in favor of lowering TN might work the opposite way to TSS or TP.

5.2. Provide the Means to Optimize BMP Planning by Using the Relationship

Taking advantage of the predictive equations for BMP removal efficiency, BLONDE was created to derive the optimal BMP building schemes in the Shoal Creek Watershed based on two criteria: the goal concentrations only, and combination of the budget constraint and goal concentrations. It was found that the optimal areal ratio of the four types of BMPs (detention-impervious : detention-pervious : infiltration : retention) should be around 4 : 1 : 2 : 2. If budget is considered, the optimal ratio of the four types of BMPs (detention-impervious : detention-pervious : infiltration : retention) turns to be around 4 : 3 : 1 : 1. It was also found that maintenance cost becomes the dominant reason in deciding the optimal plan after about 30 years.

Even though this study successfully derived predictive equations for BMP removal efficiency, there still exists space for improving. The major concern of this study was that it relies solely on the publicly available data, such GIS databases. Important data might be missing from the public data. For example, design attributes (e.g. capture volume, dimension of release structure, etc.) of each BMP are missing.

In addition to improving functionality of BLONDE, or incorporating the predictive equations in established BMP planning software, a major direction for this study in the future is to apply the same procedure to cities in other geographic regions. This study utilizes BMPs from the same city to eliminate the influence of environmental factors such as intervals between storms, soil group, and water temperature. By comparing results from different geographic regions, the influence of these factors becomes apparent. The ultimate goal is to provide a set of equations that can predict BMP efficiencies for not only one city, but any city in the world.

5.3. Provide Recommendations to Improve Municipal Regulations Regarding BMP Installation Based on the Relationship

5.3.1. Parts That Need Improving

This study has direct implication in improving city ordinances regarding water quality mitigation by BMPs. Using Austin, TX for example, a few parts of the Environmental Criteria Manual (City of Austin, 2014d) require improving, which are:

1. Erosion and sedimentation control has a specific criteria (§1.4.0), but not for other kinds of pollutants. Sediment (erosion control) is the only concern in the

ordinances, and other pollutants (bacteria, nutrients and metals) are considered to be associated with sediment (§1.6.1), i.e. reducing sediment automatically reducing other pollutants. This is not wrong, but is an oversimplification;

2. Calculation of BMP dimensions is based on "water quality volume" (§1.6.2), which is the volume of storm water based on the area of impervious surface. This is a proper criterion for flood detention, but probably not a good one for water quality mitigation; and

3. The ordinances clearly state that "sedimentation/filtration basins are the standard water quality control for new development" (§1.6.1, direct quote) and "sedimentation/filtration is the primary structural water quality control to reduce non-point source pollution" (§1.6.4, direct quote), which might incorrectly bias building of BMPs.

5.3.2. Suggested Revisions

Therefore, the following revisions are suggested for the Environmental Criteria Manual:

1. The city of Austin (or the state of Texas) needs to develop water quality criteria for nutrients. Many states have had developed such criteria, or will develop them in the near future (U.S. EPA, 2014c). After water quality criteria for nutrients are established, planning BMP can start to base on all pollutants instead of a single pollutant (i.e. sediment) like it is today;

2. Similar to §1.4.0 (erosion and sedimentation control criteria), a new section is needed for nutrients in order to provide a resource document for water quality mitigation based on findings from this study;

3. The current design guidelines are based on criteria of flood detention, not water quality mitigation. The finding from this study can be incorporated to sub-sections in §1.6.0 (design guidelines for water quality controls). In the beginning, it is suggested to keep both systems (the old system based on storm size, and the new system based on water quality mitigation from this study) working in parallel, as what will be discussed below. It is presumed that planning of BMPs happens in drafting a site plan, because engineering details of development plan are under consideration in a site plan. During land annexation, zoning, and subdivision, engineering details are not being scrutinized. Depending on whether the state (or municipal) criteria in nutrients and TSS are established, there are three ways to incorporate findings of this study to §1.6.0.:

(a) The simplest way: The simplest way to utilize the findings from this study is incorporating the optimal areal ratio of BMPs. The optimal areal ratio of BMP types (detention-impervious : detention-pervious : infiltration : retention) under budget constraint is should be around 4 : 3 : 1 : 1. Compared with the cost determined from the old system, a developer can choose to install four different kinds of BMPs (detention-impervious : detention-pervious : infiltration : retention) with the areal ratio 4 : 3 : 1 : 1 for the same total cost.

(b) If criteria in TSS and nutrients have been established: The effluent concentration from a development site cannot be higher than the criteria,

probably under s design storm. BMP plans are to be enacted from the old system and the new system and compared with each other. For the new system, using BLONDE is recommended to ensure that the plan is the most economic one. In BLONDE, the "goal criterion" is used since the water quality criteria must be met. The results from two systems are compared and the less conservative one (i.e. building more BMPs) is adopted; or

(c) If criteria in TSS and nutrients have yet been established: There is no criteria for effluent concentration from a development site, so a criterion to decide whether a BMP installation plan is satisfactory must be established first. Similarly, BMP plans are to be enacted both from the old system and the new system and compared with each other. For the new system, using BLONDE is recommended to ensure that the plan is the most economic one. In BLONDE, the "combined criterion" is used, and the weight for cost is much higher than the weight for goal concentrations since no regulatory concentration criteria is available. The cost criterion is the same as the total cost from the old system. However, a set of goal concentrations is still required by BLONDE, so it is recommended to use the goal concentrations used in Chapter 4. The results from two systems are compared and the less conservative one (i.e. building more BMPs) is adopted.

4. Sections such as §1.6.1 and §1.6.4 need to be revised that no bias is given to any kind of BMP. Or, this section can be revised according to findings from this study so that special favor is given to a certain type of BMP under certain conditions. For

example, it was known from Chapter 3 that single family land use is a major source for TSS and TN, so §1.6.1 and §1.6.4 can encourage detention types of BMPs (impervious bottom and pervious bottom) to be built in single family land use because those two types of BMPs (detention-impervious and detention-pervious) are more efficient in removing TSS and TN, respectively.

REFERENCES

Agresti, A. 2014. *Categorical Data Analysis*. 3rd ed. Hoboken, NJ: John Wiley & Sons.

Aiken, L.S., S.G. West. 1991. *Multiple Regression: Testing and Interpreting Interactions*. Thousand Oaks, CA: Sage Publications.

Al Bakri, D., S. Rahman, and L. Bowling. 2008. Sources and management of urban stormwater pollution in rural catchments, Australia. *Journal of Hydrology*. 356(3-4):299-311.

Allen, M.P. 2004 *Understanding Regression Analysis*. Berlin, Germany: Springer.

Alparslan, E., H.G. Coskun, U. Alganci. 2010. An investigation on water quality of Darlik Dam drinking water using satellite images. *Thescientificworld*. 10:1293-1306.

Anderson, D.R., K.P. Burnham. 1999. Understanding information criteria for selection among capture-recapture or ring recovery models. *Bird Study*. 46: S14-21.

ASCE. 2001. *Guide for Best Management Practice (BMP) Selection in Urban Developed Areas*. Denver, MA: American Society of Civil Engineers.

Bach, P.M., D.T. McCarthy, A. Deletic. 2010. Redefining the stormwater first flush phenemonon. *Water Research*. 44(8): 2487-2498.

Barbini, R., F. Colao, R. Fantoni, A. Palucci, F. Borfecchia, L. De Cecco, A.B. Della Rocca, S. Martini. 1997. Integration of passive and lidar remote sensed data in monitoring sea water quality. In *Proc. 7th International Symposium on Physical Measurements and Signature in Physical Measurements and Signatures in*

Remote Sensing, 49-56. Courchevel, France: International Society for Photogrammetry and Remote Sensing (ISPRS).

Barco, O. J., C. Ciaponi, S. Papiri. 2004. Pollution in storm water runoff - Two cases: an urban catchment and a highway toll gate area. *Novatech.* 2004: 1-8.

Barrett, M.E. 2005. Performance comparison of structural stormwater Best Management Practices. *Water Environment Research* 77(1): 78-86.

Barton, K. 2014. Package 'MuMIn'. Vienna, Austria: R Foundation for Statistical Computing. Available at: http://cran.r-project.org/web/packages/MuMIn/MuMIn.pdf. Last accessed 21 June 2014.

Beven, K. 2006. A manifesto for the equifinality thesis. *Journal of Hydrology*. 320: 18-36.

Borah, D.K., G. Yagow, A. Saleh, P.L. Barnes, W. Rosenthal, E.C. Krug, and L.M. Hauck. 2006. Sediment and nutrient modeling for TMDL development and implementation. *Transactions of the ASABE*. 49(4):967-986.

Bukata, R.P. 2005. *Satellite Monitoring of Inland and Coastal Water Quality: Retrospection, Introspection, Future Directions*. Boca Raton, FL: Taylor and Francis Group.

Burnham, K. P. and D. R. Anderson. 2002. *Model Selection and Multimodel Inference: A Practical Information-Theoretic Approach*. 2nd ed. New York City, NY: Springer-Verlag.

Chatterjee, S. and Simonoff, J. S. 2013. *Handbook of Regression Analysis*. Somerset, NJ: Wiley Publication.

Chen, J.Y. and B.J. Adams. 2006. Urban stormwater quality control analysis with detention ponds. *Water Environment Research*. 78(7):744-753

Chow, M.F., Z. Yusop, M.E. Toriman. 2012. Modelling runoff quantity and quality in tropical urban catchments using Storm Water Management Model. *International Journal of Environmental Science Technology*. 9:737-748

Chow, M.F., Z. Yusop, S.M. Shirazi. 2013. Storm runoff quality and pollutant loading from commercial, residential, and industrial catchments in the tropic. *Environmental Monitoring and Assessment*. 185: 8321-8331.

City of Austin. 2012. Sewer Map in GIS layers. Personal communication.

City of Austin. 2014a. Detailed City of Austin population history: 1840 to 2014. Austin, TX: Planning and Development Review Department, City of Austin. Available at: http://www.austintexas.gov/page/demographic-data. Accessed 10 September 2014.

City of Austin. 2014b. City of Austin GIS Data Sets. Austin, TX: City of Austin. Available at: ftp://ftp.ci.austin.tx.us/GIS-Data/Regional/coa_gis.html. Accessed 10 September 2014.

City of Austin, 2014c. Austin, TX Code of Ordinances. Austin, TX: City of Austin. Available at: https://library.municode.com/index.aspx?clientId=15302. Accessed 10 September 2014.

City of Austin. 2014d. Environmental Criteria Manual. Austin, TX: Austin City Government. Available at:

https://library.municode.com/index.aspx?clientId=15306. Accessed 10 September 2014.

CSIRO. 2009. Groundwater contribution to nutrient export from the Ellen Brook catchment. Clayton South, Victoria, Australia: CSIRO. Available at: http://www.clw.csiro.au/publications/waterforahealthycountry/2009/wfhc-groundwater-Ellen-Brook-catchment.pdf. Accessed 26 August 2014.

Debo, T.N and A. J. Reece. 2003. *Municipal Stormwater Management*. Boca Raton, FL: Lewis Publishers.

Dewidar, K.H., A. Khedr. 2001. Water quality assessment with simultaneous Landsat-5 TM at Manzala Lagoon, Egypt. *Hydrobiologia*, 457: 49-58.

Doherty, J. 2010. *PEST: Model-independent Parameter Estimation User Manual*. 5th edition. Queensland, Australia: Watermark Numerical Computing.

Doherty, J. 2012. Addendum to the PEST manual. Queensland, Australia: Watermark Numerical Computing.

Duan, Q.Y., V.K. Gupta, S. Sorooshian. 1993. Shuffled complex evolution approach for effective and efficient global minimization. *Journal of Optimization Theory and App*lications. 76(3): 501-521.

Eckhardt, K. 2005. How to construct recursive digital filters for baseflow separation. *Hydrological Processes*. 19(2):507-515

Edwards, D. R., T. C. Daniels, H. D. Scott, P.A. Moore, J.F. Murdoch, P.F. Vendrell. 1997. Effect of BMP implementation on storm flow quality of two northwestern Arkansas streams. *Transactions of the ASABE* 40(5):1311-1319.

Elliot, A.H., S.A. Trowsdale, and S. Wadhwa. 2009. Effect of aggregation of on-site storm-water control devices in an urban catchment model. *Journal of Hydrologocal Engineering*. 14:975-983

Doxaran, D., J.-M. Froidefond, S. Lavender, and P. Castaing. 2002. Spectral signature of highly turbid waters application with SPOT data to quantify suspended particulate matter concentrations. *Remote Sensing of the Environment.* 81: 149-161.

EROS. 2014a. USGS Global Visualization Viewer. Sioux Falls, SD: USGS Earth Resources Observation and Science Center. Available at: http://glovis.usgs.gov/. Accessed 5 September 2013.

EROS. 2014b. Multi-Resolution Land Characteristics Consortium (MRLC). Sioux Falls, SD: Earth Resources Observation and Science (EROS) Center, U.S. Geological Survey (USGS). Available at: http://www.mrlc.gov/index.php. Accessed 15 August 2014

Exelis Inc. 2009. *Atmospheric Correction Module: QUAC and FLAASH User's Guide*. Ver. 4.7. Boulder, CO: Exelis Inc.

Frazier, P. S. and K. J. Page. 2000. Water body detection and delineation with Landsat TM data. *Photogrammetric Engineering and Remote Sensing.* 66(12): 1461-1467.

Fischer, A., P. Rouault, S. Kroll, J.V. Assel, and E. Pawlowsky-Reusing. 2009. Possibilities of sewer model simplifications. *Urban Water Journal*. 6(6):457-470.

Fischer, H. B., E. G. List, R. C. Y. Koh, J. Imberger, N. H. Brooks. 1979. *Mixing in Inland and Coastal Waters*. New York, NY: Academic Press.

Goegebeur, M., V.R.N. Pauwels. 2007. Improvement of the PEST parameter estimation algorithm through Extended Kalman Filtering. *Journal of Hydrology*. 337:436-451.

Harmel, R.D., K.W. King, B.E. Haggard, D.G. Wren, J.M. Sheridan. 2006. Practical guidance for diacharge and water quality data collection on small watersheds. *Transactions of the ASABE*. 49(4): 937-948.

Hadjimitsis, D. G., C. R. Clayton, and V. S. Hope. 2004. An assessment of the effectiveness of atmospheric correction algorithms through the remote sensing of some reservoirs. *International Journal of Remote Sensing*. 25(18): 3651-3674.

Hocking, R. R. 2013. *Methods and Applications of Linear Models: Regression and the Analysis of Variance*. 3rd ed. Somerset, NJ: Wiley Publication.

Hood, M., A. Reihan, and E. Loigu. 2007. Modeling urban stormwater runoff pollution in Tallinn, Estonia. In *International Symposium on New Directions in Urban Water Management*. Paris, France: UNESCO.

Hossain, I., M. Imteaz, S. Gate-Trinidad, and A. Shanableh. 2010. Development of a catchment water quality model for continuous simulations of pollutants build-up and wash-off. *International Journal of Civil and Environmental Engineering*. 2(4):210-217.

Hsu, M.H., S.H. Chen and T.J. Chang. 2000. Inundation simulation for urban drainage basin with storm sewer system. *Journal of Hydrology*. 234(1-2):21-37.

Huber, W.C., and R.E. Dickinson. 1988. *Storm Water Management Model, Version 4: User's Manual*. Athens, GA: U.S. EPA.

Islam, N., R. Sadiq, M.J. Rodriguez, and A. Francisque. 2011. Reviewing source water protection strategies: a conceptual model for water quality assessment. *Environmental Review.* 19:68-105

Jang, S, M. Cho, J. Yoon, Y. Yoon, S. Kim, G. Kim, L. Kim and H. Aksoy. 2007. Using SWMM as a tool for hydrologic impact assessment. *Desalination* 212(2007):344-356.

Jensen, J. R. 2007. *Remote Sensing of the Environment - an Earth Resource Perspective*. 2nd ed. Upper Saddle River, NJ: Prentice Hall.

Jia, H., Y. Yu, S.L. Yu, and Y. Chen. 2012. Planning of LID-BMPs for urban runoff control: the case of Beijing Olympic Village. *Separation and Purification Technology* 84:112-119.

Kannel, P. R., S. Lee, S. R. Kanel, S. P. Khan, Y.-S. Lee. 2007. Spatial-temporal variation and comparative assessment of water qualities of urban river system: a case study of the river Bagmati (Nepal). *Environmental Monitoring and Assessment*. 129: 433-459

Karian, Z.A., and E.J. Dudewicz. 2000. *Fitting Statistical Distributions: The Generalized Lambda Distribution and Generalized Bootstrap Methods.* Boca Raton, FL: CRC Press.

Kim, H.-J., J.E. Cavanaugh, T.A. Dallas, S.A. Fore. 2014. Model selection criteria for overdispersed data and their application to the characterization of a host-parasite relationship. *Environmental Ecological Statistics*. 21: 329-350.

Kishino, M., A. Tanaka, and J. Ishizaka. 2005. Retrieval of Chlorophyll a, suspended solids, and colored dissolved organic matter in Tokyo Bay using ASTER data. *Remote Sensing of the Environment.* 99: 66-74.

Kloiber, S. M., P. L. Brezonik, L. G. Olmanson, and M. E. Bauer. 2002. A procedure for regional lake water clarity assessment using Landsat multispectral data. *Remote Sensing of the Environment*. 82: 38-47.

Knighton, D. 1998. *Fluvial Forms and Processes*. London, U.K.: Hodder Education.

Konishi, S., G. Kitagawa. 2007. *Information Criteria and Statistical Modeling*. Berlin, Germany: Springer.

Kuhn, M., S. Weston, C. Keefer, N. Coulter, R. Quinlan. 2014. Cubist: Rule- and Instance-Based Regression Modeling. Boston, MA: Free Software Foundation. Available at: http://cran.r-project.org/web/packages/Cubist/index.html. Accessed 22 February 2014.

Lal, R. 1994. *Soil Erosion Research Methods*. Delray Beach, FL: St. Lucie Press.

LCRA. 2012. LCRA Dams Form the Highland Lakes. Austin, TX: Lower Colorado River Authority. Available at: www.lcra.org/water/dams/index.html. Accessed 5 September 2013.

Lee, S., C. Yoon, K. W. Jung and H.S. Hwang. 2010. Comparative evaluation of runoff and water quality by HSPF and SWMM. *Water Science and Technology*. 62(6):1401-1409.

Leisenring, M., J. Clary, J. Stephenson, P. Hobson. 2010. International Stormwater Best Management Practices (BMP) Database Pollutant Category Summary: Nutrients. Boca Raton, FL: Geosyntec Consultants. Available at: http://www.bmpdatabase.org/Docs/BMP%20Database%20Nutrients%20Paper%20December%202010%20Final.pdf. Accessed 20 August 2014.

Leisenring, M., J. Clary, K. Lawler, P. Hobson. 2011. International Stormwater Best Management Practices (BMP) Database Pollutant Category Summary: Solids (TSS, TDS and Turbidity). Boca Raton, FL: Geosyntec Consultants. Available at: http://www.bmpdatabase.org/Docs/BMP%20Database%20Solids%20Paper%20May%202011%20FINAL.PDF. Accessed 20 August 2014.

Leitao, J.P., N.E. Simoes, C. Maksimovic, F. Ferreira, D. Prodanovic, J.S. Matos, and A. Sa Marques. 2010. Real-time forecasting urban drainage models: full or simplified networks? *Water Science and Technology*. 62.9:2106-2114.

Lim, K.J., B.A. Engel, Z. Tang, J. Choi, K.-S. Kim, S. Muthukrishnan, and D. Tripathy. 2005. Automated web GIS based hydrograph analysis tool, WHAT. *Journal of the American Water Resources Association*. 41(6):1407-1416.

Limouzin, M., D.F. Lawler, M.E. Barrett. 2011. Performance Comparison of Stormwater Biofiltration Designs. CRWR Online Report 10-05. Austin, TX: Center for Research in Water Resources, The University of Texas at Austin.

Liu, X., X. Zhang, M. Zhang. 2008. Major factors influencing the removal efficiency of vegetated buffers on sediment trapping: a review and analysis. *Journal of Environmental Quality*. 37: 1667-1674.

Liu, Y., M. A. Islam, and J. Gao. 2003. Quantification of shallow water quality parameters by means of remote sensing. *Progresses in Physical Geography*. 27(1): 24-43

Lloyd, C.D. 2005. Assessing the effect of integrating elevation data into the estimation of monthly precipitation in Great Britain. *Journal of Hydrology*. 308:128-150.

McCullough, I. M., C. S. Loftin, and S. A. Sader. 2012. High-frequency remote monitoring of large lakes with MODIS 500 m imagery. *Remote Sensing of the Environment.* 124: 234-241.

Moeller, J., T. Connor. 2014. International Stormwater BMP Database. Alexandria, VA: Water Environment Research Foundation. Available at: www.bmpdatabase.org Accessed 5 November 2014.

Moisen, G.G., T.S. Frescino. 2002. Comparing five modelling techniques for predicting forest characteristics. *Ecological Modeling*. 157: 209-225.

Moriasi, D.N., J.G. Arnold, M.W. Van Liew, R.L. Bingner, R.D. Harmel, T.L. Veith. 2007. Model evaluation guidelines for systematic quantification of accuracy in watershed simulations. *Transactions of the ASABE*. 50(3):885-900.

MRLC. 2014. National Land Cover Database (NLCD). Sioux Falls, SD: U.S. Geological Survey. Available at: http://www.mrlc.gov/index.php. Accessed 2 June 2014.

NASA. 2013a. MODIS Atmosphere: Water Vapor. Washington, DC: NASA. Available at: http://modis-atmos.gsfc.nasa.gov/MOD05_L2/index.html. Accessed 3 September 2013.

NASA. 2013b. New Landsat Finds Clouds Hiding in Plain Sight. Washington, DC: NASA. Available at: http://earthobservatory.nasa.gov/IOTD/view.php?id=81210. Accessed 3 September 2013.

NCDC. 2014. National Climatic Data Center. Asheville, NC: National Climatic Data Center. Available at: http://www.ncdc.noaa.gov/about-ncdc. Accessed 20 May 2014.

NOAA. 2013. Earth System Research Laboratory Ground-based GPS Meteorology. Washington, DC: National Oceanic and Atmospheric Administration. Available at: http://gpsmet.noaa.gov/. Accessed 3 September 2013.

Norwine, J., J.R. Giardino, and S. Krishnamurthy. 2005. *Water for Texas*. Texas A&M University Press.

NRCS. 2013. Web Soil Survey. Washington, DC: USDA, NRCS, Office of the Chief. Available at: http://websoilsurvey.sc.egov.usda.gov/App/HomePage.htm. Accessed 2 June 2014.

NWS. 2014a. Austin/San Antonio, TX. Silver Spring, MD: National Weather Service. Available at: http://www.srh.noaa.gov/ewx/?n=ausclidata.htm. Accessed 10 September 2014.

NWS. 2014b. National Weather Service Automated Surface Observing System. Silver Spring, MD: National Weather Service. Available at: http://www.nws.noaa.gov/asos/. Accessed 10 September 2014.

NWS. 2014c. Precipitation Map. Fort Worth, TX: National Weather Service, Southern Region Headquarters. Available at: http://www.srh.noaa.gov/ridge2/RFC_Precip/. Accessed 15 August 2014.

O'Connor, T.P., R. Field, D. Fischer, R. Rovansek, R. Pitt, S. Clark, M. Lama. 1999. Urban wet-weather flow. *Water Environment Research* 25: 559-583.

Owens, P.N., D.E. Wallings. 2002. The phosphorus content of fluvial sediment in rural and industrialized river basins. *Water Research*. 36: 685-701.

Pahlevan, N., A.J. Garrett, A. Gerace, et al. 2012. Integrating Landsat-7 imagery with physics-based models for quantitative mapping of coastal waters near river discharges. *Photogrammetric Engineering and Remote Sensing*. 78(11): 1163-1174.

Park, M.-H., X. Swamikannu, and M.K. Stenstrom. 2009. Accuracy and precision of the volume concentration method for urban stormwater modeling. *Water Research*. 43:2773-2786

Patton, C. J., E. P. Truitt. 1992. Methods of analysis by the U. S. Geological Survey National Water Quality Laboratory – determination of total phosphorous by a Kjeldahl digestion method and an automated colorimetric finish that includes dialysis. Open-file Report 92-146. Reston, VA: U. S. Geological Survey.

Reeves, J.B. III, S.R. Delwiche, V.B. Reeves. 2006. Least squares means multiple comparison testing of reference versus predicted residuals for evaluation of partial least squares spectral calibrations. *Journal of Near Infrared Spectroscopy*. 14(6): 371-377.

Roesner, L.A. and P.Traina. 1994. Overview of Federal Law and USEPA Regulations for Urban Runoff. *Water Science and Technology*. 29(1-2):445-454.

Rossman, L.A. 2010. *Storm Water Management Model User's Manual Version 5.0*. Cincinnati, OH: National Risk Management Research Laboratory.

Royston, P., W. Sauerbrei. 2008. *Multivariable Model-Building: A Pragmatic Approach to Regression Anaylsis based on Fractional Polynomials for Modelling Continuous Variables*. Hoboken, NJ: John Wiley & Sons.

Ruelland, D., S. Ardoin-Bardin, G. Billen, and E. Servat. 2008. Sensitivity of a lumped and semi-distributed hydrological model to several methods of rainfall interpolation on a large basin in West Africa. *J.ournal of Hydrology*. 361:96-117.

Sarangi, R.K., T. Thangaradjou, A.S. Kumar, T. Balasubramanian. 2011. Development of nitrate algorithm for the southwest Bay of Bengal water and its implication using remote sensing satellite datasets. *IEEE Journal of Selected Topics in Applied Earth Observations and Remote Sensing*. 4(4): 983-991.

SAS. 2014. *JMP User's Manual*. Ver. 6.0. Cary, NC: SAS.

Schott, J.R., J.A. Barsi, B.L. Nordgren, et al. 2001. Calibration of Landsat thermal data and application to water resource studies. *Remote Sensing of the Environment.* 78: 108-117.

Socolofsky, S.A., G.H. Jirka. 2005. Special Topics in Mixing and Transport Processes in the Environment. College Station, TX: Texas A&M University. Available at: https://ceprofs.civil.tamu.edu/ssocolofsky/ocenx89/downloads/book/socolofsky_jirka.pdf. Accessed 12 May 2014.

Soonthornnonda, P., E.R. Christensen, Y. Liu, J. Li. 2008. A washoff model for stormwater pollutants. *Science of the Total Environment*. 402: 248-256.

Su, S. 2009. Confidence intervals for quantiles using generalized lambda distributions. *Computational Statistics and Data Analysis*. 53:3324-3333

Su, S. 2007. Fitting single and mixture of generalized lambda distributions to data via discretized and maximum likelihood methods: GLDEX in R. *Journal of Statistical Software*. 21(9): 1-17.

Sun, Y., Z. Hou, M. Huang, F. Tian, L.R. Leung. 2013. Inverse modeling of hydrologic parameters using surface flux and runoff observations in the Community Land Model. *Hydrology and Earth System Sciences*, 17, 4995–5011.

State of Michigan. 2014. Total Suspended Solids. Marquette, MI: State Government of Michigan. Available at: http://www.michigan.gov/documents/deq/wb-npdes-TotalSuspendedSolids_247238_7.pdf. Accessed 13 May 2014.

Strecker, E. W., M. M. Quigley, B.R. Urbonas, J.E. Jones, J. K. Clary. 2001. Determining Urban Storm Water BMP Effectiveness. *Journal of Water Resources Planning and Management*. 127(3):144-149.

Tchobanoglous, G. and E.D. Schroeder. 1985. *Water Quality: Characteristics, Modeling, Modification*. Addison-Wesley Publishing Company

Temprano, J., O. Arango, J. Cagiao, J. Suarez, I. Tejero. 2006. Stormwater quality calibration by SWMM: A case study in Northern Spain. *Water SA*. 32(1): 55-63.

Texas State Historical Association. 2014. The Handbook of Texas Online. Denton, TX: Texas State Historical Association. Available at: http://www.tshaonline.org/handbook/online. Accessed 10 September 2014.

TWDB. 2009. Volumetric Survey of Lady Bird Lake. Austin, TX: Texas Water Development Board.

Urbonas, B. and P. Stahre. 1993. *Stormwater Best Management Practices and Detention for Water Quality, Drainage, and CSO Management*. Englewood Cliffs, NJ: PTR Prentice-Hall.

Urbonas, B. 1994. Assessment of stormwater BMPs and their technology. *Water Science and Technology*. 29(1-2): 347-353.

USDA. 2013. Web Soil Survey. Washington, DC: United States Department of Agriculture. Available at: http://websoilsurvey.sc.egov.usda.gov/App/HomePage.htm. Accessed 12 May 2014.

U.S. EPA. 1983. Results of the nationwide urban runoff program. WH-544. Washington, DC.: Water Planning Division, U.S. EPA. Available at: http://www.epa.gov/npdes/pubs/sw_nurp_vol_1_finalreport.pdf . Accessed at 1 October 2013.

U.S. EPA. 1999. Preliminary Data summary of Urban Stormwater Best Management Practices. Washington, DC: U.S. Environmental Protection Agency. Available at:

http://water.epa.gov/scitech/wastetech/guide/stormwater/index.cfm. Accessed 13 May 2014.

U.S. EPA. 2000. Stormwater Phase II Final Rule: An Overview. EPA 833-F-00-001. Washington, DC: U.S. Environmental Protection Agency.

U.S. EPA. 2013. STEPL Models and Documentation. Washington, DC: U.S. Environmental Protection Agency. Available at: http://it.tetratech-ffx.com/steplweb/models$docs.htm. Accessed 15 May 2014.

U.S. EPA. 2014a. Measurable Goals Guidance for Phase II Small MS4s. Washington, DC: U.S. Environmental Protection Agency. Available at: http://www.epa.gov/npdes/pubs/measurablegoals.pdf. Accessed 15 August 2014.

U.S. EPA. 2014b. State Development of Numeric Criteria for Nitrogen and Phosphorous Pollution. Washington, DC: U.S. Environmental Protection Agency. Available at: http://cfpub.epa.gov/wqsits/nnc-development/. Accessed 13 May 2014.

U.S. EPA. 2014c. State Development of numeric Criteria for Nitrogen and Phosphorus Pollution. Washington, DC: U.S. Environmental Protection Agency. Available at: http://cfpub.epa.gov/wqsits/nnc-development/. Accessed 15 May 2014.

U.S. EPA. 2014b. Storm Water Management Model (SWMM). Washington, DC: U.S. Environemntal Protection Agency. Available at: http://www.epa.gov/nrmrl/wswrd/wq/models/swmm/. Accessed 16 May 2014.

U.S. EPA. 2014e. SUSTAIN: System for Urban Stormwater Treatment and Analysis Integration Model. Washington, DC: U.S. Environmental Protection Agency.

Available at: http://www.epa.gov/nrmrl/wswrd/wq/models/sustain/. Accessed 16 may 2014.

U.S. EPA. 2014f. Watershed Assessment, Tracking & Environmental Results System (WATERS). Washington, D.C.: U.S. Environmental Protection Agency. Available at: http://water.epa.gov/scitech/datait/tools/waters/index.cfm. Accessed 10 September 2014.

USGS. 2004. Predicting water quality by relating secchi-disk transparency and chlorophyll a measurements to satellite imagery for Michigan inland lakes, August 2002. Scientific Investigations Report 2004-5086. Reston, VA: U.S. Geological Survey.

USGS. 2010. Nitrate Loads and Concentrations in Surface-Water Base Flow and Shallow Groundwater for Selected Basins in the United States, Water Years 1990–2006. Scientific Investigations Report 2010–5098. Reston, VA: U.S. Geological Survey. Available at: http://pubs.usgs.gov/sir/2010/5098/pdf/SIR10-5098.pdf. Accessed 25 August 2014.

USGS. 2014a. The national map viewer and download platform. Reston, VA: USGS Headquarters. Available at: http://viewer.nationalmap.gov/viewer/. Accessed at 10 September 2014.

USGS. 2014b. USGS Water Data for the Nation. Reston, VA: U.S. Geological Survey. Available at: http://waterdata.usgs.gov/nwis. Accessed 10 September 2014.

USGS. 2014c. Frequently Asked Questions about the Landsat Missions. Reston, VA: U.S. Geological Survey. Available at: http://landsat.usgs.gov/tools_faq.php. Accessed 10 September 2014.

Van Griensven, A., T. Meixner. 2007. A global and efficient multi-objective auto-calibration and uncertainty estimation method for water quality catchment models. *Journal of Hydroinformatics*. 9(4): 277-291.

Vienna University of Economics and Business. 2014. The R Project for Statistical Computing. Vienna, Austria: Vienna University of Economics and Business. Available at: http://www.r-project.org/index.html. Accessed 1 June 2014.

Wang, B., and T. Li. 2009. Buildup characteristics of roof pollutants in the Shanghai urban area, China. *Journal of Zhenjiang University*. 10(9):1374-1382

WERF. 2014. WERF SELECT Model. Alexandra, VA: Water Environment Research Foundation. Available at: http://www.werf.org/i/c/Tools/SELECT.aspx. Accessed 15 May 2014.

Wicke, D., T.A. Cochrane, and A. O'Sullivan. 2012. Build-up dynamics of heavy metals deposited on impermeable urban surfaces. *Journal of Environmental Management*. 113:347-354

Widen-Nilsson, E., L. Gong, S. Halldin, C.-Y. Xu. 2009. Model performance and parameter behavior for varying time aggregations and evaluation criteria in the WASMOD-M global water balance model. *Water Resources Research*. 45: W05418.

Walsh, K. 2005. Data mining to determine local effects of mercury emissions. DNR 12-10212005-69: PPRP-133. Annapolis, MD: Maryland Department of Natural Resources.

Wilby, R.L. 2005. Uncertainty in water resource model parameters used for climate change impact assessment. *Hydrological Processes*. 19: 3201-3219

Yan, X. 2009. *Linear Regression Analysis: Theory and Computing*. Singapore: World Scientific Publishing.

Young, E.O., D.S. Ross, C. Alves, T. Villars. 2012. Soil and landscape influences on native riparian phosphorus availability in three Lake Champlain Basin stream corridors. *Journal of Soil and Water Conservation*. 67(1):1-7.

Yu, S.L., J.-T. Kuo, E.A. Fassman, H. Pan. 2001. Field test of grasses-swale performance in removing runoff pollution. *Journal of Water Resources Planning and Management*. 127(3): 168-171.

APPENDIX A

The appendix provides modifications to source code of SWMM which allows SWMM to compute BMP removal efficiency of individual subcatchment. A strikethrough (~~example~~) means deletion and underline (<u>example</u>) means addition.

objects.h

```
//--------------------
// SUBCATCHMENT OBJECT
//--------------------
typedef struct
{
  char*        ID;             // subcatchment name
  char         rptFlag;        // reporting flag
  int          gage;           // raingage index
  int          outNode;        // outlet node index
  int          outSubcatch;    // outlet subcatchment index
  int          infil;          // infiltration object index
  TSubarea     subArea[3];     // sub-area data
  double       width;          // overland flow width (ft)
  double       area;           // area (ft2)
  double       fracImperv;     // fraction impervious
  double       slope;          // slope (ft/ft)
  double       curbLength;     // total curb length (ft)
  double*      initBuildup;    // initial pollutant buildup (mass/ft2)
  TLandFactor* landFactor;     // array of land use factors
  TGroundwater* groundwater;   // associated groundwater data
  TSnowpack*   snowpack;       // associated snow pack data

  double       lidArea;        // area devoted to LIDs (ft2)            //(5.0.019 - LR)
  double       rainfall;       // current rainfall (ft/sec)
  double       losses;         // current infil + evap losses (ft/sec)
  double       runon;          // runon from other subcatchments (cfs)
  double       oldRunoff;      // previous runoff (cfs)
  double       newRunoff;      // current runoff (cfs)
  double       oldSnowDepth;   // previous snow depth (ft)
  double       newSnowDepth;   // current snow depth (ft)
```

```
  double*      oldQual;        // previous runoff quality (mass/L)
  double*      newQual;        // current runoff quality (mass/L)
  double*      pondedQual;     // ponded surface water quality (mass/ft3)
  double*      totalLoad;      // total washoff load (lbs or kg)
  double       BMP_slp_1;      // regression line slope of overall removal efficiency for
pollutant#1 in the subcatchment
  double       BMP_slp_2;     // regression line slope of overall removal efficiency for
pollutant#2 in the subcatchment
  double       BMP_slp_3;     // regression line slope of overall removal efficiency for
pollutant#3 in the subcatchment
  double       BMP_icp_1;     // regression line intercept of overall removal efficiency
for pollutant#1 in the subcatchment
  double       BMP_icp_2;     // regression line intercept of overall removal efficiency
for pollutant#2 in the subcatchment
  double       BMP_icp_3;     // regression line intercept of overall removal efficiency
for pollutant#3 in the subcatchment
}  TSubcatch
```

subcatch.c

```
……

//=============================================================

int  subcatch_readParams(int j, char* tok[], int ntoks)
//
//  Input:   j = subcatchment index
//           tok[] = array of string tokens
//           ntoks = number of tokens
//  Output:  returns an error code
//  Purpose: reads subcatchment parameters from a tokenized  line of input data.
//
//  Data has format:
//    Name  RainGage  Outlet  Area  %Imperv  Width  Slope CurbLength BMP_eff_1
BMP_icp_1 BMP_eff_2 BMP_icp_2 BMP_eff_3 BMP_icp_3 Snowmelt
//
{
   int    i, k, m;
   char*  id;
   double x[9];
   double x[15];
```

```
// --- check for enough tokens
if ( ntoks < 8 ) return error_setInpError(ERR_ITEMS, "");

// --- check that named subcatch exists
id = project_findID(SUBCATCH, tok[0]);
if ( id == NULL ) return error_setInpError(ERR_NAME, tok[0]);

// --- check that rain gage exists
k = project_findObject(GAGE, tok[1]);
if ( k < 0 ) return error_setInpError(ERR_NAME, tok[1]);
x[0] = k;

// --- check that outlet node or subcatch exists
m = project_findObject(NODE, tok[2]);
x[1] = m;
m = project_findObject(SUBCATCH, tok[2]);
x[2] = m;
if ( x[1] < 0.0 && x[2] < 0.0 )
   return error_setInpError(ERR_NAME, tok[2]);

// --- read area, %imperv, width, slope, & curb length
for ( i = 3; i < 8; i++)
for ( i = 3; i < 14; i++)
{
   if ( ! getDouble(tok[i], &x[i]) || x[i] < 0.0 )
      return error_setInpError(ERR_NUMBER, tok[i]);
}

// --- if snowmelt object named, check that it exists
x[8] = -1;
if ( ntoks > 8 )
{
   k = project_findObject(SNOWMELT, tok[8]);
   if ( k < 0 ) return error_setInpError(ERR_NAME, tok[8]);
   x[8] = k;
}
x[14] = -1;
if ( ntoks > 14 )
{
   k = project_findObject(SNOWMELT, tok[14]);
   if ( k < 0 ) return error_setInpError(ERR_NAME, tok[14]);
   x[14] = k;
}
```

```
    // --- assign input values to subcatch's properties
    Subcatch[j].ID = id;
    Subcatch[j].gage        = (int)x[0];
    Subcatch[j].outNode     = (int)x[1];
    Subcatch[j].outSubcatch = (int)x[2];
    Subcatch[j].area        = x[3] / UCF(LANDAREA);
    Subcatch[j].fracImperv  = x[4] / 100.0;
    Subcatch[j].width       = x[5] / UCF(LENGTH);
    Subcatch[j].slope       = x[6] / 100.0;
    Subcatch[j].curbLength  = x[7];
    Subcatch[j].BMP_slp_1  = x[8];
    Subcatch[j].BMP_icp_1  = x[9];
    Subcatch[j].BMP_slp_2  = x[10];
    Subcatch[j].BMP_icp_2  = x[11];
    Subcatch[j].BMP_slp_3  = x[12];
    Subcatch[j].BMP_icp_3  = x[13];

    // --- create the snow pack object if it hasn't already been created
    if ( x[8] >= 0 )
    {
       if ( !snow_createSnowpack(j, (int)x[8]) )
    if ( x[14] >= 0 )
    {
       if ( !snow_createSnowpack(j, (int)x[14]) )
          return error_setInpError(ERR_MEMORY, "");
    }
    return 0;

}

……

//=============================================================

void combineWashoffQual(int j, double pondedQual[], double washoffQual[],
                        double tStep)
//
//  Input:   j           = subcatchment index
//           pondedQual[]  = quality of ponded water (mass/ft3)
//           washoffQual[] = quality of washoff (mass/ft3)
//           tStep         = time step (sec)
//  Output:  updates Subcatch[j].newQual[]
//  Purpose: computes combined concentration of ponded water & washoff streams
```

```
//// ---- This function was re-written for Release 5.0.014. ---- ////      //(5.0.014 - LR)
{
   int   p;
   double qOut, cOut, cPonded, bmpRemoval, massLoad;
   double qOut, cOut, cPonded, bmpRemoval, massLoad, cOut_new;

   qOut = Subcatch[j].newRunoff;

   for (p = 0; p < Nobjects[POLLUT]; p++)
   {
      // --- zero concen. if no runoff flow
      if ( qOut <= FUDGE ) cOut = 0.0;                              //(5.0.017 - LR)
      else
      {
         // --- apply any BMP removal to ponded water
         cPonded = pondedQual[p];
         bmpRemoval = getBmpRemoval(j, p) * cPonded;
         if ( bmpRemoval > 0.0 )
         {
            massLoad = bmpRemoval * qOut *  tStep * Pollut[p].mcf;
            massbal_updateLoadingTotals(BMP_REMOVAL_LOAD, p, massLoad);
            cPonded -= bmpRemoval;
         }

         // --- add concen. of ponded water to that of washoff
         cOut = cPonded + washoffQual[p];

         if ( p == 0 )
         {
         cOut_new = ((1- Subcatch[j].BMP_slp_1) * cOut) + Subcatch[j].BMP_icp_1;
         bmpRemoval = cOut - cOut_new;
         massLoad = bmpRemoval * qOut * tStep * Pollut[p].mcf;
         massbal_updateLoadingTotals(BMP_REMOVAL_LOAD, p, massLoad);
         cOut = cOut_new;
         }
         else if ( p == 1 )
         {
         cOut_new = ((1- Subcatch[j].BMP_slp_2) * cOut) + Subcatch[j].BMP_icp_2;
         bmpRemoval = cOut - cOut_new;
         massLoad = bmpRemoval * qOut * tStep * Pollut[p].mcf;
         massbal_updateLoadingTotals(BMP_REMOVAL_LOAD, p, massLoad);
         cOut = cOut_new;
         }
         else if ( p == 2 )
```

```
            {
            cOut_new = ((1- Subcatch[j].BMP_slp_3) * cOut) + Subcatch[j].BMP_icp_3;
            bmpRemoval = cOut - cOut_new;
            massLoad = bmpRemoval * qOut * tStep * Pollut[p].mcf;
            massbal_updateLoadingTotals(BMP_REMOVAL_LOAD, p, massLoad);
            cOut = cOut_new;
            }
        }

        // --- save new outflow runoff concentration (in mass/L)
        Subcatch[j].newQual[p] = MAX(cOut, 0.0) / LperFT3;


        // --- update total runoff pollutant load from subcatchment
        massLoad = 0.5 * (Subcatch[j].oldQual[p]*Subcatch[j].oldRunoff +
                          Subcatch[j].newQual[p]*Subcatch[j].newRunoff) *
                          LperFT3 * tStep * Pollut[p].mcf;
        Subcatch[j].totalLoad[p] += massLoad;

        // --- update mass balance if runoff goes to an outlet node
        if ( Subcatch[j].outNode >= 0 )
        {
            massbal_updateLoadingTotals(RUNOFF_LOAD, p, massLoad);
        }
    }
}
```

text.h

```
#define FMT01 \
 "\n Correct syntax is:\n swmm5mod <input file> <report file> <output file>\n"
#define FMT02 "\n... EPA-SWMM 5.0 (Build 5.0.022)\n"                    //(5.0.022 - LR)
#define FMT02 "\n... EPA-SWMM Build 5.0.022 with individual BMP efficiency - by Min-cheng Tu\n"
#define FMT03 " There are errors.\n"
#define FMT04 " There are warnings.\n"
#define FMT05 "\n"
#define FMT06 "\n o  Retrieving project data"
#define FMT07 "\n o  Writing output report"
#define FMT08 \
 "\n  EPA STORM WATER MANAGEMENT MODEL - VERSION 5.0 (Build 5.0.022)"      //(5.0.022 - LR)
```

```
#define FMT08 \
  "\n  EPA STORM WATER MANAGEMENT MODEL - Build 5.0.022 with individual
BMP consideration - by Min-cheng Tu"
#define FMT09 \
  "\n  ------------------------------------------------------------"
#define FMT10 "\n"
#define FMT11  "\n    Cannot use duplicate file names."
#define FMT12  "\n    Cannot open input file "
#define FMT13  "\n    Cannot open report file "
#define FMT14  "\n    Cannot open output file "
#define FMT15  "\n    Cannot open temporary output file"
#define FMT16  "\n  ERROR %d detected. Execution halted."
#define FMT17  "at line %d of input file:"
#define FMT18  "at line %d of %s] section:"
#define FMT19  "\n  Maximum error count exceeded."
#define FMT20  "\n\n  Analysis begun on:  %s"
#define FMT20a "  Analysis ended on:  %s"                    //(5.0.011 - LR)
#define FMT21  "  Total elapsed time: "
```